2020•2021

Faculteit Industriële Ingenieurswetenschappen

master in de industriële wetenschappen: nucleaire technologie

Masterthesis

Validation of ALEPH2 burn-up code using benchmarks from SFCOMPO

PROMOTOR :

Prof. dr. ir. Gert VAN DEN EYNDE

PROMOTOR :

Dr. ir. Pablo ROMOJARO

COPROMOTOR :

Dr. ir. Luca FIORITO

Linde Pollet

Scriptie ingediend tot het behalen van de graad van master in de industriële wetenschappen: nucleaire technologie, afstudeerrichting nucleaire en medisch

Gezamenlijke opleiding UHasselt en KU Leuven

2020•2021

Faculteit Industriële Ingenieurswetenschappen

master in de industriële wetenschappen: nucleaire technologie

Masterthesis

Validation of ALEPH2 burn-up code using benchmarks from SFCOMPO

PROMOTOR :

Prof. dr. ir. Gert VAN DEN EYNDE

PROMOTOR :

Dr. ir. Pablo ROMOJARO

COPROMOTOR :

Dr. ir. Luca FIORITO

Linde Pollet

Scriptie ingediend tot het behalen van de graad van master in de industriële wetenschappen: nucleaire technologie, afstudeerrichting nucleaire en medisch

UHASSELT

KU LEUVEN

Acknowledgments

With the support of SCK CEN, I'm proud to present you my master's thesis. This thesis is a good completion of my education of industrial engineering in nuclear technology at Hasselt University. From the beginning till the end of my school career, I have never regretted my choice for this career path. I have experienced that these courses resonate with the person I am, which made studying the subjects given very engaging. During my time in class and this internship at SCK CEN, I have learned a lot, which I will take with me during my further career. Although I could not have accomplished any of this without the help of a number of individuals, whom I would like to thank.

First, I want to give a special thanks to Prof. Van den Eynde for offering this great learning opportunity. He motivated me to stand up for myself when I didn't dare to speak up for what I wanted. Also, I can't forget the much-needed advice he gave which allowed me to grow as a person.

Additionally, I want to thank my mentors Pablo Romojaro and Luca Fiorito for the close supervision last year. At the beginning, I had a hard time finding my way around the topic. Thanks to their guidance and support, I was able to complete this manuscript.

Finally, I would like to express my greatest thanks to my family and friends. They gave me strength and motivation during my master's thesis. The long hours writing and discussing together are unforgettable. It was a great comfort knowing I had all these people by my side.

Table of contents

List of figures

List of tables

Glossary of terms

AD	Analysis Date
ADS	Accelerator Driven System
AGR	Advanced Gas-cooled Reactor
BOC-X	Begin Of Cycle X
BWR	Boiling Water Reactor
CANDU	CANada Deuterium Uranium
DOD	Day Of Discharge
ENDF	Evaluated Nuclear Data File
EOC-X	End Of Cycle X
HTML	HyperText Markup Language
JAERI	Japan Atomic Energy Research Institution
LWR	Light Water Reactor
MCNP	Monte Carlo N-Particle Transport
NEA	Nuclear Energy Agency
OECD	Organisation for Economic Co-operation and Development
PWR	Pressurized Water Reactor
SCALE	Standardized Computer Analysis for Licensing Evaluations
SCK CEN	Belgian Nuclear Research Centre
SFCOMPO	Spent Fuel Isotopic Composition
SNF	Spent Nuclear Fuel

Abstract

Spent Nuclear Fuel (SNF), irradiated nuclear fuel, is highly radioactive and dangerous when not handled correctly. An accurate characterization of SNF, in terms of nuclide composition, gives the possibility to accurately quantify integral responses such as decay heat, neutron and gamma emission, and criticality for its safe handling, transport, and storage. So-called depletion codes are used to predict these nuclide compositions. ALEPH2 is a Monte-Carlo depletion code developed by SCK CEN since 2004. In the past, ALEPH2 has been validated to solve a limited number of light water reactor (LWR) cases. As a part of its maintenance and verification process, a continuous work of validation against experimental measurements is needed. In this Master's thesis, a validation exercise was performed by simulating several LWR SNF benchmark cases using the experimental assay data available in SFCOMPO, a database developed and maintained by the OECD/NEA. Experimentally measured nuclide compositions were compared against ALEPH2 predictions. Initially, a simple model was developed for each case, which, after analysis, was refined. A good agreement between calculated nuclide concentrations and measured data was found, hence validating ALEPH2 capabilities to provide good representation of the actual nuclide composition.

Abstract (NL)

Gebruikte of bestraalde splijtstof is hoog radioactief en gevaarlijk indien deze niet op de juiste manier wordt behandeld. Een nauwkeurige karakterisering van deze splijtstof, in termen van nuclide samenstelling, biedt de mogelijkheid om integrale parameters, zoals restwarmte, neutron- en gamma-emissie en kritikaliteit nauwkeurig te kwantificeren met het oog op een veilige behandeling, vervoer en opslag ervan. Zogenaamde evolutiecodes worden gebruikt om deze nuclidesamenstellingen te voorspellen. ALEPH2 is een Monte Carlo evolutiecode die sinds 2004 door het SCK CEN is ontwikkeld. In het verleden werd ALEPH2 reeds gevalideerd door een beperkt aantal studies van splijtstof van licht water reactoren (LWR). Als onderdeel van het onderhouds- en verificatieproces, is er nood aan een continue validatie aan de hand van experimentele metingen. In deze masterproef werd een validatieoefening uitgevoerd door verschillende LWR bestraalde splijtstof benchmarkgevallen te simuleren en te vergelijken met de experimentele gegevens in SFCOMPO, een database ontwikkeld en onderhouden door het OECD/NEA. De experimenteel gemeten nuclidesamenstellingen werden vergeleken met de ALEPH2 voorspellingen. Aanvankelijk werd voor elk geval een eenvoudig model ontwikkeld, dat na analyse werd verfijnd. Er werd een goede overeenkomst gevonden tussen de berekende nuclideconcentraties en de gemeten gegevens. ALEPH2 geeft dus een goede weergave van de werkelijke nuclidesamenstelling.

1 Introduction

Nuclear fuel is irradiated in nuclear power plants. After the irradiation process, the nuclear fuel is discharged from the reactor and is considered as used nuclear fuel or Spent Nuclear Fuel (SNF). Handling of SNF is limited by its characteristics:

- decay heat: the heat released through the decay of the fuel;
- radioisotopic inventory: the source term that could be released in case of a breach of confinement;
- criticality: the possibility to sustain a fission reaction chain, to assure that it does not occur;
- neutron emission: the number of neutrons emitted;
- gamma emission: the number of gamma rays emitted.

SNF needs to be transported and handled safely between the different processing steps with the ultimate goal to be reprocessed or stored in a deep geological repository. SNF is first stored in short-term wet storage, where short-lived nuclides decay and the produced decay heat is removed. Afterward, the SNF is transported to intermediate storage, dry or wet [1]. At the moment, a final disposal solution is not yet realized, however, research is in progress. Finland expects to operate its repository in 2023 and Sweden in the next 10 years. In Belgium, plans are in the making [2]. Throughout all these steps, the control of the criticality, the decay heat removal, and the integrity of the containment are extremely important for its safe handling.

1.1 The three safety functions

1.1.1 Criticality

The SNF should always remain in a subcritical condition after being discharged from the reactor (the neutron absorption rate is larger than the neutron production rate). Due to the potential interaction between fuel elements, neutrons that exit one fuel element can enter another fuel element that is situated nearby, which causes an increase in the number of neutrons in the volume, and thus also the possibility to induce a reaction. For this reason, fuel elements need to be stored according to the predetermined criteria (e.g., a minimal distance between fuel elements is respected or shielding of the fuel elements) to avoid re-criticality of the material and that the fission chain reaction becomes self-sustained, something that is undesirable outside a nuclear reactor.

1.1.2 Decay heat removal

At all times, the decay heat needs to be adequately evacuated. In wet storage, this is realized by heat transfer from the SNF to the water in the pools, which, in turn, are then cooled. In dry storage, the heat is removed through convection in the air. In case the decay heat is not sufficiently removed, the fuel could start to melt due to a rising temperature.

1.1.3 Containment

Depending on the accidental conditions, a release of SNF can potentially affect both nearby and far populations and the environment. The containment of the SNF itself has two functions: shielding

against radiation and providing mechanical integrity in normal and accidental conditions, to avoid a possible release of radionuclides to the environment. The shielding not only protects the workers but also allows more flexible placement of the fuel elements concerning the danger of possible re-criticality since the structural material will also absorb neutrons and hence fewer neutrons will reach neighboring fuel elements reducing the neutronic coupling.

1.2 The need for spent nuclear fuel characterization

To assess these risks, the nuclide composition of the SNF must be known. Accurate quantification of assembly integral responses such as nuclide inventory, neutron- and gamma-emission rates, and decay heat rate are of vital importance for safe handling, transport, and storage of SNF. Predictions of these responses are derived from the nuclide content. It is not possible to measure every integral response for each and all fuel assemblies in an acceptable time [3]. In addition, not all nuclides are easy to measure, for example, nuclides present in small quantities or alpha-emitters. By the time spent fuel is sufficiently cooled to perform the experimental measures, most very short-lived fission products have already decayed and are not measurable anymore.

A set of equations (implemented in fuel depletion or burn-up codes) allows predicting the evolution of nuclide concentrations under particle irradiation, in a reactor context typically neutrons, and radioactive decay. They are considered of utmost importance. These equations rely on the use of nuclear data, which define interactions, such as, cross sections, decay data, branching ratios, fission yields, and Q-values. They are used to make model predictions and to give a good estimate of the real-life response in different situations. Depending on different versions of the nuclear data libraries, a slightly different outcome is expected, since some nuclear data differ between libraries.

The concept of burn-up credit is possible due to good characterization. It implies taking credit for the reduction in reactivity of the spent fuel element due to irradiation of nuclear fuel (loss of fissile material and production of neutron-absorbing fission products) when the criticality safety analysis is carried out for the spent fuel [4]. This methodology is implemented as part of licensing protocols and regulatory practices to optimize transport as well as both optimize and increase SNF storage capacities [5].

1.3 Parameters that influence the nuclide composition of spent fuel

A higher enrichment of ^{235}U in the fuel is the most common way to raise the level of burn-up (a measure for the amount of energy released in the fuel) because more fissile material is available in the same volume of nuclear fuel and thus, more fissions can occur before discharging the fuel from the reactor. Not only does the level of enrichment affect the burn-up, but also the distribution of different fuel rods to reduce rod thermal loads, as well as the reconstitution and reshuffling of spent fuel bundles [6]. Depending on the position and the type of fuel in the reactor, the neutron flux changes. There is an angular, axial, and radial dependence [7]. A local increase in neutron flux causes an increase in the number of fissions, which results in a higher burn-up and a different nuclide composition in that area.

In addition, the cooling time also has an impact on the nuclide composition of the SNF. Radioactive nuclides decay during that time, not only releasing energy but also producing other nuclides, thus resulting in a different nuclide composition. Secondly, spontaneous fissions occur, generating more fission products and fast neutrons. The number of neutrons produced this way is not sufficient to maintain the chain reaction in a nuclear reactor, but will in their turn be moderated and possibly result in

other fissions. Since also neutron loss occurs in a reactor (through non-fission absorption or leakage), this rate drops fast.

The reactivity [ρ] of a reactor is a value that expresses the state of the reactor compared to criticality, described in three states: subcritical, critical, and supercritical. It is defined by the ratio between the neutron production rate and the neutron absorption rate. The reactor is subcritical when more neutrons are absorbed than produced. In a supercritical reactor, it is the other way around. When absorption and production are perfectly balanced, the reactor is critical. The longer nuclear fuel is irradiated in a reactor, the more fissioning nuclides deplete. When the number of fissioning nuclides in the system decreases, the fission reaction rate also decreases. To keep the reactivity constant, anti-reactivity measures are taken, such as diluting boric acid in the moderator, integrating gadolinium in the fuel rods, and using control rods. Fuel shuffling strategies are devised to minimize such measures. Boric acid functions as a neutron absorber. It is mixed into the cooling water/moderator to ensure homogeneous distribution. Over the reactor lifetime, the boric acid helps to control the reactivity. The fission reaction rate is higher at the beginning of the irradiation period than at the end, which is balanced by the boric acid to maintain a constant reactivity. A certain concentration of boric acid is pumped into the cooling water and as the reactivity decreases, non-borated water is added and the boric acid concentration reduces because the fission reaction rate is reduced at higher burn-up of the sample.

The Doppler effect, otherwise known as the fuel prompt temperature coefficient, is an important phenomenon to maintain reactor stability [8]. In the epithermal range of neutron energy, the neutron absorption cross section has resonances. These resonances are seen as high peaks, which causes a possibility of absorption of neutrons during their moderation from fast to thermal energies. The width of these peaks depends on the fuel temperature (Figure 1). With rising temperature, the peaks flatten, but still, the neutron absorption cross section remains high, which causes the probability of neutron absorption to rise and more neutrons are absorbed during their moderation. This is a negative reactivity effect, i.e., it the temperature of the fuel increases, the reactivity in the reactor decreases due to an increasing number of resonance captures in the fuel (mainly in ^{238}U). As a result, simulating a temperature higher than the actual temperature ensures the simulation of too many neutron absorptions.

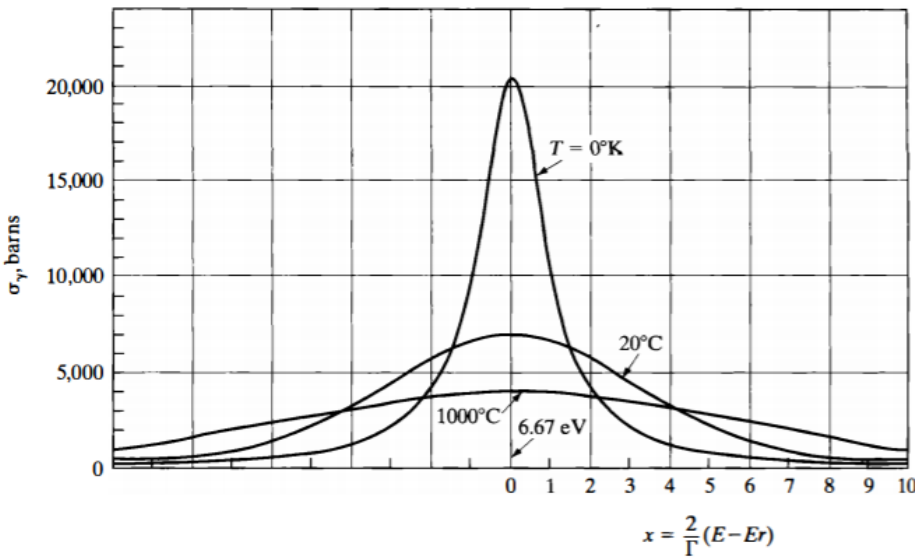

Figure 1: Doppler resonance peak of the neutron capture cross-section of ^{238}U at 6.67 eV resonance [8]

1.4 Computer codes for spent fuel characterization

The integral responses of SNF are predicted through simulations and computational modeling [5]. They predict the nuclide evolution using interaction data, decay data, branching ratios, fission yields, and Q-values. With the nuclide evolution, the nuclide composition is calculated at a certain point in time. Starting from the nuclide composition, the decay heat and emitted radiation are estimated using decay data. Those integral responses during the storage period are predicted for every SNF batch, regardless of the initial composition or irradiation time. Over time, several so-called depletion codes for coupled neutron transport have been developed [9].

These burn-up codes need verification and validation to ensure correct results in design and safety studies for spent nuclear fuel handling and storage. To validate these burn-up codes, simulations are made for well-described cases. A sample (with known initial nuclide composition) is irradiated under known conditions (reactor type, irradiation history, moderator and fuel temperature, and boron concentration) in a nuclear reactor [10]. The outcome (e.g., final nuclide composition and burn-up level) of the simulation is compared with experimental data.

The main goal of this research is to validate the ALEPH2 burn-up code by using the experimental assay data of SNF from SPCOMPO [11]. The benchmarks have been selected according to the level of complexity to offer a variety of cases (i.e., different levels of burn-up, enrichment, fuel type, and reactor type) for a widespread validation of ALEPH2. In addition, information that is not mentioned in SFCOMPO to run the simulations will be retrieved from operation reports of the concerned reactors. Inconsistencies (or missing information) found in the SFCOMPO database, compared to the official reports, is reported in Appendix A. The burn-up level and nuclide composition were calculated with the simulations and compared with the experimental data from SFCOMPO, obtained by isotopic destruction techniques. The results of this work will allow validating not only ALEPH2 but also the nuclear data libraries used in the burn-up calculations.

The thesis begins with a brief description of the physical quantities as a background, followed by a literature study about the nuclide composition, burn-up calculations, ALEPH2, and SFCOMPO as a provider of experimental data. In method and materials, the input and model of each case are discussed. The assumptions made are also justified for every case in this section. In the results section, the important and relevant information of the output files is presented, followed by a discussion of the results. Finally, conclusions are presented and the capability of ALEPH2 to predict the nuclide compositions for the considered range of burn-up, initial enrichment, and cooling time will be assessed.

2 Theory

2.1 Description of physical quantities

2.1.1 Cross sections

A cross section expresses the probability for a particle (e.g., a neutron) to interact with a nucleus and undergo a specific reaction, e.g., fission, radiative capture, scattering, or threshold reactions. Cross sections are expressed in terms of area (barns or 10^{-24} cm^2).

Transmutation is a reaction type where an incident particle (either neutron or proton) is absorbed in the target nucleus that will result in a transformation of that target nucleus into another isotope. When the target is placed in an irradiating environment, the nuclides initially presented will undergo different nuclear reactions and other isotopes are formed. Afterward, these newly formed nuclides can either decay, transmute again, or fission depending on the cross section of the nuclide for that specific reaction. The likeliness of those reactions is determined by the structure of the nucleus. Nuclides with an odd number of nucleons are more likely to absorb a neutron followed by fission than nuclides with an even number of nucleons [12].

The most common reactions in nuclear fuel are fission, absorption, and elastic collision reactions. Heavy fissile nuclides, such as ^{235}U or ^{239}Pu, absorb a neutron, causing the creation of a very unstable nuclide that will likely undergo fission. The probability for both steps to happen, the cross section of this reaction, is much higher when the incident neutron is a thermal neutron (kinetic energy of about 0.025 eV) instead of a fast neutron (kinetic energy of more than 0.1 MeV). The nucleus splits into at least two lighter nuclei (also known as fission products), two or three fast neutrons, and gamma irradiation. To maintain the fission chain reaction, these released neutrons are used to induce the next fission reaction. However, since the cross section of the fission reaction is higher when using thermal neutrons instead of fast neutrons, the fast neutrons need to be moderated through elastic scattering. Moderation is typically done with a material of low mass with a high scattering cross section and a low absorption cross section, to lose as little as possible neutrons through neutron absorption.

Cross sections are available in evaluated nuclear data files and obtained by energy-dependent measurements supplemented with theoretical model calculations. This combination/evaluation is done through critical comparison and renormalization by evaluators to obtain a representative model of the real values that define nuclear reactions. Nuclear data are stored as tabulated, computer-readable databases called nuclear data libraries. The adopted format is called ENDF, as in Evaluated Nuclear Data File, and it is currently at its sixth revision (ENDF-6) [13]. Modern graphical user interfaces such as JANIS [14] from OECD/NEA help to access and display nuclear data files.

2.1.2 Neutron flux

The neutron flux is a quantity that describes the number of neutrons that cross a defined surface in a certain time. It is calculated by multiplying the neutron density (n), in neutrons/m^3, by the neutron velocity (v), in m/s, and is expressed in neutrons/m^2 s (equation (1)). The energy distribution of neutrons is called the neutron spectrum and in a Pressurized Water Reactor (PWR), one typically considers three sorts of neutrons: fast, intermediate, and thermal neutrons (Figure 2). Fast neutrons are released during fission, they are then moderated (slowed down) to intermediate energies and then up to thermal energies to increase the probability for fission.

$$\varphi = nv \tag{1}$$

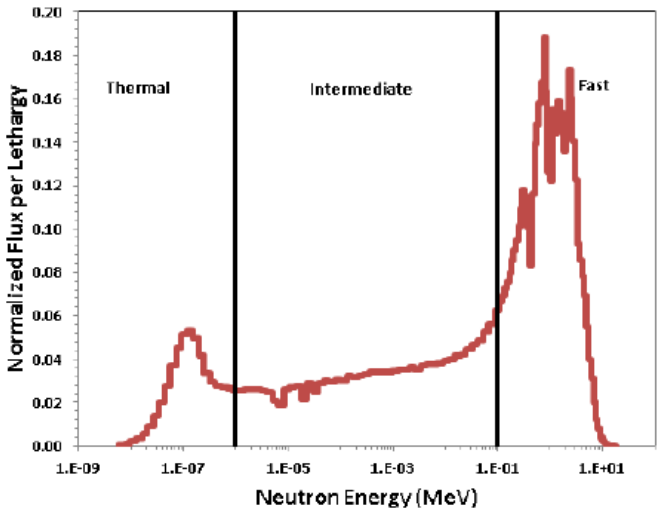

Figure 2: Typical neutron spectrum in a PWR [15]

2.1.3 Nuclear decay

Nuclear decay (also known as radioactive decay) occurs in unstable nuclides. Energy is spontaneously emitted in the form of radiation (alpha, beta, and gamma radiation). Nuclear decay is characterized by the half-life ($T_{1/2}$ = ln(2)/λ, decay constant λ) of the nuclide, a theoretic time interval after which half of the initially present unstable nuclides have decayed. The number of nuclides *N(t)* remaining after a certain decay time *t* is calculated with equation (2), starting from the original number of nuclides N_0.

$$N(t) = N_0 e^{-\lambda t} \tag{2}$$

2.1.4 Fission product yields

The fission yield is the fraction of a fission product that is produced through fission. This yield changes according to the mass of the initial fissioned nuclide and the energy of the incident neutron. An example of a fission yield distribution as a function of the target mass is displayed in Figure 3.

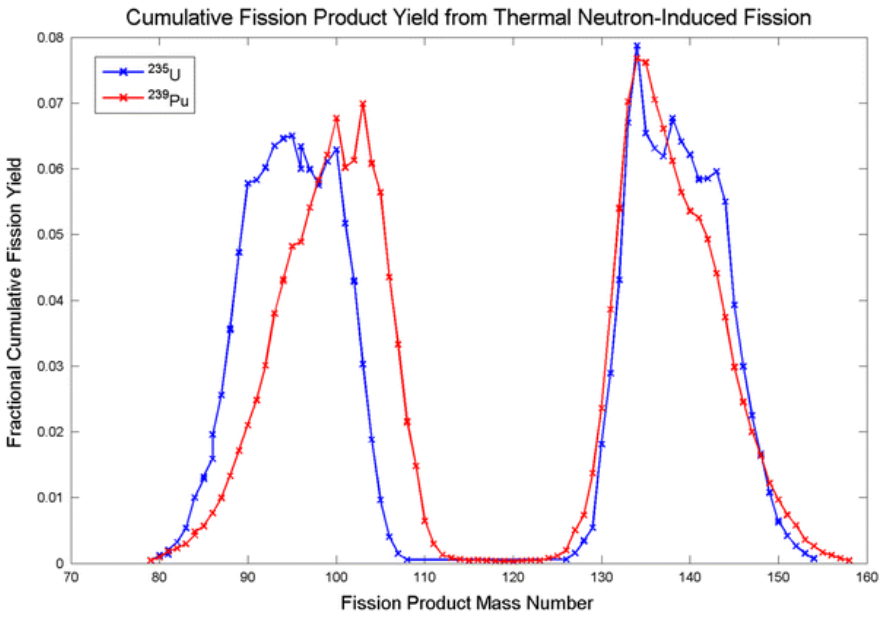

Figure 3: Fission yield distribution by mass of fission products for thermal neutrons for ^{235}U and ^{239}Pu [17]

2.2 Neutron transport

Neutron transport can be described using the Boltzmann transport equation, which is time-dependent. In this application, steady state is assumed, since there is no interest in start-up and shutdown processes but rather in the long period that the reactor operates at nominal power. This allows a simplification, the assumption that the number of neutrons in the volume stays equal, so-called steady state. There is considered no time dependence in the system. The number of neutrons produced is the same as the number of neutrons lost, through either collision/absorption or leaking out of the volume. In steady state, the neutron transport is represented by equation (3) consisting of the neutron loss rate through leakage out of the system $[\boldsymbol{\Omega} \cdot \nabla\varphi]$, the total reaction rate for collision and absorption $[\sum_t(\boldsymbol{r}, E)\varphi]$, and the generation rate through scatter $[\sum_s f\varphi]$, fission $[Q_f]$, and external neutron sources $[S]$.

$$\boldsymbol{\Omega} \cdot \nabla\varphi + \sum_t(\boldsymbol{r}, E)\varphi = \int_0^\infty \int_{\Omega'} \sum_s(\boldsymbol{r}, E')f(\boldsymbol{r}, E' \rightarrow E, \boldsymbol{\Omega}' \rightarrow \boldsymbol{\Omega})\,\varphi(\boldsymbol{r}, E', \boldsymbol{\Omega}', t)dE'd\boldsymbol{\Omega} + Q_f(\boldsymbol{r}, E, \boldsymbol{\Omega}, t) + S(\boldsymbol{r}, E, \boldsymbol{\Omega}, t) \quad (3)$$

There is a direct relation between the thermal power in a reactor and the neutron flux. The thermal power is determined by the rate at which the heat, as a result of fission, is produced. The reaction rate [*RR]* at which fission occurs is determined by the neutron flux $[\varphi(E, t)]$ and the macroscopic cross section [$\sum_f$] (atom number density [*N(t)*] multiplied by the microscopic cross section [*σ(E)*] and is given by equation (4). The thermal power per unit time (equation (5)) can be calculated by multiplying the total number of reactions in a volume per unit of time, defined by the reaction rate multiplied by the volume of fission material [*V*], by the energy released per fission [E_r].

$$RR = \varphi\sum = \varphi N\sigma \quad (4)$$

$$P = RR\,E_rV = \varphi\sum_f E_rV \quad (5)$$

2.3 Nuclide composition

When irradiating nuclear fuel with neutrons, the nuclide composition of the fuel changes. After neutron absorption, the nuclides can either undergo fission, with the production of fission products, or transmute into heavier nuclides, which will decay in their turn. Any possible reaction contributes to changing fuel composition. At every point in time, after irradiation and/or decay, the new nuclide composition can be calculated with the Bateman equations (equation (6)). Each equation always consists of two terms. First, the production part tells how many nuclides per unit of time are produced in certain conditions, which occurs in three different ways:

- fission $\left[\gamma_j \sum_f \varphi\right]$;
- transmutation $\left[\sigma^{i\to j} \varphi n_i\right]$;
- decay from other nuclides $\left[b_{j\to i}\, \lambda^{i\to j} n_i\right]$.

with γ_j the fission yield, $\sum_f$ the macroscopic cross section for fission, φ the neutron flux, $\sigma^{i\to j}$ microscopic cross section for the reaction transmuting nuclide *i* in nuclide *j*, n_i the number of atoms of nuclide *i*, $b_{j\to i}$ the branching ratio, and $\lambda^{i\to j}$ the decay constant from nuclide *i* to nuclide *j.* The number of the formed nuclide will, in its turn, decrease through

- neutron absorption $\left[\sigma_a^j \varphi n_j\right]$;
- decay (only if unstable) $\left[\lambda^j n_j\right]$.

with σ_a^j the cross section for neutron absorption by nuclide *j*. The reduction of nuclides is described in the second part of the equation, the destruction part.

$$\frac{\partial n_j}{\partial t} = \gamma_j \sum_f \varphi + \sum_i (b_{j\to i} \lambda^{i\to j} + \sigma^{i\to j} \varphi) n_i - (\lambda^j + \sigma_a^j \varphi) n_j \qquad (6)$$

γ_j is the fission product yield when producing fission product *j*, $\lambda^{i\to j}$ is the decay rate of isotope *i* to produce isotope *j* for the different decay forms, and $\sigma^{i\to j}$ is the cross section for the transmutation of isotope *j* by neutron capture. The cross section used in this equation is one-group-averaged. This means that the cross section is averaged out over the energy of a particular neutron flux while preserving the reaction rate. To remove the non-linear character of the cross section in the depletion equation, the neutron flux is assumed to remain constant (in amplitude and spectrum) for a certain time (in this case, an irradiation step). This assumption allows less complex calculations. Time steps are chosen in such a way that the linearization does not impact the final result too much.

The production of fission products is also a consequence of "burning"[1] nuclear fuel. Two intermediate-mass nuclei, together with two or three neutrons, are produced per fission. Due to the structure of the nucleus, the distribution of the nucleus particles over the fission products is not equal. As shown in Figure 3, this distribution has two peaks, where the mass of the isotopes is about 100 and 140 amu. The shape of the peaks, especially the first one, depends on the mass of the fissioned nuclide, which results in a different fission yield for different isotopes. These fission products can also undergo neutron capture and/or, when not stable, radioactive decay. The change in the concentration of these fission products can be described with the general production-destruction equation (6) for nuclide *j.*

The evolution of nuclides depends on different reactor parameters. A different initial nuclide concentration of the nuclear fuel results in a different final nuclide composition. The occurring reaction rates

[1] Subjected to a neutron flux

depend on the nuclides present. The density of the cladding, moderator, and fuel, which is also correlated with its temperature, influences the local neutron flux, which results in a different neutron distribution, and different reaction rates. Likewise, the rod and assembly dimensions have an impact on the neutron distribution.

2.4 Fuel burn-up

Fuel burn-up [*BU*] is a measure of how much energy is extracted from nuclear fuel and is commonly defined as the total energy released per unit mass of heavy elements initially present in the fresh fuel. Approximately 200 MeV of recoverable energy is released per fission of ^{235}U. To calculate the burn-up, the integral of the power [*P*] per initial mass of heavy metal (or uranium) [m_0] over the time of the irradiation [*T*] is taken and Equation (7) is obtained. The longer the nuclear fuel is irradiated with a steady neutron flux, the more fissions occur, and the higher the burn-up. The more fissile material is present in the fuel material, the more fissions can occur and the more energy will be emitted during operation.

$$BU\ [MWd/kgHMi] = \frac{1}{m_0}\int_0^T P(t)dt \tag{7}$$

The number of fissionable isotopes decreases in time and fission products are produced, resulting in a changing nuclide composition of the nuclear fuel. Fertile isotopes (e.g., ^{238}U) undergo transmutation through neutron capture and, in this case, produce ^{239}U, which decays ($T_{1/2}$ = 23.45 min [18]) with β^--decay into ^{239}Np, which decays ($T_{1/2}$ = 2.356 d [18]) with β^--decay into ^{239}Pu, a fissile isotope, that becomes the main fission contributor after a burn-up of a few dozen of GWd/tHMi. ^{239}Pu transmutes into ^{240}Pu through neutron capture, which is a strong neutron absorber. This reaction occurs very easily due to the high absorption cross section for thermal neutrons (Figure 4). ^{240}Pu has a half-life of 6561 y [18] and a high cross section for the capture of a thermal neutron. It is therefore likely that it will undergo transmutation through neutron capture into ^{241}Pu. This specific isotope of plutonium has a high cross section for neutron capture [14] but also a much shorter half-life ($T_{1/2}$ = 14.329 y [18]) as compared to other plutonium isotopes. Because the half-life has the same order of magnitude as the irradiation time of a fuel assembly, a significant amount of decay will occur, and ^{241}Am, the first minor actinide in the neutron-capture chain, is produced. Due to its long half-life ($T_{1/2}$ = 432.6 y [18]) and high cross section for thermal neutrons [14], the majority of the ^{241}Am nuclides will capture a thermal neutron and transmute into ^{242}Am, a nuclide with both a very large capture cross section for capture [14] and a short half-life ($T_{1/2}$ = 16.02 h [18]) for β^-- decay. As a result, ^{243}Am will be produced through transmutation and ^{242}Cu, another minor actinide, will be produced through the β^--decay of ^{242}Am. To produce ^{243}Cm and ^{244}Cm, respectively one and two neutrons are captured in ^{242}Cm since both ^{242}Cm and ^{243}Cm have high cross sections for the capture of thermal neutrons. In Figure 5 is a schematic representation of this chain is shown.

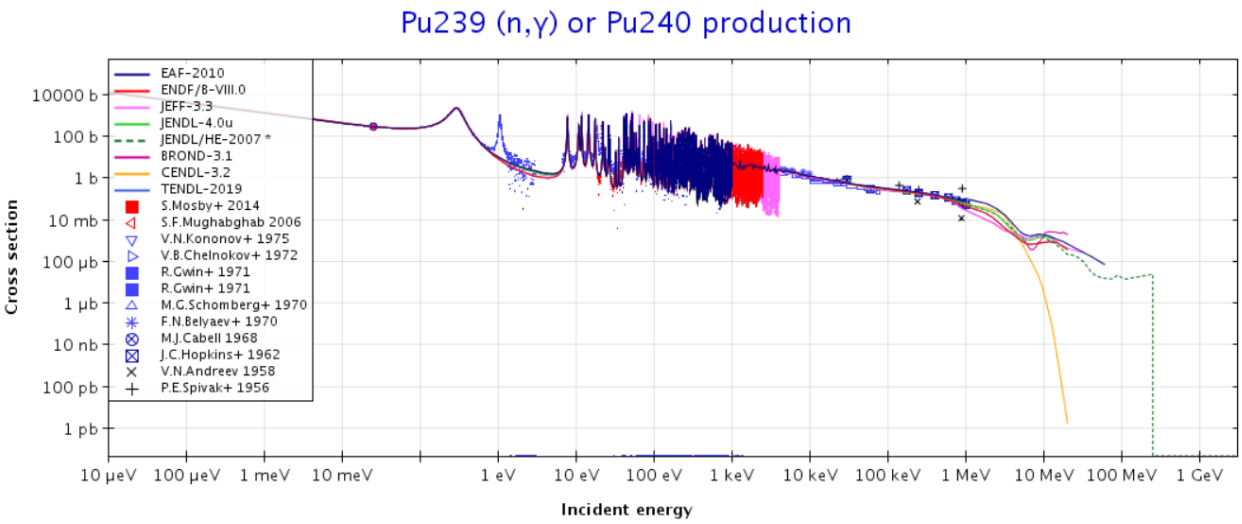

Figure 4: Cross section for $^{239}Pu(n,\gamma)^{240}Pu$ reaction (figure generated using the JANIS software [14]*)*

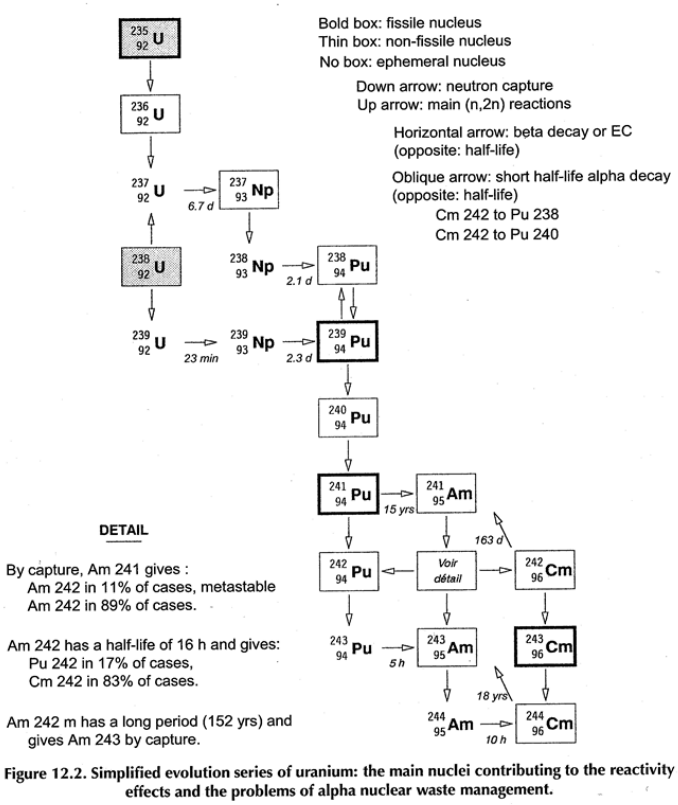

Figure 12.2. Simplified evolution series of uranium: the main nuclei contributing to the reactivity effects and the problems of alpha nuclear waste management.

Figure 5: Schematic overview of transmutation reactions and decay starting from uranium [19]

The build-up of the different actinides occurs as a function of burn-up. Figure 6 shows the evolution of the nuclide composition of plutonium and uranium isotopes as a function of the burn-up. The production of the isotopes further up in the neutron capture chain is time-dependent. A sufficient amount of the parent nuclides must be produced before the next reaction in the chain can occur.

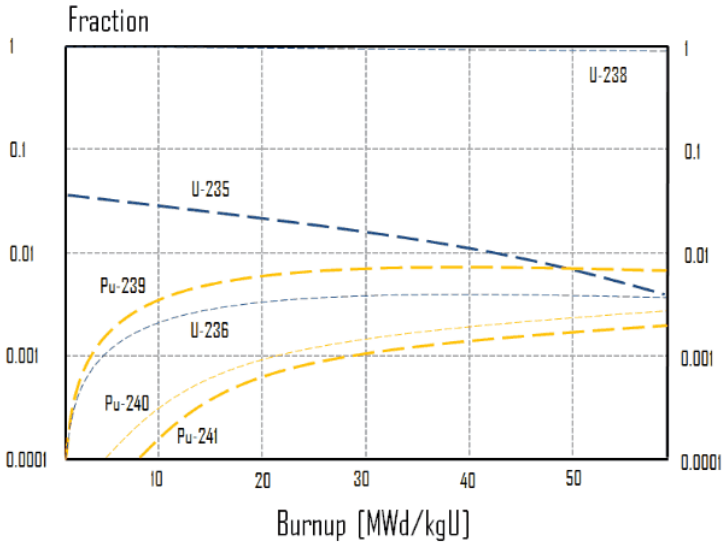

Figure 6: Evolution of nuclide composition of actinides as a function of fuel burn-up [20]

2.5 Experimental spent fuel characterization

Samples of spent fuel are characterized in a laboratory. The nuclide composition is determined both with destructive and non-destructive analysis. Destructive analysis is composed of several stages: (1) dissolution of fuel samples, (2) radiochemical analysis of components, (3) determination of nuclide composition of the element, (4) estimation of mass fraction of the element and their isotopes, and (5) evaluation of the burn-up [21]. This is also known as radiochemical analysis. Non-destructive analysis is based on the measurement of neutron and gamma emission from the fuel. This is performed without damaging the fuel assembly and takes place at the storage location [22].

With the experimental assessment of the nuclide composition of the spent fuel, comes the determination of the burn-up. This value is calculated based on the concentration of the burn-up indicators (nuclides produced through fission) and are thus, in direct proportion to the burn-up of the fuel. A good burn-up indicator must have a low cross section for neutron capture and be insensitive to other irradiation parameters such as fuel composition, power density, and cooling time [23]. The ^{148}Nd isotope is a well-known burn-up indicator. It is a stable nuclide, so the cooling time has no influence, and it is produced through neutron-induced fission, which is the dominant production path, or decay of short-lived fission products (the β^--decay chain starting from ^{148}Xe until ^{148}Nd is reached). Additionally, ^{148}Nd is also produced through neutron capture of ^{147}Nd. Fresh fuel does not contain ^{148}Nd and ^{148}Nd does not physically relocate in the fuel once it is present. Moreover, the fission yield is nearly independent of the neutron energy and the fuel type [24]. Other nuclides that can be used as a burn-up indicator are ^{137}Cs [25],^{134}Cs [26], and the total number of ^{139}La and ^{244}Cm [25].

2.6 Fuel depletion simulations

2.6.1 ALEPH2

Among existing fuel depletion codes, the Belgian Nuclear Research Centre (SCK CEN) has developed its own Monte Carlo burn-up code, ALEPH2, since 2004 [27]. This code is an interface between Monte Carlo N-Particle Transport (MCNP) [28] and a depletion solver, i.e., a routine that solves the Bateman

equations. MCNP is a general-purpose transport code that is used by ALEPH2 to calculate particle spectra in materials needed to generate one-group averaged cross sections. The code is ideal to solve heterogeneous reactors and/or lattices/assemblies containing burnable poison [29]. It permits exact modeling of all geometrical details without any spatial or energy homogenization of neutron cross section [29], [30]. Steady-state calculations of neutron fluxes and spectra are executed, followed by solving the system for first-order ordinary differential equations with constant coefficients for a given time step using the reaction rates calculated from these fluxes and spectra [31].

A depletion solver is a routine that solves the Bateman equations, which are used to characterize the evolution in time of materials during irradiation [32]. In the first version of ALEPH, ALEPH-1, ORIGEN 2.2 [33] was used as a depletion solver [31]. At that time, it was only possible to treat a limited number of reactions, namely radiative capture, fission, (n,2n), (n,3n), (n,p), and (n,α) [31], [34]. In the second version of ALEPH, ALEPH2, the depletion solver is changed to RADAU5 and on-the-fly generated one group cross sections were used to calculate the neutron spectrum [34].

Unlike other burn-up codes, ALEPH2 contains some important features such as a full consistency of cross section data [34], the ability of reaching/matching the predetermined concentrations of nuclides, the ability to reflect in a single run the time evolution of many parameters [35], and the ability to calculate the accumulation of spallation products in Accelerator Driven Systems (ADS) [27]. During the initialization, ALEPH2 also performs crosscheck of the MCNP/X part of the input file for consistency. If possible, it tries to correct the user when the provided description is not complete enough to run the ALEPH calculations [31].

Figure 7 shows the typical calculation flow within ALEPH2. First, the input file is processed, which contains an MCNP/X part before additional ALEPH2 specific commands [31]. After this processing, ALEPH2 generates a new MCNP/X input file based upon the input and starts the MCNP/X calculation with the multi-particle cross section data from the chosen library. The particle spectra for the considered irradiation zones are then used to calculate the reaction rates, which are then passed on to the built-in depletion solver, and the concentrations at the end of the time step are obtained. During this part of the calculation flow, two assumptions are made: the fluxes and spectra are independent in space and time in the given region of phase space and at the given time step [31]. After the depletion calculations, the new material compositions are stored. Then, the choice can be made to either apply a predictor-corrector method or not. This feature was added to the second version of ALEPH2 by changing the depletion solver from ORIGEN 2.2 to one based on RADAU5. Enabling the predictor-corrector algorithm allows to change the neutron flux and spectrum changes within an irradiation step. The fluxes and spectra are calculated at the beginning of the time step, after which the concentrations are obtained in the middle of the time step to recalculate the fluxes and spectra. Otherwise, it is recommended to take small irradiation steps to keep these parameters nearly constant. Keeping in mind that increasing the number of irradiation steps results in a longer simulation time, since after each step, amongst others, the nuclide composition in each material is calculated, which increases the complexity of the simulation. Therefore, a healthy balance must be found between the need for detail (an accurate spectrum) and the complexity of the simulation (and thus a longer simulation time).

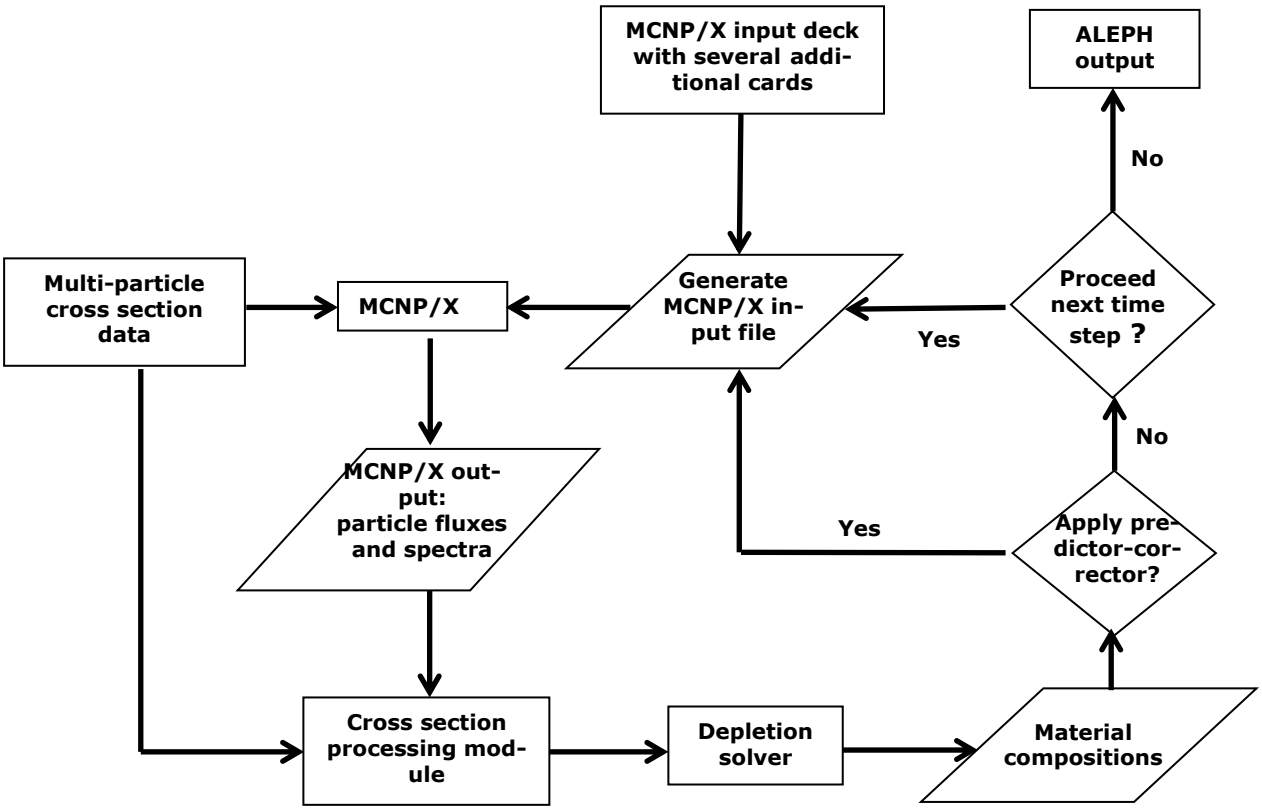

Figure 7: Calculation flow inside ALEPH2 [31]

2.6.2 SFCOMPO-2.0

Spent Fuel Isotopic Composition (SFCOMPO) [11], developed by the Organisation for Economic Co-operation and Development's (OECD) Nuclear Energy Agency (NEA), is a relational database of measured nuclide concentrations of SNF of reviewed experimental datasets [5]. It is well documented, including the open-source bibliographical references wherefrom the data was retrieved. Operating information and design specifications are also included [5]. The most relevant parameters for this validation (discussed in §1.3) are included in the database; the boron concentration, coolant pressure and temperature, rod and assembly dimensions, initial (and when mentioned in the official report, final) nuclide concentration of the fuel, sample burn-up, and the density and temperature of the different components (cladding, moderator, and fuel). These properties all influence the final nuclide composition of the sample, which is related to the burn-up of the sample and thus, also the properties of SNF [36]. The assessment of the final nuclide composition of the sample is performed by destructive radiochemical analysis [5].

The Japan Atomic Energy Research Institute (JAERI) was the first to initiate an open compilation of SNF experimental measurements in 1993 [5], [36], [37]. This compilation consisted already of existing nuclide composition data of SNF obtained from the open literature of post-irradiation experiments [11], which resulted in the creation of the first version of SFCOMPO. The SNF database underwent several improvements over the years, among which, a conversion into HyperText Markup Language (HTML) format for hosting on a website and a move to the NEA web server in 2001 [5], [11]. In 2012, an early prototype was developed to expand and modernize the database structure [5].

The current version of SFCOMPO, SFCOMPO-2.0, is a relational H2-SQL database and is accessible through an open Java application [5], [38]. SFCOMPO-2.0 can freely be accessed without any charge

and downloaded from the internet. The user can rapidly search the database and find the information needed for a specific application [5]. All measured data are shown in the same way as mentioned in the reference reports, including the units [11]. For example, dimensions and heights can be found in both millimeters and inches. This fits the philosophy of SFCOMPO: to preserve the original information provided by the primary sources [11].

All information is stored in the database according to a hierarchical system, beginning with the reactor type. Eight different types can be found: Advanced Gas-cooled Reactor (AGR), Boiling Water Reactor (BWR), CANada Deuterium Uranium (CANDU), Magnox, PWR, RBMK, VVER-1000, and VVER-440. For each specific reactor, a distinction is made out of which assembly and specific rod, the samples were taken. Figure 8 shows an overview of the hierarchic system that is used in SFCOMPO-2.0.

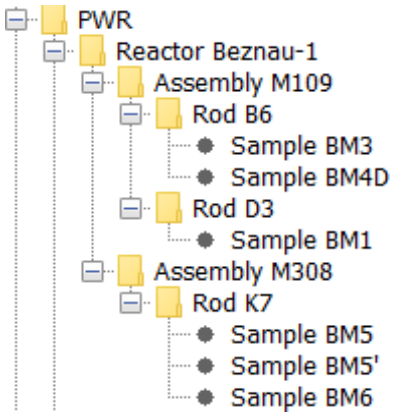

Figure 8: Hierarchic overview within SFCOMPO [5]

12 different BWR's are listed in the database, including 31 assemblies and 93 rods [5]. The estimated burn-up varies from 2.185 GWd/tHMi in the Japan Power Demonstration Reactor-1 (assembly A-20, rod C3, sample KC-1333-660) up to 86.42 GWd/tHMi in the reactor Fukushima-Daini-1 (assembly 2F1ZN3, rod C3, sample UM). (Figure 9)

The 16 PWR's in SFCOMPO-2.0 include measurements out of 43 assemblies, from a total of 95 rods. The estimated burn-up is distributed over a range between 3.399 GWd/tHMi, measured in the Trino Vercellese-1 reactor (assembly 509-104, rod A12, sample 1) and 75 GWd/tHMi in the Vandellos-2 reactor (assembly EC45 and EF05, rod WZtR165, sample WZtR165-2a). (Figure 9)

In most cases, the place in the rod wherefrom the sample was taken was recorded. This was written either as the position from the end plug or as the position from the bottom of the fuel stack. For the Turkey Point-3 reactor, in assembly D01 and D04, calculations of the estimated burn-up in the complete rod, besides one sample, were also made.

The irradiation history is always mentioned in SFCOMPO, except for the Tsuruga-1 reactor, where no operation history is given. The irradiation time is the sum of all the days the reactor was in operation. The time between irradiation periods is also given. This is important to determine the final nuclide composition. For BWR's the irradiation varies between 239 and 2784 days and for PWR's this varies between 215 and 1970 days. (Figure 9)

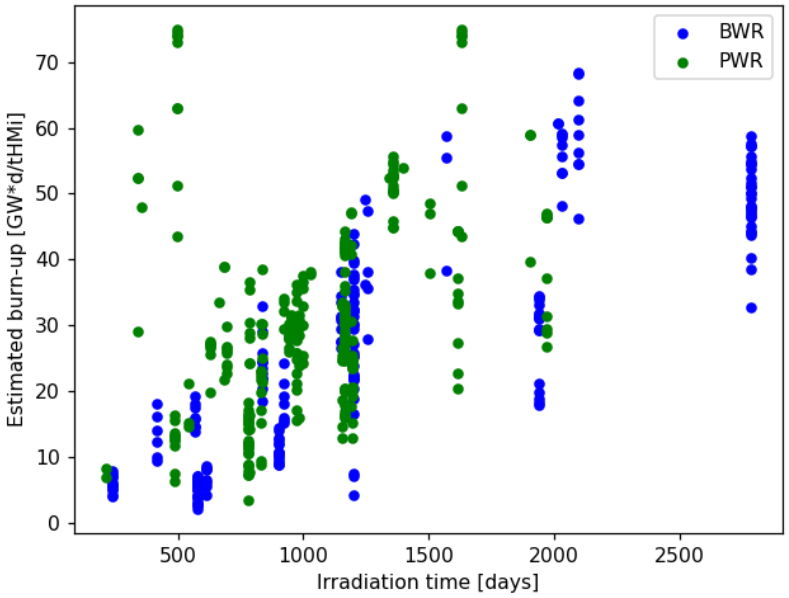

Figure 9: Data assessment SFCOMPO burn-up distribution as function of irradiation time

3 Description of cases

Different simulations were made per case. First, a simple model was made, with the information provided in the SFCOMPO database (i.e., the geometry of the assembly, the material composition, and the irradiation history). The missing information was completed with the information in the official reports of the cases. The modeling assumptions in the simple model are based on assumptions made with SCALE system during their modeling of that particular case. SCALE is a modular code system for performing Standarized Computer Analyses for Licensing Evaluation. It utilizes well-established computer codes and methods within standard analysis sequences [39].

Then, cases were refined based on the previously obtained results for improvement, keeping in mind that with modeling assumptions, uncertainties are expected. For example, time steps can be divided in such a way that they do not contribute more than 1 GWd/tHMi to the sample burn-up since in each irradiation step the neutron flux is assumed to be constant, which in reality it is not. With minimizing modeling assumptions, the complexity of the simulation increases, which is not always outweighed by the improvement in the results.

One of the most challenging parts of modeling reactor fuel is modeling MOX fuel since all the plutonium isotopes are unstable. Depending on the moment of the characterization of the fuel, the nuclide composition at the beginning of the irradiation is different. Knowing exactly when the characterization took place will allow for an accurate simulation. This cooling period is simulated beforehand to simulate a starting nuclide composition as close as possible to the real one. When these needs cannot be met and information is missing (i.e., starting nuclide composition or cooling time before irradiation), the results contain a large bias.

3.1 Case 1: Gösgen-1 GU1

3.1.1 Simple model Gösgen-1 GU1

The first simulated case was sample GU1 of the Gösgen-1 reactor in the assembly 1240, situated in rod 14H13 (or M13 in coordinates used in the initial report [40]). The assembly consists of 205 fuel rods (UO_2 initially enriched with 3.5 wt% ^{235}U) and 20 guide tubes, arranged in a 15x15 lattice (Figure 10). The 33 mm sample was taken 960.5 mm from the end plug. It was irradiated for four consecutive cycles, from cycle 12 up to and including cycle 15. The estimated burn-up of the sample is 59.66 GWd/tHMi.

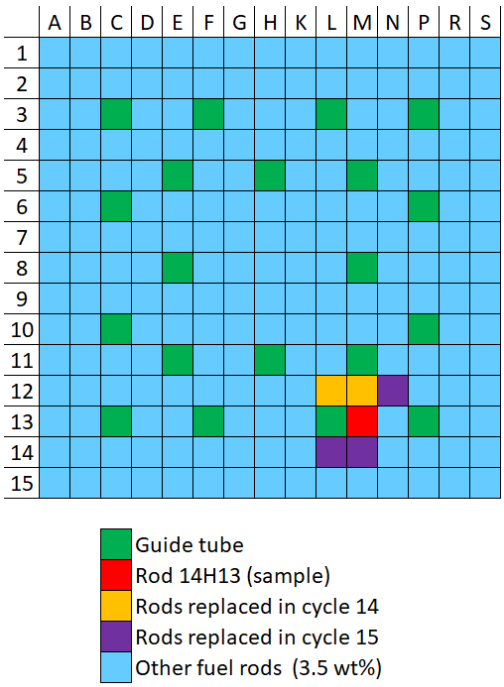

Figure 10: Overview of assembly 1240 at the end of cycle 15

Before the start of cycles 14 and 15, modifications were made in the fuel rod configuration of the assembly. First, before the start of cycle 14, the 3 rods at positions L12, M12, and N12 were replaced with rods that were irradiated elsewhere, with a burn-up of 30.25, 30.29, and 42.85 GWd/tHMi, respectively [40]. Before the start of irradiation cycle 15, once again 3 rods were replaced with rods that were irradiated elsewhere, L14, M14, and N12 with a burn-up of 51.78, 41.64, and 53.81 GWd/tHMi respectively [40].

For every replaced rod, the initial burn-up was compared with the burn-up of the newly introduced rod. An alteration in burn-up, and thus the nuclide composition, has an impact on the local neutron flux distribution and the occurring physics. No information was provided about the burn-up of the to-be-replaced rods at End Of Cycle 13 (EOC-13). Since no information is provided to model this rod replacement, models with the SCALE system contained the assumption that this rod replacement negligible, and therefore, it will also not be included in this model.

In the transition from cycle 14 to cycle 15, the rod replacement was also evaluated. In this case, the burn-up in EOC-14 of the replaced rods is provided in the official report [40], which was 42.70, 42.33, and 54.60 GWd/tHMi for respectively rod L14, M14, and N12. The burn-up of the newly inserted rods was respectively 51.78, 41.64, and 53.81 GWd/tHMi which results in a variation in burn-up of 21.26%, -1.63%, and -1.45%, respectively. Although, the rod shuffle of L14 results in an increase of burn-up of more than 20%, all rod shuffles were neglected. However, this was kept in mind as a possible improvement of the simulation.

For the geometry definition of the assembly, all the dimensions were retrieved from SFCOMPO and can be found in Table 1. Reflective boundary conditions were applied on all outer surfaces of the model. The resulting flat buckling of the neutron flux resulting from these boundary conditions is a good approximation considering the axial position from where the sample was taken (close to the

center of the fuel rod). The rod pitch[2] is 14.3 mm and the assembly pitch 215.6 mm. When calculating the width of the assembly based on the rod pitch, a width of 214.5 mm was obtained. An extra 0.55 mm thick water layer surrounds the assembly. Although the real sample taken from the reactor is only 3.3 cm, the height of the assembly in the simulation was set to 10 cm. The diffusion length of neutrons in water is 2.54 cm, so to make sure that neutrons interact at least a few times with the fuel before being reflected, a height of 10 cm was taken. A quasi-2D geometry was obtained since the height of the modeled assembly is much smaller than the height of the real-live assembly. The initial fuel nuclide composition of the assembly was also retrieved from SFCOMPO, from which the mass percentage for all the nuclides in the fuel was calculated (Table 2). The sample was located next to a guide tube. This is known to affect the neutron flux distribution because no fissions occur in this area (and thus, no neutrons are produced). The homogeneity in the neutron flux distribution is affected. Therefore, the fuel rods next to the sample (north, south, and east) were modeled as different materials but with the same nuclide composition as the rest of the fuel. This ensures that the nuclide composition of these rods is not averaged out by the other rods in the assembly.

Table 1: Main core data Gösgen-1 GU1

General information	
Type of reactor	PWR
Nominal thermal power	3002 MW
Pressure primary system	153 kg/cm²
Coolant inlet temperature	292.0°C
Coolant average temperature	309.0°C
Coolant outlet temperature	326.0°C
Number of assemblies	177
Number of rods per assembly	205
Lattice type	15x15
Rod pitch	14.3 mm
Assembly pitch	215.6 mm
Number of guide tubes	20
Fuel rod	
Fuel material	UO_2
Fuel density	10.4 g/cm³
Cladding	Zr-4
Pellet diameter	9.11 mm
Cladding inner diameter	9.30 mm
Cladding outer diameter	10.75 mm
Active fuel length	3400 mm
Guide tube	
Inner diameter	12.4 mm
Outer diameter	13.8 mm
Material	Zr-4

[2] Distance between the center of two adjacent rods

Table 2: Nuclide composition used for modeling sample GU1 in Gösgen-1

Nuclide	Mass percent [wt%]
UO_2 initially enriched with 3.5 wt% ^{235}U	
^{16}O	11.9
^{234}U	0.032
^{235}U	3.09
^{238}U	85

For a correct simulation, the temperature of the sample and moderator had to be determined (§1.3). Both quantities were monitored during the irradiation cycles, provided in the official report [40] and shown in Table 3. The temperature of the sample varied between 709 K[3] and 1171 K, with an average of 919.6 K. The temperature of the moderator varied between 279.6 °C and 309.9 °C, with an average of 305.81 °C. The cross section data, used in the simulations, is only available for temperatures rounded up to a hundred (in kelvin). For the fuel, the nuclear data files were used for a temperature of 900 K while for the moderator they were used for 600 K. The temperature of the cladding is not available and thus the nuclear data files were also used for 600 K, same as the moderator. ALEPH2 allows changing the temperature over the irradiation steps but this was not applied in the model because the average temperature is expected to balance the Doppler effect (§1.3). However, when the results from the calculations still have big discrepancies, this could be a second improvement to include in the simulation.

[3] Values have the same units as mentioned in SFCOMPO

Table 3: Irradiation history Gösgen-1 GU1

Elapsed time for every cycle [d]	Sample burn-up [MWd/tHMi]	Sample power [MW]	Boron concentration [ppm]	Moderator temperature [°C]	Sample tempera-ture [K]
Cycle 12 (Begin date: 06.07.1990 – End date: 01.06.1991)					
0	0	0	1511	307.6	1151.3
6	354	0.003326	1179	308.1	1171.5
150	9195	0.003677	565	308	1136
294.9	17454	0.003422	8	308.3	1078.3
317	18649	0.003132	8	298.6	1046.7
Cycle 13 (Begin date: 03.07.1991 – End date: 30.05.1992)					
0	18649	0	1477	306.9	919.3
6	18899	0.00249	1145	307.3	967.7
150	25572	0.002644	542	307.1	957.9
292.3	3262	0.002935	7	307.5	943.1
321.3	33594	0.002744	7	294.4	842
Cycle 14 (Begin date: 15.06.1992 – End date: 05.06.1993)					
0	33594	0	1517	308.2	888.9
6	33789	0.001942	1178	308.7	894.4
150	39879	0.002527	549	308.6	854.8
290.1	45757	0.002507	5	308.9	841.4
331.3	47911	0.003124	5	289.5	709.8
Cycle 15 (Begin date: 01.07.1993 – End date: 04.06.1994)					
0	47911	0	1594	309.4	806.6
6	40121	0.002091	1243	309.8	829.8
150	53506	0.002234	605	309.6	810.6
301.9	58842	0.002099	5	309.9	804
326.7	59656	0.001961	5	279.6	738

ENDF/B-VII.1 [41] nuclear data library was used to initially compare the simulation results with the results obtained using the SCALE system since they also used this nuclear data library. To achieve a certain burn-up level in the fuel, the fuel pins have to be irradiated. This way, the nuclide composition is provided in the output between the different irradiation steps. To simulate the changing boron concentration in the moderator, the nuclide composition in the moderator also needed to be modeled. This affects the neutron flux distribution, thus also how the fuel composition changes. The effect on the reactivity of burning the cladding is negligible since it has barely an impact on the neutron flux distribution. The only reason for burning the cladding is to be able to examine the nuclide composition since only then the evolution of the nuclide composition will be included in the output file. It is important to create a representative image of reality, but on the other hand, assumptions have to be made to simplify the model and to have an acceptable number of discrepancies.

There are two sets of experimental results available in the official report. The first set contains the experimental measurements obtained on the analysis date (AD). The second set contains measurements recalculated to the day of discharge (DOD) of the SNF. The measurement uncertainties are only

provided for the results obtained on the AD, except for a limited number of nuclides (^{95}Mo, ^{99}Tc, ^{101}Ru, ^{106}Ru, ^{103}Rh, ^{109}Ag, and ^{125}Sb). These measurement uncertainties are only provided for the recalculated results to the DOD.

The irradiation history was also retrieved from SFCOMPO together with the boron concentration and the burn-up from the sample at the measured times (Table 3). The power in the sample was derived from the sample burn-up (Table 3).

Since the experimental burn-up is calculated through the ^{148}Nd concentration and the burn-up in ALEPH2 through the irradiation history, it is necessary to achieve the same ^{148}Nd concentration to ensure the sample was sufficiently irradiated. When this concentration was achieved, the irradiation of the assembly was interrupted. As already mentioned in §2.4, ^{148}Nd is a suitable burn-up indicator due to the fission yield being independent of the neutron energy and the fuel type, the stability of the nuclide, and low cross section for further reactions. If during simulations the concentration matches the predetermined ^{148}Nd concentration within the uncertainty, the simulation is terminated. The experimentally determined concentration is reported in [40] and thus, also in SFCOMPO, and is 7.24 x 10^{-4} g^{148}Nd/g^{238}U. The ALEPH2 input file of the best simple model is included in Appendix B as an example.

3.1.2 Optimization Gösgen-1 GU1

As a first optimization, the previous calculation was repeated with ENDF VIII.0 [42] and JEFF 3.3 [43] nuclear data libraries. Since these contain updated nuclear data, it is expected that the results should slightly improve.

Because the sample is situated next to a guide tube, the neutron flux next to the guide tube may deviate from the neutron flux in the rest of the assembly, and the physics within the sample may not be represented correctly. To counteract this, as an optimization, the sample will also be divided into smaller pieces, in half along the z-axis and as smaller annular zones (formed by circles on each third on the radius of the fuel rod) into each other. This would provide a better and thus, more accurate neutron flux distribution within the sample since the different zones have a different neutron flux distribution and this would not be averaged out over the whole sample. The irradiation history is averaged over the whole sample, as well as the nuclide composition. Since the provided irradiation history does not ensure a sufficient sample burn-up, the irradiation history was extended until the concentration of ^{148}Nd matches the experimentally determined measurement (within the experimental uncertainty).

3.2 Case 2: Vandellos-2 WZtR165-2a

3.2.1 Simple model Vandellos-2 WZtR165-2a

The second case simulated was the sample WZtR165-2a taken from the Vandellos-2 reactor in rod WZtR165. This rod was irradiated in two different assemblies: EC45 (cycle 7 – cycle 10) and EF05 (cycle 11). The black arrows show the position switch of the rods before cycle 11 (Figure 11). Both assemblies consisted of 264 fuel rods, 24 guide tubes, and 1 instrumental tube, arranged in a 17x17 square lattice. The 2 mm sample was taken 1060 mm from the bottom of the fuel stack. The estimated burn-up of the sample is 75 GWd/tHMi.

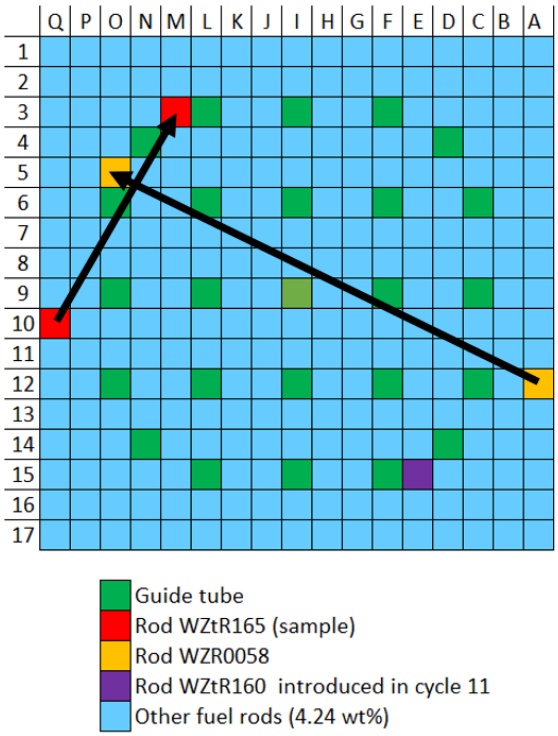

Figure 11: Overview of rod replacement before cycle 11

The fuel placed in assembly EC45 is UO_2 fuel enriched with 4.498 wt% ^{235}U. After the irradiation in cycle 7 up and including cycle 10, both rod WZR0058 and rod WZtR165 were taken from the assembly and placed into assembly EF05. An additional rod was taken from a separate assembly (EC46) and placed in assembly EF05 (Figure 11). Because the placement of this additional pre-irradiated rod (WZtR160) is relatively far from the two rods, the effect on the neutron flux was expected to be minimal, even though the rod burn-up is almost twice the burn-up of the rest of the assembly. Therefore, this rod was modeled with the same nuclide composition as the fuel introduced in assembly EF05, keeping in mind that modeling this rod can serve as a possible improvement of the model if large deviations between the experimentally determined and simulated nuclide compositions are obtained. In addition to both rods from assembly EC45, assembly EF05 was filled with UO_2 fuel initially enriched with 4.24 wt% ^{235}U and with an estimated burn-up of 26.5 GWd/tHMi at Begin Of Cycle 11 (BOC-11).

For the geometry definition of the assembly, all the dimensions were retrieved from SFCOMPO and can be found in Table 4. The rod pitch is 12.6 mm and the assembly pitch 215.04 mm. When calculating the width of the assembly based on the rod pitch, a width of 214.2 mm was obtained. Since the assembly pitch is 215.04 mm, an extra 0.42 mm thick water layer surrounds the assembly, the difference of the assembly pitch and 17 times the rod pitch divided over the two sides. Reflective boundary conditions were applied to all outer surfaces of the model. A sample height of 10 cm was chosen, which resulted in a quasi-2D geometry, same as in the first case (§3.1.1). The initial fuel nuclide composition of the sample was also retrieved from SFCOMPO, from which the mass percentage for all the nuclides in the fuel was calculated (Table 5). First, assembly EC45 was simulated (cycle 7 - 10). The final nuclide composition of both rods (WZtR165 and WZR0058) was then copied as initial composition to assembly EF05 (cycle 11), which was hereinafter simulated. The nuclide composition of the remaining fuel rods of assembly EF05 at BOC-11 was simulated through a simple model, starting from the nuclide composition provided in Table 5.

Table 4: Main core data Vandellos-2

General information	
Type of reactor	PWR
Nominal thermal power	2940.6 (Cycles 7-10) - 3070 (Cycle 11) MW
Pressure primary system	158.191 kg/cm²
Coolant inlet temperature	565 K
Coolant outlet temperature	601 K
Number of assemblies	157
Lattice type	17x17
Rod pitch	12.6 mm
Assembly pitch	215.04 mm
Number of fuel rods	264
Number of guide tubes	24 + 1 instrumental tube
Fuel rod	
Fuel material	UO_2
Fuel density	10.47 g/cm³
Fuel temperature	928 K
Cladding	Zirlo, MDA
Pellet diameter	8.191 mm
Cladding inner diameter	8.356 mm
Cladding outer diameter	9.5 mm
Active fuel length	3657.6
Guide tube / instrumental tube	
Inner diameter	11.25 mm
Outer diameter	12.05 mm
Material	Zirlo, MDA

Table 5: Nuclide composition used for modeling sample WZtR165-2a in Vandellos-2

Nuclide	Mass percent [wt%]
UO_2 initially enriched with 4.5 wt% ^{235}U	
^{16}O	11.85
^{234}U	0.036
^{235}U	3.97
^{236}U	0.0026
^{238}U	84.1
UO_2 initially enriched with 4.24 wt% ^{235}U	
^{16}O	11.9s
^{235}U	3.74
^{238}U	84.4

An important assumption in this model is not modeling the reshuffling of the core after each irradiation cycle. Some discrepancies in the results were expected due to the peripheral placement of the sample

in the assemblies and the applied reflective boundary conditions that did not match the real physics of the case. However, no further information about the irradiation history and the nuclide composition of the adjacent assemblies was provided.

A correct simulation of the temperature is crucial in order to simulate the right number of fissions (§1.3). The fuel temperature is only mentioned once in the official report, 928 K (Table 4). The moderator temperature is mentioned at the end of each cycle (Table 6). For the fuel, the nuclear data files were used for a temperature of 900 K while for the moderator they were used for 600 K. The temperature of the cladding is not available and thus the nuclear data files were also used for 600 K, same as in the first case (§3.1.1).

Table 6: Irradiation history Vandellos-2 WZtR165-2a: *EC45 (cycle 7-10) & EF05 (cycle 11)*

Elapsed time for every cycle [d]	Sample power [MW]	Boron concentration [ppm]	Moderator temperature [K]
Cycle 7 (Begin date: 19.06.1994 – End date: 12.06.1995)			
0	0	1320	
60	0.001939	1140	
179	0.001939	684	
298	0.001939	229	
358	0.001939	0	574.3
Cycle 8 (Begin date: 15.07.1995 – End date: 09.06.1996)			
0	0	1200	
55	0.0023261	1018	
165	0.0023261	599	
275	0.0023261	181	
330	0.0023261	0	574.3
Cycle 9 (Begin date: 14.07.1996 – End date: 25.08.1997)			
0	0	1300	
34	0.0022030	1241	
102	0.0022030	1009	
170	0.0022030	776	
238	0.0022030	543	
306	0.0022030	310	
374	0.0022030	78	
407	0.0022030	0	574.3
Cycle 10 (Begin date: 25.09.1997 – End date: 14.03.1999)			
0	0	1920	
44	0.00066079	1774	
133	0.00066079	1449	
222	0.00066079	1124	
311	0.00066079	799	
401	0.00066079	474	
490	0.00066079	149	
535	0.00066079	0	569.3
Cycle 11 (Begin date: 03.05.1999 – End date: 10.09.2000)			
0	0	1800	
41	0.0020166	1650	
124	0.0020166	1350	
206	0.0020166	1050	
289	0.0020166	750	
372	0.0020166	450	
455	0.0020166	150	
496	0.0020166	0	573.2

As in Case 1, the ENDF/B-VII.1 [41] nuclear data library was used. The irradiation was simulated for all fuel pins and for the moderator (with boron). This is already discussed in §3.1.1. The experimental results, used for the comparison, were only provided for the AD. The power for each irradiation step was calculated for the simulation code. The sample power, provided in SFCOMPO, was used to calculate the sample burn-up per irradiation cycle, which was divided over the irradiation steps, assuming the burn-up evolved linear in time. From this sample burn-up per irradiation step, the power in that step was calculated. The intervals for the irradiation steps are the same as the moments where the boron concentration was provided. (Table 6).

Since the 95% uncertainty on the experimentally determined ^{148}Nd and ^{137}Cs concentration is very high (4.05% and 6.51%), there is no benefit in reaching/matching the concentration of the burn-up indicators with the experimentally determined concentration. The provided irradiation history is used. The concentration of these burn-up indicators must be checked, together with the concentration of the fissile isotopes and the sample burn-up provided in the output file. By evaluating and weighing these three aspects, it is possible to evaluate to what extend the fuel has been irradiated and measures can be taken to irradiate the fuel to a good level. This can be lengthening or shortening the irradiation history in a way that these three parameters are within acceptable ranges.

3.2.2 Optimization Vandellos-2 WZtR165-2a

The assemblies were moved through the core after each irradiation cycle. The WZtR165-2a sample followed the blue path (Figure 12), as assembly EC45 starting with cycle 7 in M4, cycle 8 in D12, cycle 9 in F10, and cycle 10 in H15 and as assembly EF05 during cycle 11 in H11. The official report provides additional information on burn-up at the BOC and initial enrichment of the east and west adjacent assemblies during the reshuffling, but only for cycle 7 till cycle 10 (Table 7). The first simulation took place without taking the reshuffling into account. As optimization of the model, this reshuffling was implemented in a second model. However, no further information about the irradiation history and the nuclide composition of the adjacent assemblies was provided. Before adding these assemblies to the model, they were irradiated separately in advance. This was done through a simple model. The nuclide composition was added into the simulation code that corresponded to that specific cycle. In addition, the irradiation cycles that contributed more than 1 GWd/tHMi to the sample, were subdivided into smaller steps to counteract this.

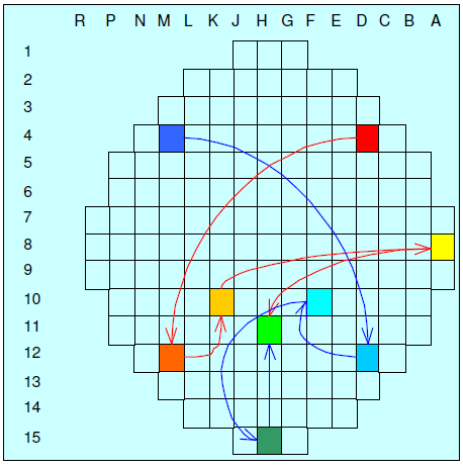

Figure 12: Reshuffling assemblies through reactor core [26]

Table 7: Data of assemblies adjacent to EC45

	East of EC45		West of EC45	
Cycle	Enrichment [wt% ^{235}U]	BOC burn-up [GWd/tHMi]	Enrichment [wt% ^{235}U]	BOC burn-up [GWd/tHMi]
7	3.60	22.125	3.60	32.204
8	3.60	31.333	3.60	14.032
9	4.23	0	3.60	13.648
10	3.60	34.678	3.60	34.678

3.3 Case 3: Gösgen-1 GU3

3.3.1 Simple model Gösgen-1 GU3

The third case simulated was the sample GU3 taken from the Gösgen-1 reactor in rod 16B05. This rod is irradiated in two consecutive assemblies: 1601 (cycle 16 – cycle 17) and 1701 (cycle 18). The black arrow shows the rod repositioning of the sample between the two assemblies (Figure 13). Both assemblies consisted of 205 fuel rods and 20 guide tubes, arranged in a 15x15 square lattice. The 50 mm sample was taken 1224.2 mm from the end plug. The estimated burn-up of the sample is 52.5 GWd/tHMi.

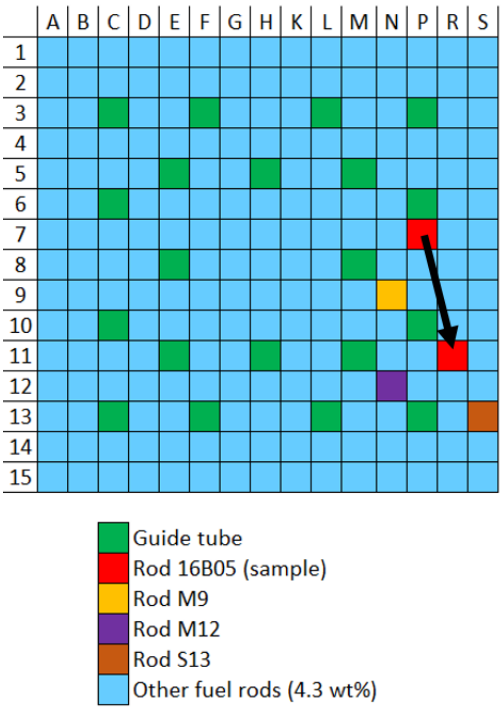

Figure 13: Overview of rod replacement before cycle 18

Starting as non-irradiated UO_2 fuel (enriched with 4.1 wt%), assembly 1601 was irradiated for two consecutive cycles (cycle 16 and cycle 17). Together with three other rods (M9, M12, and S13), rod 16B05 was retrieved from the assembly after the irradiation and placed in assembly 1701, filled with depleted UO_2 fuel (initially enriched with 4.3 wt% ^{235}U and 20 GWd/tHMi burn-up). Rod 16B05 (sample)

was moved from P7 into position R11. The three other rods (M9, M12, and S13) were placed in the same position as in assembly 1601.

For the geometry definition of the assembly, all the dimensions were retrieved from SFCOMPO and can be found in Table 8. The rod pitch is 14.3 mm and the assembly pitch 215.6 mm. When calculating the width of the assembly based on the rod pitch, a width of 214.5 mm was obtained. An extra 0.55 mm thick water layer surrounds the assembly. Reflective boundary conditions were applied to all outer surfaces of the model. A sample height of 10 cm was chosen, which resulted in a quasi-2D geometry, same as in the first case (§3.1.1). Both assemblies were simulated separately and the nuclide composition of the four relocated rods was copied between the assemblies. The initial fuel nuclide composition was retrieved from SFCOMPO, from which the mass percentage for all the nuclides in the fuel was calculated (Table 9). The material composition of assembly 1701 at BOC-18 was retrieved from [44] and is presented in Table 10.

Table 8: Main core data Gösgen-1 GU3

General information	
Type of reactor	PWR
Nominal thermal power	3002 MW
Pressure primary system	153 kg/cm²
Coolant inlet temperature	292.0°C
Coolant average temperature	309.0°C
Coolant outlet temperature	326.0°C
Number of assemblies	177
Number of rods per assembly	205
Lattice type	15x15
Rod pitch	14.3 mm
Assembly pitch	215.6 mm
Number of guide tubes	20
Fuel rod	
Fuel material	UO_2
Fuel density	10.4 g/cm³
Cladding	Zr-4
Pellet diameter	9.11 mm
Cladding inner diameter	9.30 mm
Cladding outer diameter	10.75 mm
Active fuel length	3400 mm
Guide tube	
Inner diameter	12.4 mm
Outer diameter	13.8 mm
Material	Zr-4

Table 9: Nuclide composition used for modeling sample GU3 in Gösgen-1

Nuclide	Mass percent [wt%]
UO_2 initially enriched with 4.1 wt% ^{235}U	
^{16}O	11.9
^{234}U	0.0037
^{235}U	3.62
^{238}U	84.5

Table 10: Nuclide composition from fuel in assembly 1701

Nuclide	Atom density [atoms/barn cm]
Depleted fuel of 1701 fuel assembly (4.3 wt% ^{235}U and 20 GWd/tHMi)	
^{16}O	4.64387×10^{-2}
^{83}Kr	2.12697×10^{-6}
^{95}Mo	1.86090×10^{-5}
^{97}Mo	2.81624×10^{-5}
^{99}Tc	2.83842×10^{-5}
^{101}Ru	2.57791×10^{-5}
^{103}Rh	1.31574×10^{-5}
^{105}Pd	9.06319×10^{-6}
^{105}Rh	6.99709×10^{-8}
^{109}Ag	1.52633×10^{-6}
^{113}Cd	4.32513×10^{-9}
^{131}Xe	1.21680×10^{-5}
^{133}Cs	2.97603×10^{-5}
^{134}Cs	1.87642×10^{-6}
^{135}Cs	8.15147×10^{-6}
^{135}Xe	1.11704×10^{-8}
^{139}La	3.00937×10^{-5}
^{141}Pr	2.40582×10^{-5}
^{143}Nd	2.26147×10^{-5}
^{145}Nd	1.73142×10^{-5}
^{147}Pm	6.64546×10^{-6}
^{147}Sm	9.09277×10^{-7}
^{148m}Pm	3.91359×10^{-8}
^{149}Sm	1.00802×10^{-7}
^{150}Sm	6.06198×10^{-6}
^{151}Sm	4.33435×10^{-7}
^{152}Sm	2.59933×10^{-6}
^{153}Eu	1.86747×10^{-6}
^{154}Eu	2.58602×10^{-7}
^{155}Eu	1.08952×10^{-7}
^{157}Gd	2.37812×10^{-9}

Table 10: Nuclide composition from fuel in assembly 1701 (continued)

Nuclide	Atom density [atoms/barn cm]
Depleted fuel of 1701 fuel assembly (4.3 wt% ^{235}U and 20 GWd/tHMi)	
^{235}U	5.62272 x 10^{-4}
^{236}U	8.08732 x 10^{-5}
^{237}Np	4.55531 x 10^{-6}
^{238}Pu	6.75976 x 10^{-7}
^{238}U	2.19114 x 10^{-2}
^{239}Np	2.36188 x 10^{-6}
^{239}Pu	1.07298 x 10^{-4}
^{240}Pu	2.59970 x 10^{-5}
^{241}Am	1.71209 x 10^{-7}
^{241}Pu	1.38650 x 10^{-5}
^{242}Pu	2.09731 x 10^{-6}

For a correct simulation, the temperature of the sample and moderator has to be determined (§1.3). Both quantities were monitored during the irradiation cycles, provided in the official report [40], and copied to Table 11. The determination of the fuel temperature occurs for both assemblies separately. In assembly 1601 (cycle 16 - 17), the fuel temperature varied between 865.4 K and 1244.1 K, with an average of 1083 K. In assembly 1701, the fuel temperature varied between 944.7 K and 794.9 K, with an average of 879.56 K. In both assemblies, the average moderator temperature was respectively 306.66 °C and 306.34 °C. For the fuel, the nuclear data files were used for a temperature of 1100 K and 900 K respectively for both assemblies while for the moderator these were used for 600 K for the same reason as discussed in §3.1.1. The temperature of the cladding is not available and thus the nuclear data files were also used for 600 K. ALEPH2 allows changing the temperature over the irradiation steps. No use was made of this feature because the range of the temperature is less than 400 K and 200 K respectively and the expected impact is minimal.

Table 11: Irradiation history Gösgen-1 GU3: 1601 (cycle 16 - 17) & 1701 (cycle 18)

Elapsed time for every cycle [d]	Sample power [MW]	Boron concentra-tion [ppm]	Moderator temperature [°C]	Sample temperature [K]
Cycle 16 (Begin date: 26.06.1994 - End date: 10.06.1995)				
0	0	1705	308.7	1203.1
6	0.0038744	1347	308.7	1244.1
15.2	0.003976	1305		
30.3	0.0039509	1278		
45.55	0.0039204	1209		
60.9	0.0038893	1138		
76.4	0.0038576	1068		
92	0.003826	997		
107.75	0.0037943	925		
123.65	0.0037619	852		
139.65	0.0037298	779		
150	0.0037029	690	308.7	1194.6
155.8	0.0036885	667		
172.05	0.0036736	601		
188.4	0.0036515	535		
204.85	0.0036294	467		
221.4	0.0036073	402		
238.05	0.0035852	335		
254.8	0.0035631	268		
271.65	0.0035404	200		
288.65	0.0035177	131		
305.75	0.0034949	62		
320	0.003474	5	308.7	1154.1
323	0.0034244	5		
336.8	0.003183	5	300.2	1065.2
Cycle 17 (Begin date: 05.07.1995 - End date: 08.06.1996)				
0	0	1601	308.7	1052.5
6	0.0030725	1247	308.7	1068.5
19.2	0.0031346	1179		
38.4	0.0031131	1148		
57.75	0.003088	1048		
77.25	0.0030629	947		
96.9	0.003072	845		
116.75	0.0030115	743		
136.75	0.0029853	639		
150	0.0029637	602	308.7	1005
156.95	0.0039536	574		
177.25	0.0029458	494		
197.6	0.0029351	413		

Table 11: Irradiation history Gösgen-1 GU3: 1601 (cycle 16 - 17) & 1701 (cycle 18) (continued)

Elapsed time for every cycle [d]	Sample power [MW]	Boron concentration [ppm]	Moderator temperature [°C]	Sample temperature [K]
Cycle 17 (Begin date: 05.07.1995 - End date: 08.06.1996)				
218.05	0.0029237	332		
238.6	0.002913	251		
259.2	0.002916	169		
279.9	0.0028902	87		
299.5	0.0028795	9	308.4	978.7
300.65	0.002846	9		
323.55	0.0026698	9		
328.7	0.0024146	9	297.1	865.4
Cycle 18 (Begin date: 30.06.1996 - End date: 07.06.1997)				
0	0	1675	308.7	944.7
6	0.0027719	1300	308.7	933.6
21.9	0.0027158	1213		
44.3	0.0026668	1177		
67.2	0.0026088	1052		
90.65	0.0025491	923		
114.65	0.0024887	792		
139.3	0.002426	657		
150	0.0023806	631	308.7	866.6
164.5	0.0023644	572		
189.85	0.0023567	469		
215.3	0.0023465	366		
240.85	0.0023369	262		
266.55	0.0023268	158		
292.35	0.0023166	53		
301.2	0.00231	17	308.4	858
319	0.0022097	17		
335.24	0.002022	17	297.2	794.9

As in Case 1, the ENDF/B-VII.1 [41] nuclear data library was used. The irradiation was simulated for all fuel pins and for the moderator (with boron). This is already discussed in §3.1.1. The irradiation power was retrieved from [44] (Table 11). The boron concentration was retrieved from SFCOMPO. More refined irradiation intervals (steps with a contribution to the sample burn-up less than 1 GWd/tHMi) are used for the irradiation of the sample. In previous cases, this was seen as an optimization, but due to time restriction, this was already integrated into the simple model. To be able to adjust the boron concentration for each irradiation step, the boron concentration was assumed to decrease linearly in time. This is presented in Table 11.

This model was first simulated with the given irradiation history and then, another simulation was performed normalizing to the experimentally determined ^{148}Nd concentration. The reason for this normalization has already been discussed in §3.1.1. The uncertainty on the experimental result was 2.74%,

which is sufficiently small. For this reason, both models are simulated and compared. The predetermined ^{148}Nd concentration is mentioned in the report [40] and thus, also SFCOMPO, and is 6.05 x 10^{-4} g^{148}Nd/g^{238}U.

3.3.2 Optimization Gösgen-1 GU3

The sample was placed in the periphery of the assembly 1701. Due to this placement and the applied reflective boundary conditions, it is possible that the real physics were not represented correctly into this simple model. Since no information about the adjacent assemblies was provided, it was not possible to model these. The implemented alternative consisted of modeling the two outer fuel rows as two different materials, different from the fuel pins in the center, but with the same nuclide composition. This ensured that the flux distribution and nuclide composition within these outer rows were better represented, together with the applied physics within these volumes.

3.3.3 Influence of different nuclear data libraries

In this section, the influence of using different nuclear data libraries is evaluated. Simulations with three additional nuclear data libraries were executed with the same model as the best simple model of §3.3.1: ENDF/B-VIII.0 [42], JEFF3.3 [43], and JENDL4.0 [45]. Since the calculation of the experimental burn-up was based on the experimentally determined ^{148}Nd concentration using a version of the ENDF library, only the model with the ENDF/B-VIII.0 library was normalized to the ^{148}Nd concentration. For the simulation with the other two libraries, this normalization was not applied since nuclear data is different between nuclear data libraries, which already has a different effect on the final nuclide composition. The irradiation history and spatial arrangement were kept the same for all the different models.

When using the JENDL4.0 nuclear data library, no nuclear data files were available for the defined temperatures in the simple model (600 K and 1100K). Instead, the temperature of the moderator was deemed to be 500 K and the fuel temperature 1000 K. The neutron absorption cross section varies with the temperature (§1.3) and therefore a small differences in the results are expected [8]. Additionally, the neutron cross section of ^{17}O is not available in this library, which results in an error when using the same model as the other libraries. At first, the error was suspected to be caused by the changing boron concentration. Therefore, the averaged boron concentration was modeled in the material card of the moderator. This material composition is retrieved from [44] for the three different cycles, which are simulated with different inputs and each time the material composition of the fuel copied too the input of the next cycle. Afterward, the actual problem was found to be the absence of the nuclear data of ^{17}O. An additional model was modeled with the changing/detailed boron concentration. The difference between the averaged and detailed boron concentration is also discussed.

3.4 Case 4: Beznau-1 BM5

The fourth case simulated was the sample BM5 irradiated in the Beznau-1 reactor in rod K7. This rod was irradiated in assembly M308 for six consecutive cycles (cycle 20 - 25, Figure 14). The assembly consisted of 179 fuel rods, 16 guide tubes, and 1 instrumental tube, arranged in a 14x14 square lattice. The 72 mm sample was taken 894 mm from the end plug. The estimated burn-up of the sample is 58.9 GWd/tHMi.

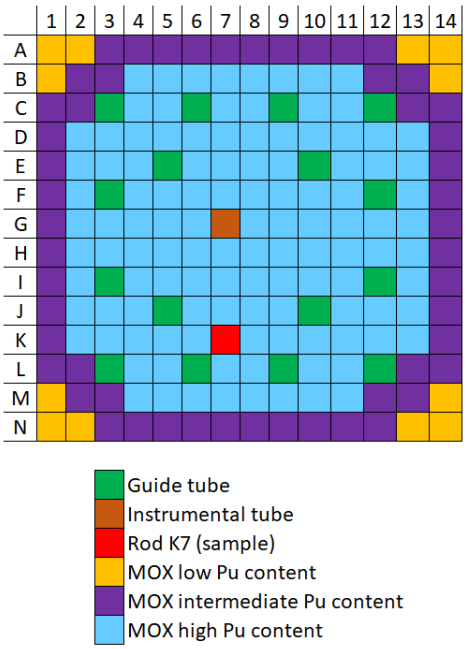

Figure 14: Overview of assembly M308

In the official report [40], only the initial nuclide composition of the rod from where the sample was retrieved was given. This composition was used to calculate the mass percent of each nuclide in the fuel. This nuclide composition was measured in March 1990. The insertion of the fuel rod in the reactor core did not happen until July 1990. Therefore, a decay period of 4 months (122 days) was modeled. In the ARIANE program [40], a second assembly of the Beznau-1 reactor was examined, assembly M109. This assembly had the same configuration as assembly M308 and the examined rod was MOX fuel with high Pu content (0.231 wt% ^{235}U - 6.011 wt% Pu). The nuclide composition of all fuel rods was given for May 1988, i.e., two years before irradiation in another assembly of this reactor, irradiated prior to this assembly. It was assumed that the same fuel was used in assembly M308. Therefore, a decay period of 791 days was also modeled before introducing the MOX fuel in the assembly. For the MOX rods with low and intermediate Pu content, only the concentration (Pu+Am)/(U+Pu+Am) were given, which was respectively 3.36 wt% and 4.28 wt% in assembly M109. Because no further information was available, the proportion between the Pu isotopes and ^{241}Am was kept the same as for the MOX fuel with high Pu content. The fuel nuclide composition was calculated for May 1988 and a decay period of 791 days was simulated before introducing the nuclide composition in the simulation. Because these are all assumptions, the above-described decay periods of the unknown fuel are additionally simulated at 122 days of decay. The impurity in the fuel was simulated by introducing boron in its natural composition in the fuel rods: 1.153 ppm in the sample rod and 0.529 ppm in the other fuel rods [46]. Table 13 shows the initial nuclide composition used for the different types of fuel used in assembly M308. In consequence of the good representation obtained with the modeling of the previous cases, it may be possible to provide an estimation of the cooling time of the other rods in the assembly before being introduced in the reactor core, since the neutron flux distribution is different for both models (122 and 791 days cooling time).

For the geometry definition of the assembly, all the dimensions were retrieved from SFCOMPO and can be found in Table 12. The rod pitch is 14.12 mm and the assembly pitch 198.2 mm. Reflective

boundary conditions were applied to all outer surfaces of the model. A sample height of 10 cm was chosen, which resulted in a quasi-2D geometry, same as in the first case (§3.1.1).

Table 12: Main core data Beznau-1

General information	
Type of reactor	PWR
Nominal thermal power	1130 MW
Pressure primary system	158.2 kg/cm²
Coolant inlet temperature	283.8°C
Coolant average temperature	300.9°C
Coolant outlet temperature	316.9°C
Number of assemblies	121
Number of rods per assembly	179
Lattice type	14x14
Rod pitch	14.12 mm
Assembly pitch	198.2 mm
Number of guide tubes	16
Number of instrumental tubes	1
Fuel rod	
Fuel material	MOX
Fuel density	10.38 g/cm³
Cladding	Zr-4
Pellet diameter	9.292 mm
Cladding inner diameter	9.48 mm
Cladding outer diameter	10.72 mm
Active fuel length	3023 mm
Guide tube	
Inner diameter	9.48 mm
Outer diameter	10.72 mm
Material	Zr-4

Table 13: Nuclide composition used for modeling sample BM5 in Beznau-1

Nuclide	Mass percent [wt%]
MOX (0.231 wt% ^{235}U - 5.5 wt% Pu)	
^{10}B	1.70×10^{-6}
^{11}B	7.52×10^{-6}
^{16}O	11.8
^{234}U	1.67×10^{-3}
^{235}U	1.92×10^{-4}
^{238}U	81.3
^{238}Pu	0.0295
^{239}Pu	3.23
^{240}Pu	1.13
^{241}Pu	0.321
^{242}Pu	0.129
^{241}Am	0.0448
MOX (0.231 wt% ^{235}U - 6.011 wt% Pu)	
^{10}B	7.79×10^{-7}
^{11}B	3.45×10^{-6}
^{16}O	11.8
^{234}U	0.00164
^{235}U	0.195
^{236}U	8.21×10^{-4}
^{238}U	82
^{238}Pu	0.0603
^{239}Pu	3.71
^{240}Pu	1.41
^{241}Pu	0.513
^{242}Pu	0.235
^{241}Am	0.0634
MOX (0.237 wt% ^{235}U - 4.28 wt% Pu)	
^{10}B	7.79×10^{-7}
^{11}B	3.45×10^{-6}
^{16}O	11.8
^{234}U	0.00168
^{235}U	0.199
^{236}U	8.39×10^{-4}
^{238}U	83.7
^{238}Pu	0.0429
^{239}Pu	2.64
^{240}Pu	1.01
^{241}Pu	0.378
^{242}Pu	0.167
^{241}Am	0.0452

Table 13: Nuclide composition used for modeling sample BM5 in Beznau-1 (continued)

Nuclide	Mass percent [wt%]
MOX (0.237 wt% ^{235}U - 3.36 wt% Pu)	
^{10}B	7.79×10^{-7}
^{11}B	3.45×10^{-6}
^{16}O	11.8
^{234}U	0.00170
^{235}U	0.201
^{236}U	8.48×10^{-4}
^{238}U	84.6
^{238}Pu	0.0337
^{239}Pu	2.07
^{240}Pu	0.791
^{241}Pu	0.297
^{242}Pu	0.131
^{241}Am	0.0354

For a correct simulation, the temperature of the fuel and of the moderator have to be determined (§1.3). Both quantities were monitored during the irradiation cycles, provided in the official report [40], and copied to Table 14. The temperature of the sample varied between 399 °C and 1004 °C. The temperature of the moderator varied between 285 °C and 296 °C, with an average of 291.2 °C. For the moderator, the nuclear data files were used for a temperature of 600 K, for the same reason as discussed in §3.1.1. The temperature of the cladding is not available and therefore, the nuclear data files were also used for a temperature of 600 K. ALEPH2 allows changing the fuel temperature over the irradiation steps, which was applied in this model since the sample temperature varies. To model these temperature changes, the nuclear data files were used for every hundred temperatures starting from 700 K up to 1300 K for the fuel.

Table 14: Irradiation history Beznau-1 (cycle 20 - 25)

Elapsed time for every cycle [d]	Sample burn-up [MWd/tHMi]	Power [MW]	Boron concentration [ppm]	Moderator temperature [°C]	Sample temperature [°C]
Cycle 20 (Begin date: 02.07.1990 - End date: 09.05.1991)					
1	7	0.000434	1099	286	429
2.5	30	0.000952	944	288	525
4.5	77	0.001458	822	291	722
5.5	110	0.002048	712	294	848
6.5	126	0.000993	933	288	533
34	1015.75	0.002008	560	294	845
61.5	1905.5	0.002008	543	291	717
89	2795.25	0.002008	526	291	717
116.5	3685	0.002008	509	291	717

Table 14: Irradiation history Beznau-1 (cycle 20 - 25) (continued)

Elapsed time for every cycle [d]	Sample burn-up [MWd/tHMi]	Power [MW]	Boron concentration [ppm]	Moderator temperature [°C]	Sample temperature [°C]
Cycle 20 (Begin date: 02.07.1990 - End date: 09.05.1991)					
117	3697	0.001489	492	291	717
142.33	4513.33	0.001997	286	294	843
167.67	5327.67	0.001997	329	294	843
193	6143	0.001997	372	294	843
193.5	6150	0.000869	415	288	519
216.5	6869	0.00194	147	294	830
216.7	6872	0.000931	356	288	519
220.2	6981	0.001933	111	294	830
220.7	6993	0.001489	225	291	691
243.87	7723.33	0.001956	24	295	832
267.03	8453.67	0.001956	46	295	832
290.2	9184	0.001956	68	295	832
307.8	9719	0.001785	90	294	811
Cycle 21 (Begin date: 29.06.1991 - End date: 02.07.1992)					
0.5	9722	0.000372	1400	285	399
2.5	9748	0.000807	1244	287	506
4	9778	0.001241	1114	289	628
5	9804	0.001613	1044	290	741
6	9831	0.001676	1020	290	758
8.5	9899	0.001688	1015	291	758
9	9909	0.001241	1111	289	616
21	10239	0.001707	986	291	760
21.5	10249	0.001241	1072	289	615
47.25	10957	0.001706	889	291	762
73	11665	0.001706	876	291	762
74	11685	0.001241	915	289	609
108.5	12625.75	0.001692	617	291	766
143	13566.5	0.001692	589	291	766
177.5	14507.25	0.001692	562	291	766
212	15448	0.001692	534	291	766
212.2	15452	0.001241	506	289	627
239.87	16201	0.00168	306	291	768
297.53	16950	0.00168	349	291	768
295.2	17699	0.00168	392	291	768
296.2	17712	0.000807	435	287	499
329.2	18613.5	0.001695	102	291	770
362.2	19515	0.001695	102	291	770

Table 14: Irradiation history Beznau-1 (cycle 20 - 25) (continued)

Elapsed time for every cycle [d]	Sample burn-up [MWd/tHMi]	Power [MW]	Boron concentration [ppm]	Moderator temperature [°C]	Sample temperature [°C]
Cycle 22 (Begin date: 02.09.1992 - End date: 01.04.1993)					
0.5	19519	0.000496	1071	285	430
2.5	19547	0.000869	916	288	524
4.5	19593	0.001427	784	290	689
6.5	19650	0.001769	711	292	783
24	20203	0.001961	622	293	826
41.5	20756	0.001961	565	293	826
60.5	21350.5	0.001942	508	293	824
79.5	21945	0.001942	592	293	824
80.5	21960	0.000931	677	288	531
112.8	22928.5	0.001861	258	293	814
145.1	23897	0.001861	258	293	814
177.4	24865.5	0.001861	258	293	814
209.7	25834	0.001861	258	293	814
Cycle 23 (Begin date: 09.07.1993 - End date:17.06.1994)					
8	25988	0.001195	1211	289	597
30.97	26907.67	0.002485	850	295	906
53.93	27827.33	0.002485	882	295	906
76.9	28747	0.002485	915	295	906
79.4	28798	0.001266	947	289	603
83.4	28956	0.002451	718	295	920
88.4	29157	0.002495	702	296	905
90.4	29196	0.00121	914	289	627
110.37	29976.33	0.002425	594	296	930
130.33	30756.67	0.002425	543	296	930
150.3	31537	0.002425	493	296	930
170.27	32320	0.002434	402	296	929
190.23	33103	0.002434	343	296	929
210.2	33886	0.002434	283	296	929
230.17	34650.33	0.002376	224	296	961
250.13	35414.67	0.002376	171	296	961
270.1	36179	0.002376	119	296	961
295.05	37115	0.002328	66	296	1004
320	38051	0.002328	58	296	1004
340	38658	0.001883	50	293	886

Table 14: Irradiation history Beznau-1 (cycle 20 - 25) (continued)

Elapsed time for every cycle [d]	Sample burn-up [MWd/tHMi]	Power [MW]	Boron concentration [ppm]	Moderator temperature [°C]	Sample temperature [°C]
Cycle 24 (Begin date: 01.08.1994 - End date: 30.06.1995)					
6	38747	0.000921	1203	288	563
8	38794	0.001458	1063	290	746
9	38819	0.001551	1044	291	757
37.9	39810.33	0.002129	784	294	940
66.8	40801.67	0.002129	688	294	940
95.7	41793	0.002129	591	294	940
124.57	42788.33	0.00214	495	295	911
153.43	43783.67	0.00214	406	295	911
182.3	44779	0.00214	318	295	911
211.2	45757	0.0021	229	295	892
240.1	46735	0.0021	275	295	892
269	47713	0.0021	320	295	892
270	47728	0.000931	366	288	565
292.4	48451.5	0.002004	38	294	880
314.8	49175	0.002004	20.5	294	880
315.9	49211	0.002031	3	295	886
332.7	49740	0.001954	3	294	875
334.3	49762	0.000853	3	288	559
Cycle 25 (Begin date: 30.07.1995 - End date: 28.06.1996)					
7.8	49861	0.000788	1160	287	541
38.1	50676	0.001669	827	292	799
68.4	51491	0.001669	889	292	799
69.4	51504	0.000807	915	288	553
98.2	52307	0.00173	627	293	815
127	53110	0.00173	535	293	815
155.8	53953	0.001816	442	294	840
184.6	54796	0.001816	452	294	840
185.6	54817	0.001303	462	291	700
212.45	55592	0.001791	272	294	828
239.3	56367	0.001791	353	294	828
240.3	56380	0.000807	434	288	570
273	57318.5	0.001781	102	294	812
305.7	58257	0.001781	55	294	812
306.7	58286	0.0018	8	294	845
327.2	28842	0.001683	20	293	794
328.2	58854	0.000745	246	287	542

As in Case 1, the ENDF/B-VII.1 [41] nuclear data library was used. The irradiation was simulated for all fuel pins and for the moderator (with boron). This is already discussed in §3.1.1. The irradiation history was also retrieved from SFCOMPO together with the boron concentration and the burn-up from the sample at the given intervals (Table 14). This irradiation history was adjusted in a way that the irradiation steps have a maximum burn-up of 1 GWd/tHMi, by simply subdividing the steps with more than 1 GWd/tHMi into smaller steps. The power for each irradiation step was derived from the sample burn-up (Table 14). The fuel and cladding temperature were kept constant over the subdivision of the irradiation steps. The boron concentration is assumed to evolve linearly in time. Through interpolation, the missing boron concentration was calculated to be able to change this concentration in each irradiation step in the models.

With all the modeling assumptions made in the above-described models, the normalization of the concentration of a burn-up tracer to its experimental results will not improve the results. The experimental uncertainty on both burn-up tracers, ^{148}Nd and ^{137}Cs, is too high (respectively 6.65% and 3.05%) for the normalization to ensure correct burn-up normalization of the sample.

3.5 Case 5: Fukushima-Daini-2 sample 1

The fifth case simulated was sample 1 irradiated in the Fukushima-Daini-2 reactor in rod SF98. This rod was irradiated in assembly 2F2DN23 for three consecutive cycles (cycle 5 - 7, Figure 15). The assembly consisted of 62 fuel rods and 2 water rods, arranged in an 8x8-2 square lattice. The 0.5 mm sample was taken 39 mm from the bottom of the fuel stack. The estimated burn-up of the sample is 4.15 GWd/tHMi.

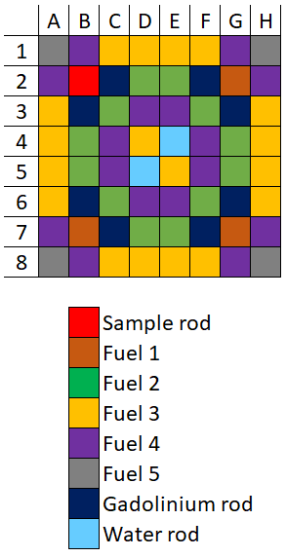

Figure 15: Overview of assembly 2F2DN23

During the irradiation, no known alterations were made to the arrangement of the fuel assembly. For the geometry definition of the assembly, all the dimensions were retrieved from SFCOMPO and can be found in Table 15. The rod pitch is 16.3 mm and the assembly pitch 152 mm. When calculating the width of the assembly based on the rod pitch, a width of 130.4 mm was obtained. Since, the assembly pitch is 152 mm, an extra 10.8 mm thick water layer surrounds the assembly, the difference of the

assembly pitch and 8 times the rod pitch divided over the two sides. Reflective boundary conditions were applied to all outer surfaces of the model. A sample height of 0.5 mm was modeled, the same as the actual sample retrieved from the fuel rod. A 3D model is modeled due to the presence of a reflector, different levels of enrichment along the z-axis, and different void fractions of the moderator along the z-axis. Each fuel rod has the two ends made of non-enriched (natural composition) UO_2. The initial fuel nuclide composition of the different rods was retrieved from SFCOMPO, from which the mass percentage for all the nuclides in the fuel was calculated and reported in Table 16.

Table 15: Main core data Fukushima-Daini-2 sample 1

General information	
Type of reactor	BWR
Nominal thermal power	3293 MW
Coolant pressure	69 bar
Coolant inlet temperature	216.0°C
Coolant outlet temperature	286.0°C
Number of assemblies	764
Lattice type	8x8-2
Rod pitch	16.3 mm
Assembly pitch	152 mm
Number of fuel rods	62
Number of water rods	2
Fuel rod	
Fuel material	UO_2
Fuel density	10.412 g/cm³
Cladding	Zr-2
Pellet diameter	10.3 mm
Cladding inner diameter	10.58 mm
Cladding outer diameter	12.3 mm
Active fuel length	371 mm
Water rod	
Inner diameter	13.5 mm
Outer diameter	15 mm
Material	Zr-2

Table 16: Nuclide composition used for modeling sample 1 in Fukushima-Daini-2

Nuclide	Mass percent [wt%]
UO_2 (non-enriched)	
^{16}O	11.85
^{234}U	1.28×10^{-4}
^{235}U	0.63
^{238}U	87.52
UO_2 initially enriched with 2 wt% ^{235}U (Fuel 1)	
^{16}O	11.85
^{234}U	0.016
^{235}U	1.76
^{238}U	86.37
UO_2 initially enriched with 2.9 wt% ^{235}U (Fuel 2)	
^{16}O	11.85
^{234}U	0.023
^{235}U	2.56
^{238}U	85.56
UO_2 initially enriched with 3.41 wt% ^{235}U (Fuel 3)	
^{16}O	11.86
^{234}U	0.026
^{235}U	3.00
^{238}U	85.12
UO_2 initially enriched with 3.45 wt% ^{235}U (Fuel 4)	
^{16}O	11.86
^{234}U	0.027
^{235}U	3.04
^{238}U	85.08
UO_2 initially enriched with 3.91 wt% ^{235}U (Fuel 5)	
^{16}O	11.86
^{234}U	0.035
^{235}U	3.45
^{238}U	84.66
UO_2-Gd_2O_3 (3.4 wt% ^{235}U - 3.0 wt% Gd)	
^{16}O	11.90
^{154}Gd	0.058
^{155}Gd	0.39
^{156}Gd	0.54
^{157}Gd	0.41
^{158}Gd	0.66
^{160}Gd	0.58
^{234}U	0.026
^{235}U	2.91
^{238}U	82.53

Table 16: Nuclide composition used for modeling sample 1 in Fukushima-Daini-2 (continued)

Nuclide	Mass percent [wt%]
UO_2-Gd_2O_3 (3.4 wt% ^{235}U - 4.5 wt% Gd)	
^{16}O	11.92
^{154}Gd	0.086
^{155}Gd	0.59
^{156}Gd	0.81
^{157}Gd	0.62
^{158}Gd	0.98
^{160}Gd	0.87
^{234}U	0.025
^{235}U	2.86
^{238}U	81.26

For a correct simulation, the temperature of the sample and moderator have to be determined (§1.3). A homogeneous fuel temperature of 900 K was provided in [47]. The input and output temperatures of the moderator are provided in [48] and are respectively 284 °C and 312 °C. The nuclear data files were used for a temperature of 600 K for the moderator and a temperature of 900 K for the nuclear fuel, for the same reason as discussed in §3.1.1. The temperature of the cladding is not available and therefore, the nuclear data files were used for a temperature of 600 K.

As in Case 1, the ENDF/B-VII.1 [41] nuclear data library was used. The irradiation was simulated for all fuel pins and for the moderator (with boron). This is already discussed in §3.1.1. The irradiation history (power to the sample) was retrieved from the official report [48], together with the boron concentration. The history of the boron concentration in each irradiation cycle was given for different time intervals than the time intervals for which the irradiation history was provided. The boron concentration was calculated through interpolation for the same days as the sample power was given (Table 17). The irradiation history was adjusted in a way that the irradiation steps have a maximum burn-up of 1 GWd/tHMi, by simply subdividing the steps with more than 1 GWd/tHMi into smaller steps. Additionally, this model was simulated with a normalization to the final experimentally determined ^{148}Nd concentration. This was calculated from the reported final nuclide composition in the official report [48] and is 4.62 x 10^{-5} $g^{148}Nd/g^{238}U$.

Table 17: Irradiation history Fukushima-Daini-2 (cycle 5 - 7)

Elapsed time for every cycle [d]	Power [MW]	Boron concentration [ppm]
Cycle 5 (Begin date: 14.01.1989 - End date: 08.03.1990)		
6	4.84917×10^{-7}	1154
3	1.22184×10^{-6}	1139
132	1.50821×10^{-6}	1132
21	0	808
5	5.46008×10^{-7}	757
244	1.31347×10^{-6}	754
8	1.52348×10^{-6}	146
Cycle 6 (Begin date: 04.07.1990 - End date: 24.08.1991)		
5	5.46008×10^{-7}	1132
158.5	1.31347×10^{-6}	1121
158.5	1.31347×10^{-6}	764
9	0	408
4	5.68918×10^{-7}	388
72	1.33638×10^{-6}	379
10	1.50821×10^{-6}	217
Cycle 7 (Begin date: 14.11.1991 - End date: 14.11.1992)		
3	6.22373×10^{-7}	1154
182.5	1.39366×10^{-6}	1146
182.5	1.39366×10^{-6}	674

4 Results & Discussion

The results of the depletion analyses are presented in the form of C/E-1 (results from calculations divided by experimental results minus 1) per case, to represent the deviation of the simulation results against the experimental ones. First, the results obtained with the simple model are presented, followed by a more refined model. By using the C/E-1 form, the deviation of the ALEPH2 results from the experimental results is presented. Since C/E-1 results with the SCALE system were available in literature [26], [49]–[51], these results are also presented as a means of comparison. The nuclide composition of samples GU3 (Gösgen-1) and BM5 (Beznau-1) were experimentally examined by two different institutions. GU3 was examined at ITU and SCK CEN and BM5 at PSI and SCK CEN. The official report [40] recommends using the experimental nuclide composition provided by SCK CEN, instead of the other laboratory, for both samples due to nuclide concentration underprediction and uncertainty underprediction in the results provided by the other institutions (ITU and PSI). Samples GU1 (Gösgen-1) and WZtR165-2a (Vandellos-2) were only examined by one lab only, SCK CEN and an independent laboratory, respectively.

4.1 Case 1: Gösgen-1 GU1

4.1.1 Simple model Gösgen-1 GU1

The MCNP geometry of the assembly is presented in Figure 16. Each material is shown in a different color, clearly showing that the adjacent rods to the sample are modeled as a different material (§3.1.1). The experimental results are retrieved from the official report [40], where a sample burn-up of 59.66 GWd/tHMi was reported. In the report, the experimental nuclide composition was provided both on the AD and recalculated to the DOD. Both are used and compared with each other along with the results obtained with the SCALE system. Each simulation was run with the given irradiation history and then, another one normalized to the experimentally determined ^{148}Nd concentration. In these models, the ENDF/B-VII.1 nuclear data library was used. With the model that included the simple irradiation history, a sample burn-up of 59.66 GWd/tHMi was reached. When the normalization to the experimentally determined ^{148}Nd concentration was executed, a sample burn-up of 60.47 GWd/tHMi was reached instead. The model with the SCALE system resulted in a burn-up of 60.7 GWd/tHMi, by using the ENDF/B-V nuclear data library and the TRITON simulation code. The experimentally determined burn-up (based on the ^{148}Nd concentration) was 59.66 GWd/tHMi. The C/E-1 results obtained with the simulation of the four models and the SCALE system of the actinides (Figure 17) are presented separately from the fission products (Figure 18), supplemented with the experimental uncertainty.

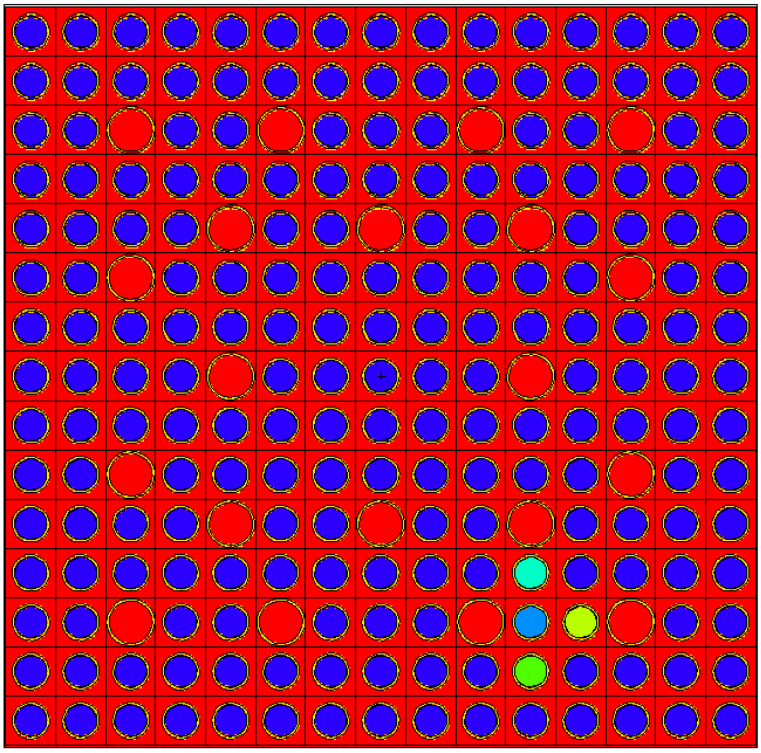

Figure 16: MCNP geometry Gösgen-1 assembly 1240

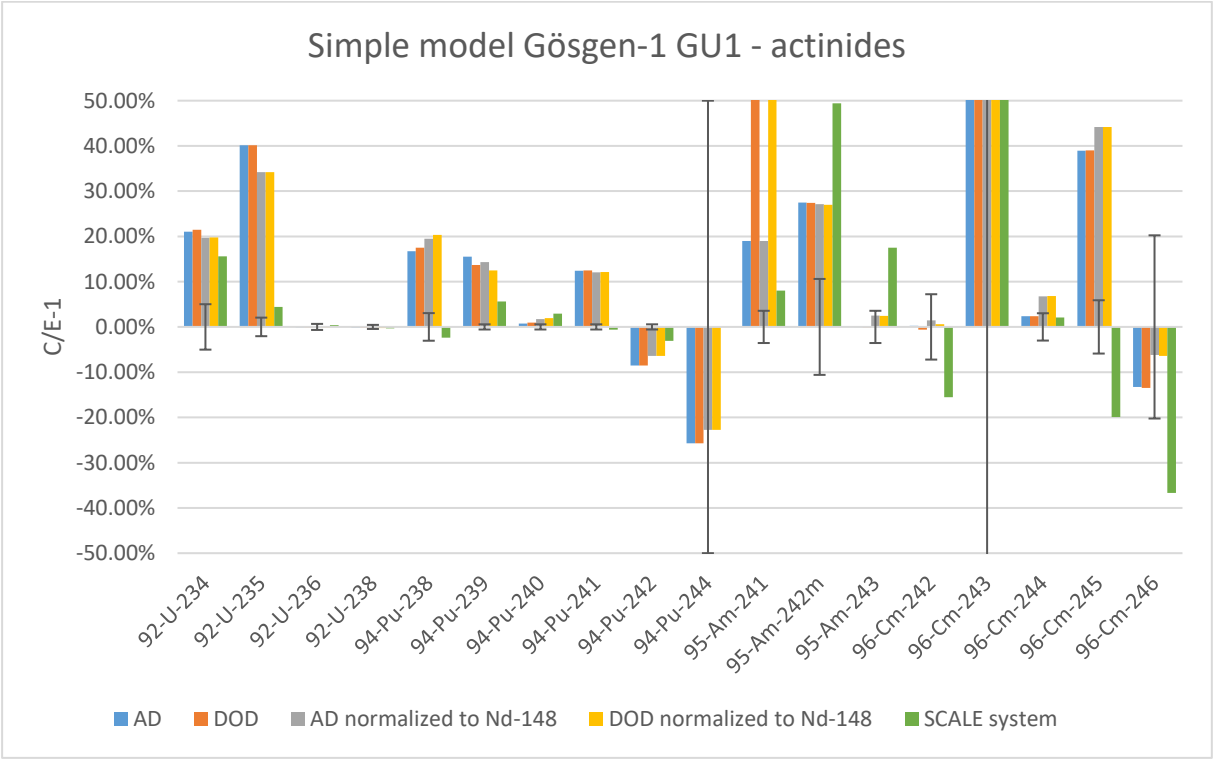

Figure 17: C/E-1 results of the simple model Gösgen-1 GU1 - actinides

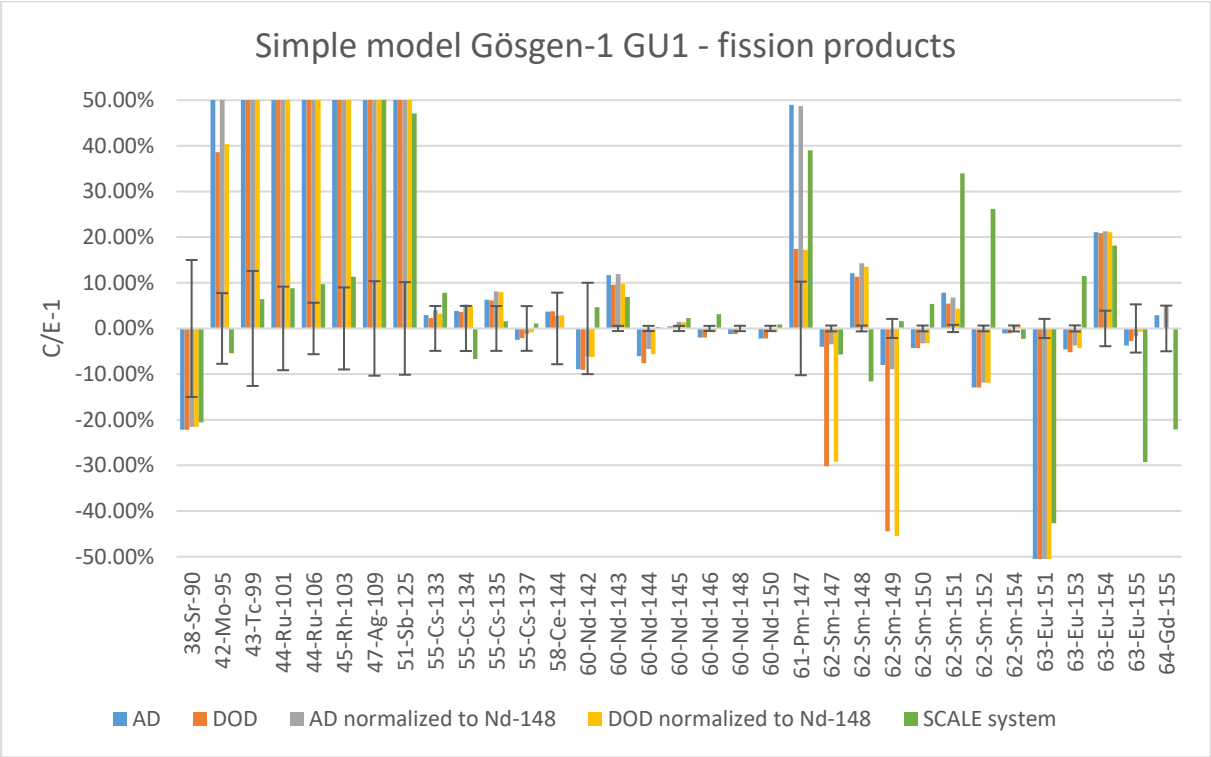

Figure 18: C/E-1 results of the simple model Gösgen-1 GU1 - fission products

In general, the C/E-1 results obtained with the models where a normalization to the experimentally determined ^{148}Nd concentration was applied, deviates less than the results obtained with the provided irradiation history. The normalization to the ^{148}Nd concentration ensures sufficient irradiation of the sample since the concentration of the burn-up indicators is matched to the experimental one. A second notable aspect in the results is that for some nuclides there is a large difference in the C/E-1 results depending on the use of the experimental results obtained on the AD or the ones recalculated to the DOD.

The further discussed results apply to the two models with the normalization to the experimentally determined ^{148}Nd concentration. The concentration of ^{241}Am, a nuclide important for the determination of the decay heat and neutron emission [23], is overestimated with 56% when the results recalculated to the DOD are used as a reference, opposed to a 19% overestimation when the results obtained on the AD where used as a reference. This is also the case for the C/E-1 results of ^{151}Eu. The C/E-1 result when using the experimental results obtained on the AD is underestimated with 55%, opposed to an underestimation of 97% when using the experimental results recalculated to the DOD. When looking at the C/E-1 results of ^{147}Sm, it is only 3% underestimated when using the experimental results obtained on the AD but 30% underestimated when using the results recalculated to the DOD as a reference. What does stand out is the fact that this is the other way around for ^{147}Pm, the predecessor of ^{147}Sm. These C/E-1 results are overestimated with 50% when using the experimental results obtained on the AD and 17% when using the results recalculated to the DOD. Keeping in mind that the experimental uncertainty is 10.25% and the C/E-1 result obtained with the SCALE system was overestimated with 39% relative to the experimental results obtained on the AD, the obtained C/E-1 results are not trustworthy to base important decisions on. The experimental result recalculated to the DOD of ^{155}Gd was even negative, something that is very unlikely and is excluded for further processing of results. Due to recalculations, the experimental results are prone to have larger uncertainties, since they rely

on the use of data from a certain nuclear data library, which is continuously evolving because in time, nuclear characteristics are better understood and thus, more accurate. Preference is given to use the experimental results obtained on the AD as a reference and to include the normalization to the experimentally determined ^{148}Nd concentration in the simulation model. This model, known as "AD normalized to Nd-148" in Figure 17 and Figure 18 and from now seen as the best simple model for this sample, is used for further discussion and is used to analyze whether the optimizations provide better results.

In the best simple model, the ^{235}U concentration is overestimated by almost 35%, which implies that the sample was insufficiently irradiated. On the other hand, the concentration of the burn-up indicators, ^{137}Cs and ^{148}Nd, lie within the experimental uncertainty, which implies that the sample was sufficiently irradiated. This was also the case with previous simulations done with this case at SCK CEN with TRITON simulation software [51]. Here, ^{234}U was overestimated with 22% and ^{235}U with 30%. The other uranium isotopes lie within the 95% uncertainty boundaries, same as the simulation with the best simple model. The concentration of the plutonium isotopes is overestimated by 19.5%, 14.3%, and 12.8% for respectively ^{238}Pu, ^{239}Pu, and ^{241}Pu. The ^{244}Pu nuclide is underestimated with 23%, which seems a lot, but still lies within the 95% experimental uncertainty (50%). Considering the overestimation of the other actinides, two possible situations could have occurred. Either too much ^{235}U and/or ^{238}U was simulated in the input file, or too few fissions have occurred, compared to the actual sample.

The discrepancies in the C/E-1 results of the fission products in the best simple model are on average also overestimated. The cesium and neodymium isotopes lie within the 95% experimental uncertainty boundaries or show acceptable deviation, except for ^{143}Nd. A few fission products have heavily been overestimated: ^{95}Mo (52%), ^{99}Tc (87%), ^{101}Ru (245%), ^{106}Ru (205%), ^{103}Rh (222%), ^{109}Ag (986%), and ^{125}Sb (136%). There is no logical explanation for this. These results should be kept in mind while analyzing the results from the other cases. However, these results are not uncommon since after simulation, Azzaoui et al. [51] reported major discrepancies for these nuclides. This is the same with the large underestimation of the ^{151}Eu concentration (-54.6%) while [51] obtained a C/E-1 result of -97%.

4.1.2 Optimization Gösgen-1 GU1

Two additional modeling approaches were explored to optimize previous calculations, i.e., dividing the sample into two halves and three annular zones in each other. The MCNP geometry is shown per geometry respectively in Figure 19 and Figure 20, showing the different materials modeled in different colors. The results after optimization are compared to the C/E-1 results of the best simple model, a model normalized to the experimentally determined ^{148}Nd concentration and with the experimental results given obtained on the AD as reference. Therefore, the optimized results are only compared to the experimental results obtained on the AD. The C/E-1 results obtained with these simulations and the best simple model of the actinides are presented in Figure 21 and the fission products in Figure 22, supplemented with the experimental uncertainty. After simulation of the model with the sample divided into two halves, a burn-up of 60.47 GWd/tHMi was reached, whereas the sample burn-up after simulation of the model with the annular zones was 62.1 GWd/tHMi.

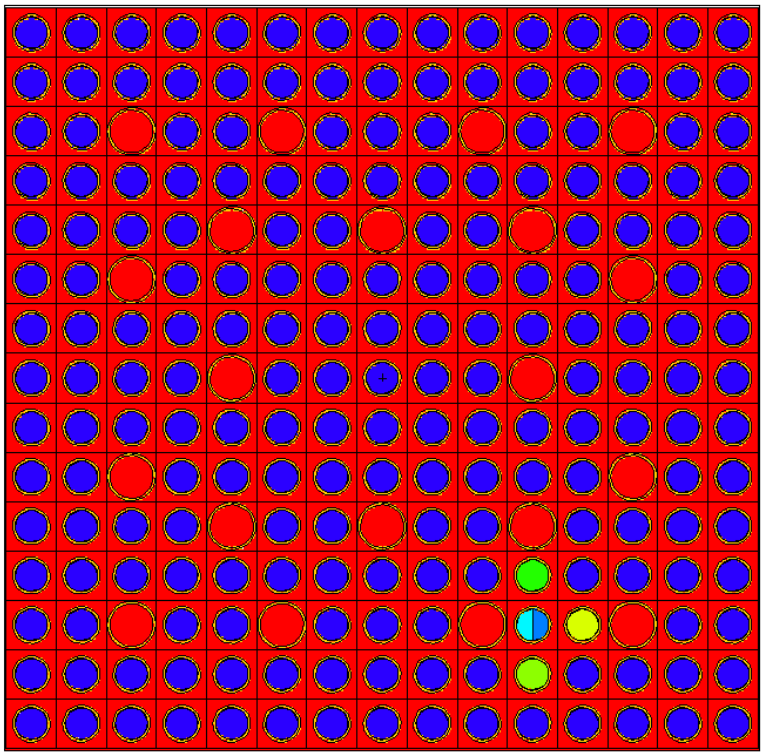

Figure 19: MCNP geometry Gösgen-1 assembly 1240 - halves

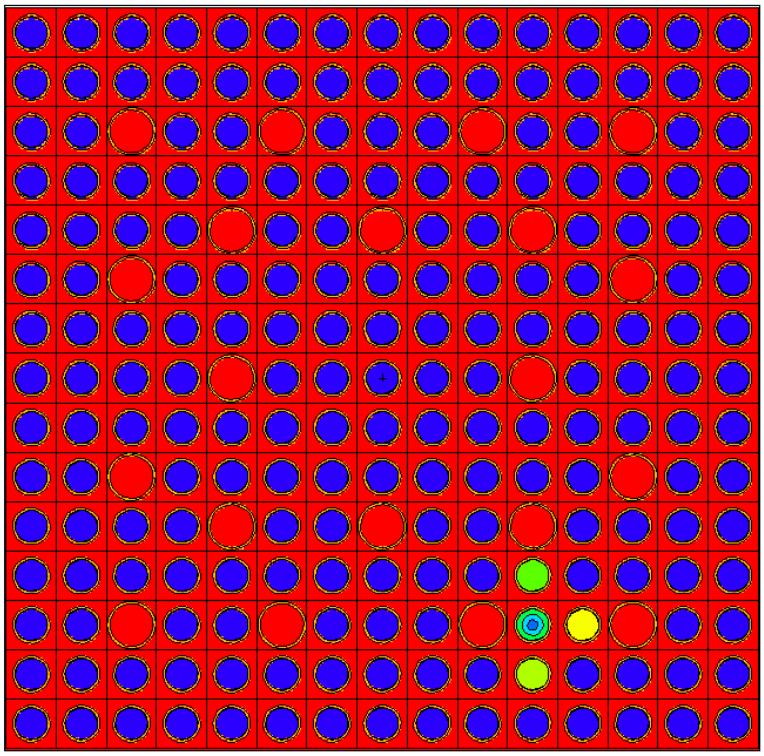

Figure 20: MCNP geometry Gösgen-1 assembly 1240 - annular zones

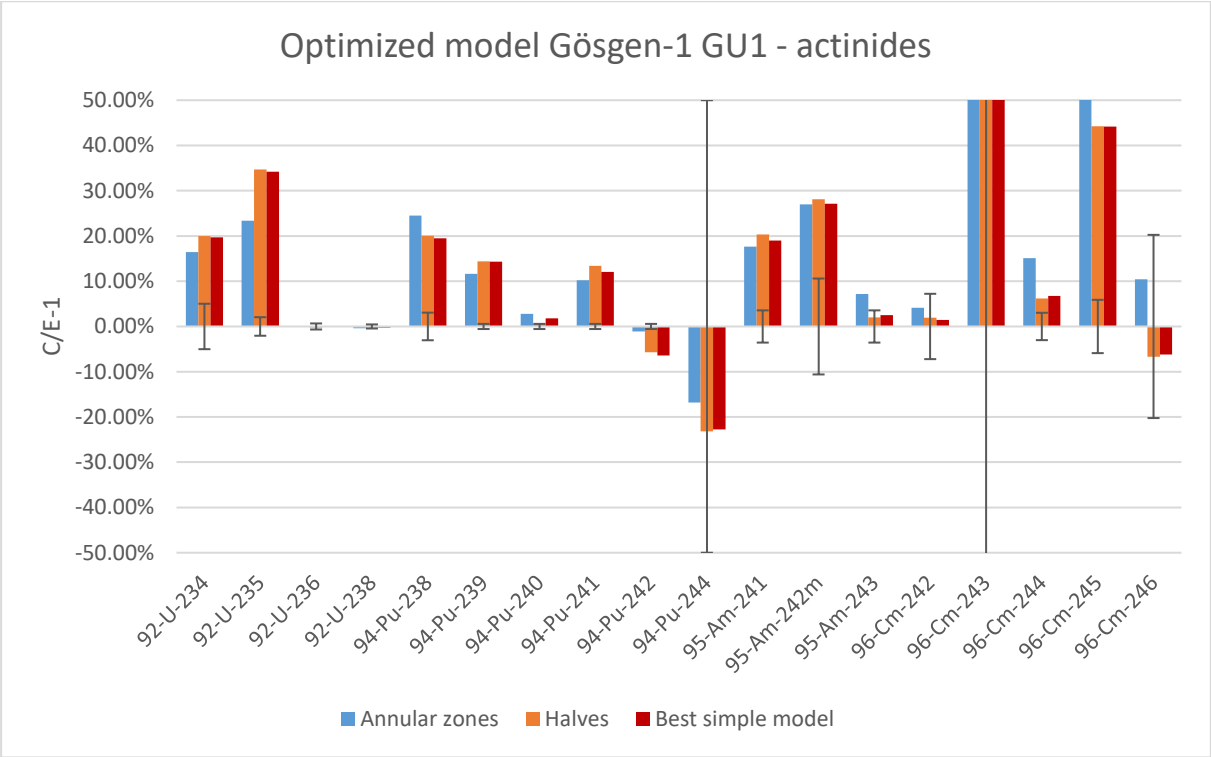

Figure 21: C/E-1 results of the optimized model Gösgen-1 GU1 - actinides

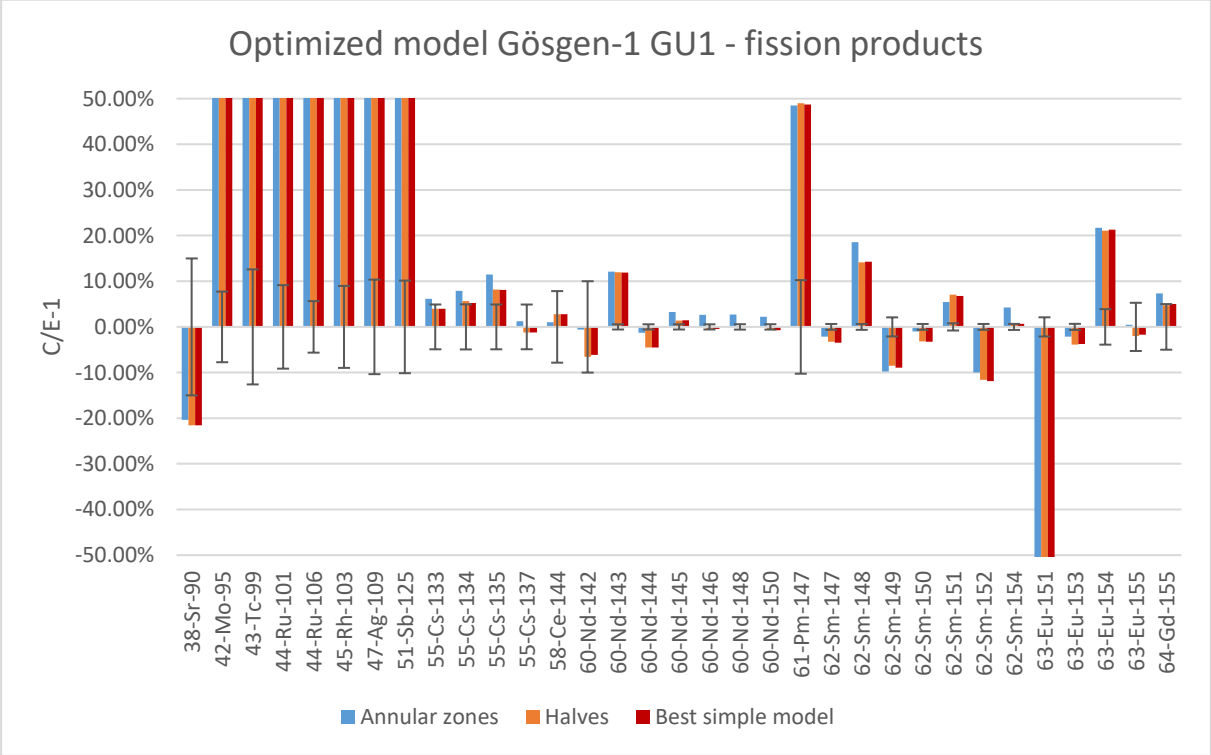

Figure 22: C/E-1 results of the optimized model Gösgen-1 GU1- fission products

The C/E-1 results after the optimization of halving the sample are the same as the best simple model from §4.1.1. There is no visible improvement in the results. The additional work required for this slightly more complex model does not show better results.

The model with the sample divided into three annular zones shows contradictory results. The C/E-1 result of ^{235}U decreased by almost 10% and ^{239}Pu with almost 3%. On the other hand, the C/E-1 result of ^{238}Pu, a nuclide important for the determination of the decay heat and neutron emission [23], rose with almost 5%. The same goes for ^{245}Cm, where the C/E-1 rose with more than 10% after the optimization by implementing a division of the fuel sample into annular zones. The C/E-1 results of the other nuclides remain within the same order of magnitude after the optimization. The severely overestimated fission products (best simple model, §4.1.1) are even more overestimated after this optimization. The C/E-1 results of these fission products are presented for both models (simple model and optimized with annular zones) in Table 18. The simulation of a model considering the rod reshuffling in cycle 14 and 15 has already been proven redundant [52] and will not be explored as an alternative optimization. The considered C/E-1 deviations of the fission products are also found in recent research [52], using ENDF/B-VII.1 and ENDF/B-VIII.0 nuclear data libraries. The obtained results are consistent with Refs. [51], [52].

Table 18: Overestimated fission products Gösgen-1 GU1

Nuclide	Best simple model	Optimized model (annular zones)	Experimental uncertainty
42-Mo-95	52.25%	55.48%	7.74%
43-Tc-99	86.53%	90.59%	12.60%
44-Ru-101	245.08%	253.94%	9.15%
44-Ru-106	205.07%	208.16%	5.64%
45-Rh-103	221.61%	225.16%	8.98%
47-Ag-109	986.02%	1024.67%	10.35%
51-Sb-125	136.12%	139.55%	10.14%

4.2 Case 2: Vandellos-2 WZtR165-2a

4.2.1 Simple model Vandellos-2 WZtR165-2a

The experimental results for the comparison with the results from the simulation were retrieved from the official report providing the sample information [53]. The MCNP geometry is shown for each assembly separately, assembly EC45 in Figure 23 and assembly EF05 in Figure 24. The experimental sample burn-up was 75 GWd/tHMi. The C/E-1 results obtained with the simulation and the SCALE system of the actinides are presented in Figure 25 and the fission products in Figure 26, supplemented with the experimental uncertainty. After the simulation, a burn-up of 76.32 GWd/tHMi was achieved. The simulated results from the SCALE system were obtained by using the ENDF/B-V library and the TRITON simulation code, after which a sample burn-up up of 76.32 GWd/tHMi was reached.

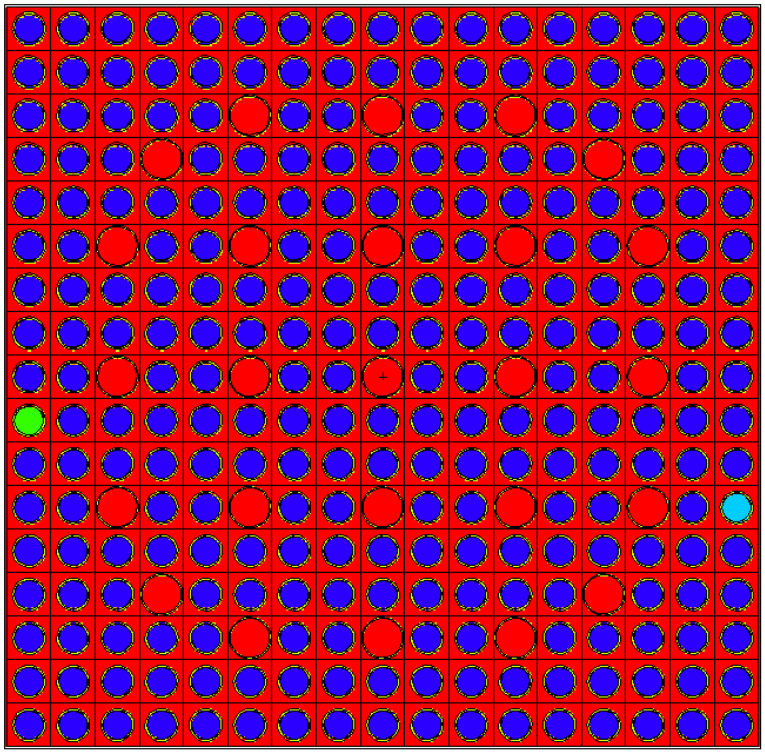

Figure 23: MCNP geometry Vandellos-2 assembly EC45

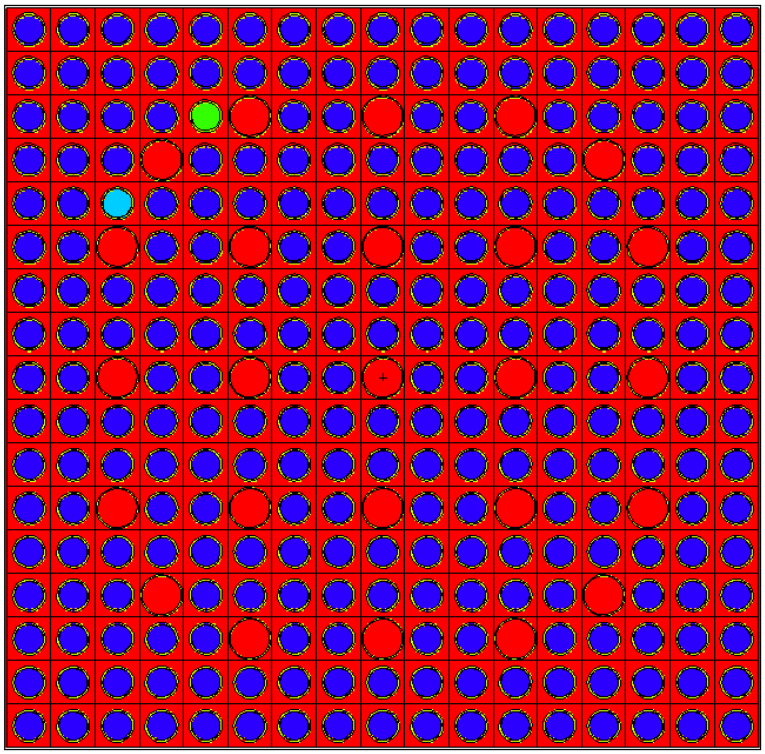

Figure 24: MCNP geometry Vandellos-2 assembly EF05

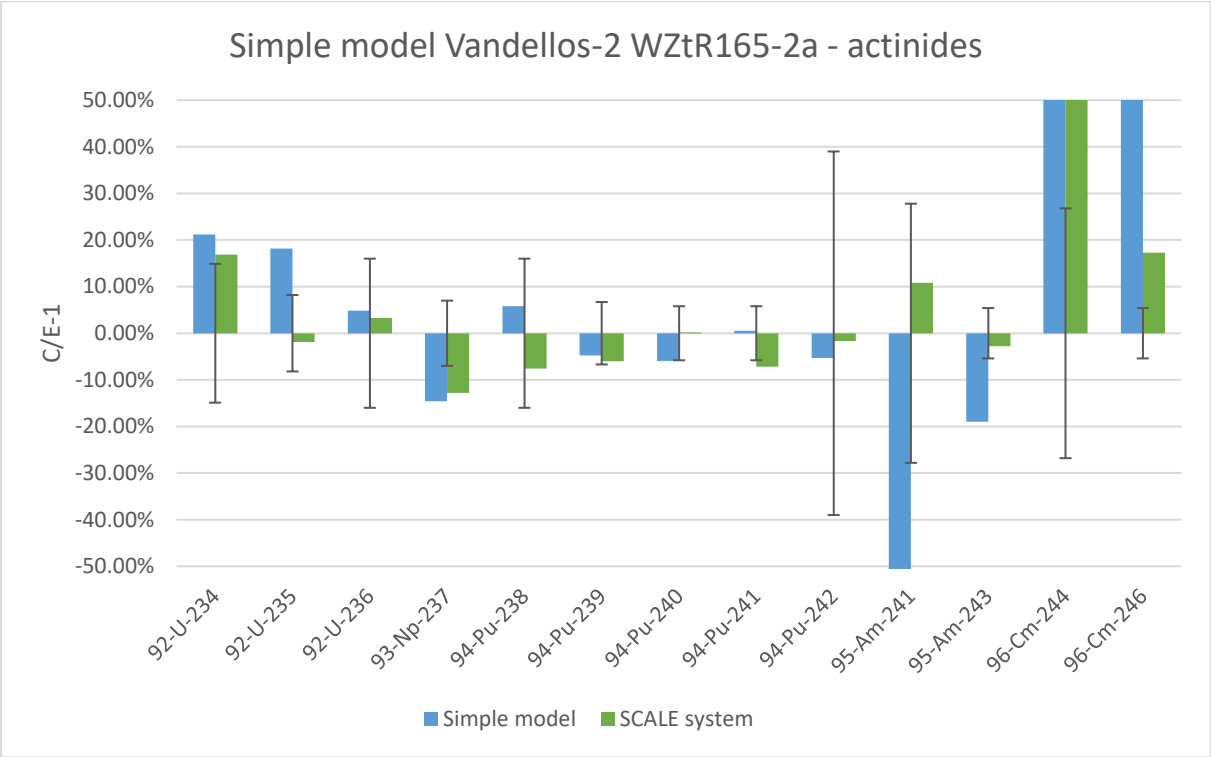

Figure 25: C/E-1 results of the simple model Vandellos-2 WZtR165-2a - actinides

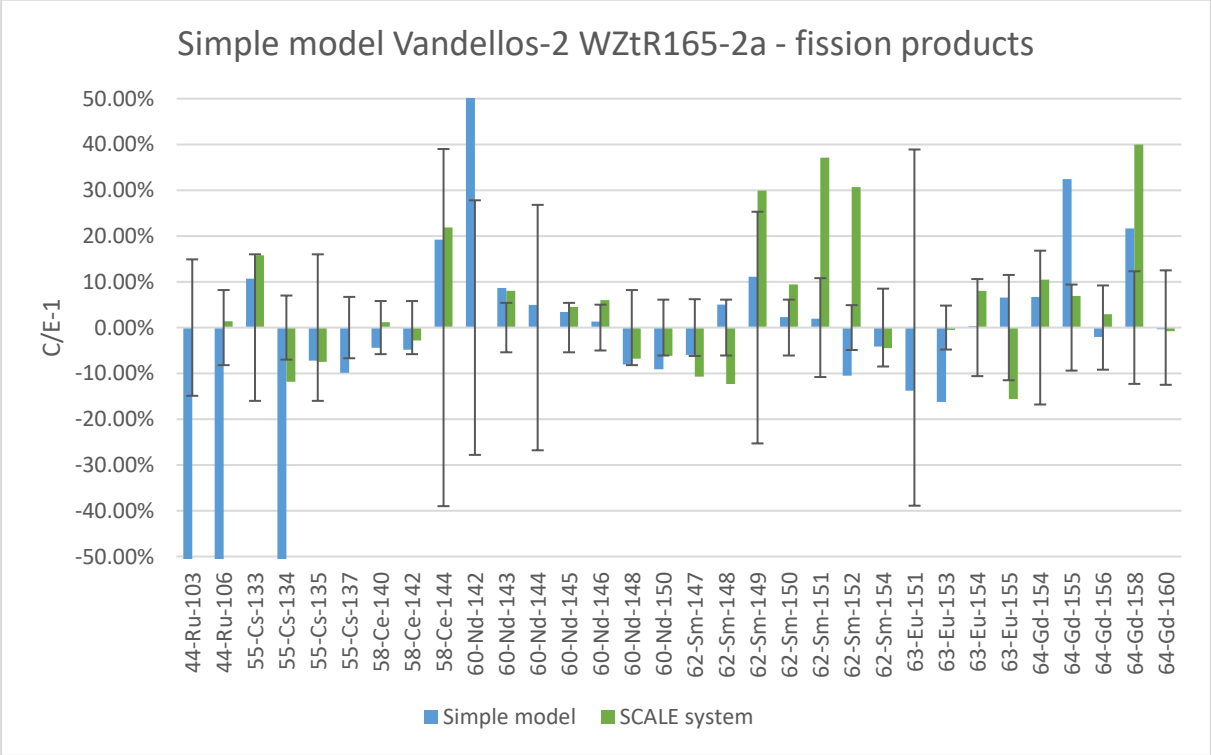

Figure 26: C/E-1 results of the simple model Vandellos-2 WZtR165-2a - fission products

The experimental results have been normalized to the final ^{238}U concentration. For the comparison, same was done with the results obtained with the simulations. Results obtained with the SCALE system were retrieved from [49]. Unfortunately, some nuclides were not provided with C/E-1 results (i.e., ^{103}Ru, ^{142}Nd, ^{144}Nd, and ^{151}Eu) and therefore, they do not appear in Figure 25 and Figure 26. The C/E-1 results after simulation present for some nuclides large discrepancies: ^{103}Ru (-100%), ^{106}Ru (-87%), ^{134}Cs (-65%), ^{142}Nd (57%), ^{155}Gd (32%), ^{235}U (18%), ^{241}Am (-77%), ^{243}Am (-18%), ^{244}Cm (55%), and ^{246}Cm (53%). Looking at ^{235}U and the burn-up indicators, it could be possible that too few fissions have occurred since they are respectively over- and underestimated. Additionally, the americium isotopes are severely underestimated and the curium isotopes overestimated, which could be explained with relatively too many neutron captures in the actinides that result in β^--decay instead of fissions. There is a good agreement between the experimental results and the simulated ones for the plutonium isotopes.

As mentioned in §3.2.1, additional simulations were executed since ^{235}U and the burn-up indicators deviate too much from the experimental concentrations. The last irradiation step was duplicated and extended with 10 days at the time. Acceptable results were found starting from 70 days extension, resulting in an increase of 5.6% in the sample burn-up (79.2 GWd/tHMi). The C/E-1 results of the actinides of both the simple and the extended model are presented in Figure 27 and the fission products in Figure 28.

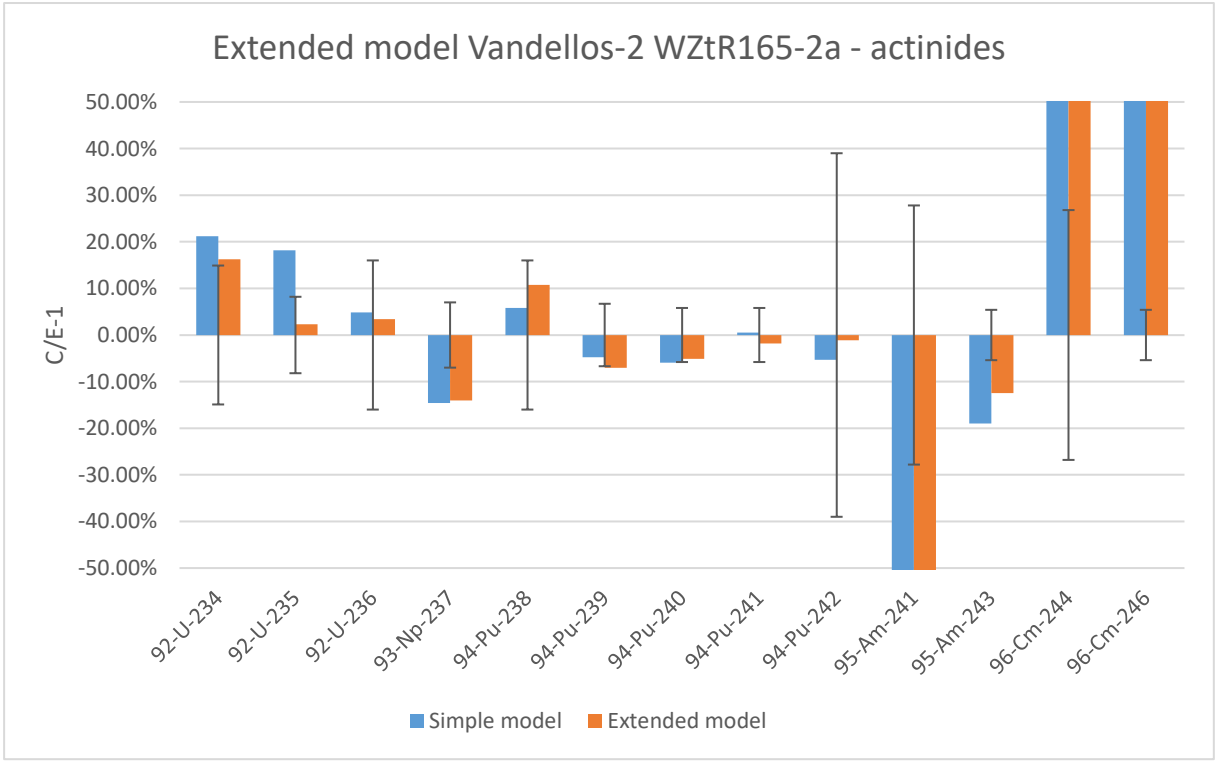

Figure 27: C/E-1 results of the extended model Vandellos-2 WZtR165-2a - actinides

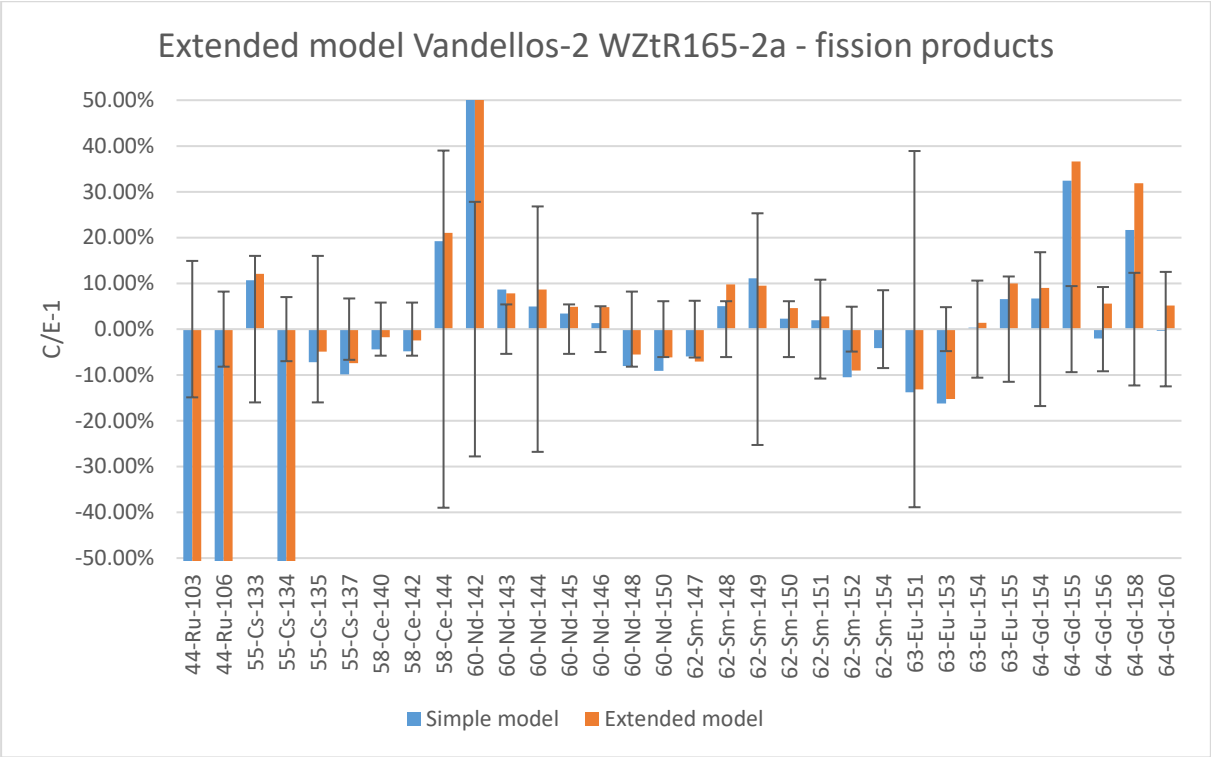

Figure 28: C/E-1 results of the extended model Vandellos-2 WZtR165-2a - fission products

The focus lays with the C/E-1 results of ^{235}U and the burn-up indicators ^{137}Cs and ^{148}Nd. In the simple model, these nuclides were respectively over- and underestimated, which may indicate insufficient irradiation. By extending the irradiation history, the sample is more irradiated which causes the sample burn-up to rise. This model is a good fit to maintain the balance between sufficient and too much irradiation.

The C/E-1 results of the different nuclides lie in the same order of magnitude. Results falling within the experimental uncertainty stay within these boundaries and the results falling outside these boundaries keep falling outside after optimization. However, the curium isotopes are more severely overestimated with the extended model (74% for ^{244}Cm and 86% for ^{246}Cm). This can be explained with the increased burn-up. The ^{241}Am nuclide is underestimated with 78%, which is in the same range as ^{244}Cm and ^{246}Cm. It is possible that too many neutron absorptions have taken place in ^{241}Am, but since this nuclide does not find itself in the same production chain as the curium isotopes, these underestimations are unrelated. Keeping in mind the modeling assumptions (the adjacent assemblies were not modeled), it is possible that the representation of the flux distribution was lacking. Further optimization by modeling the adjacent assemblies, based on the extended model, is encouraged.

4.2.2 Optimization Vandellos-2 WZtR165-2a

The MCNP geometry of the model with adjacent assemblies is shown in Figure 29. The C/E-1 results of the actinides obtained with the optimized simulation and the extended model from §4.2.1 are presented in Figure 30 and the fission products in Figure 31, supplemented with the experimental uncertainty.

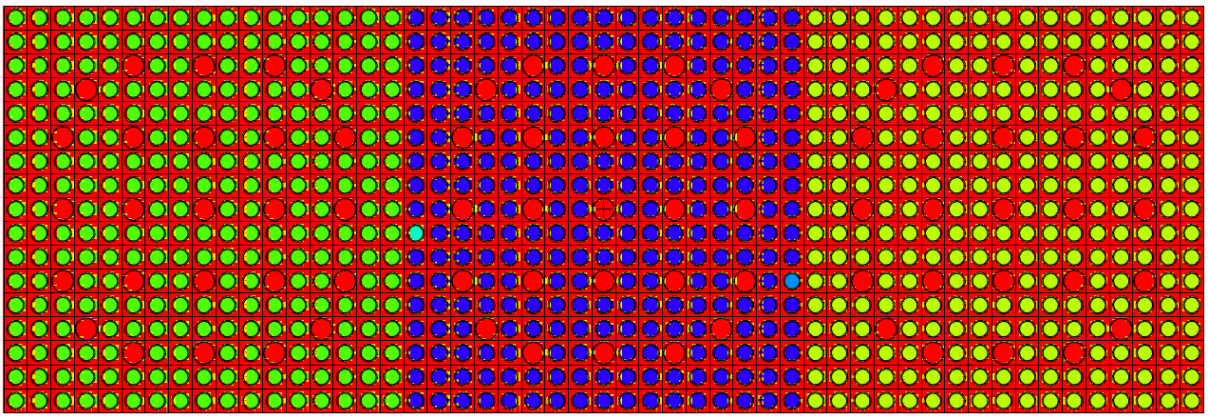

Figure 29: MCNP geometry Vandellos-2 assembly EC45 with adjacent assemblies

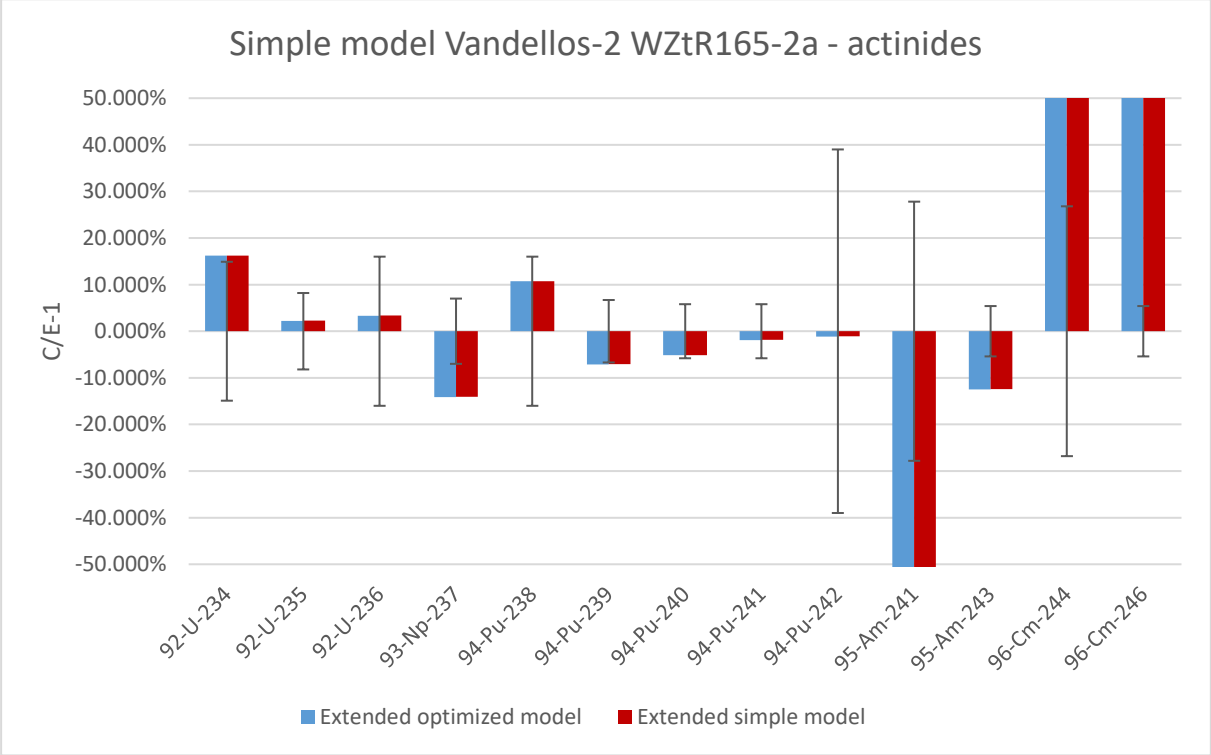

Figure 30: C/E-1 results of the optimized extended model Vandellos-2 WZtR165-2a - actinides

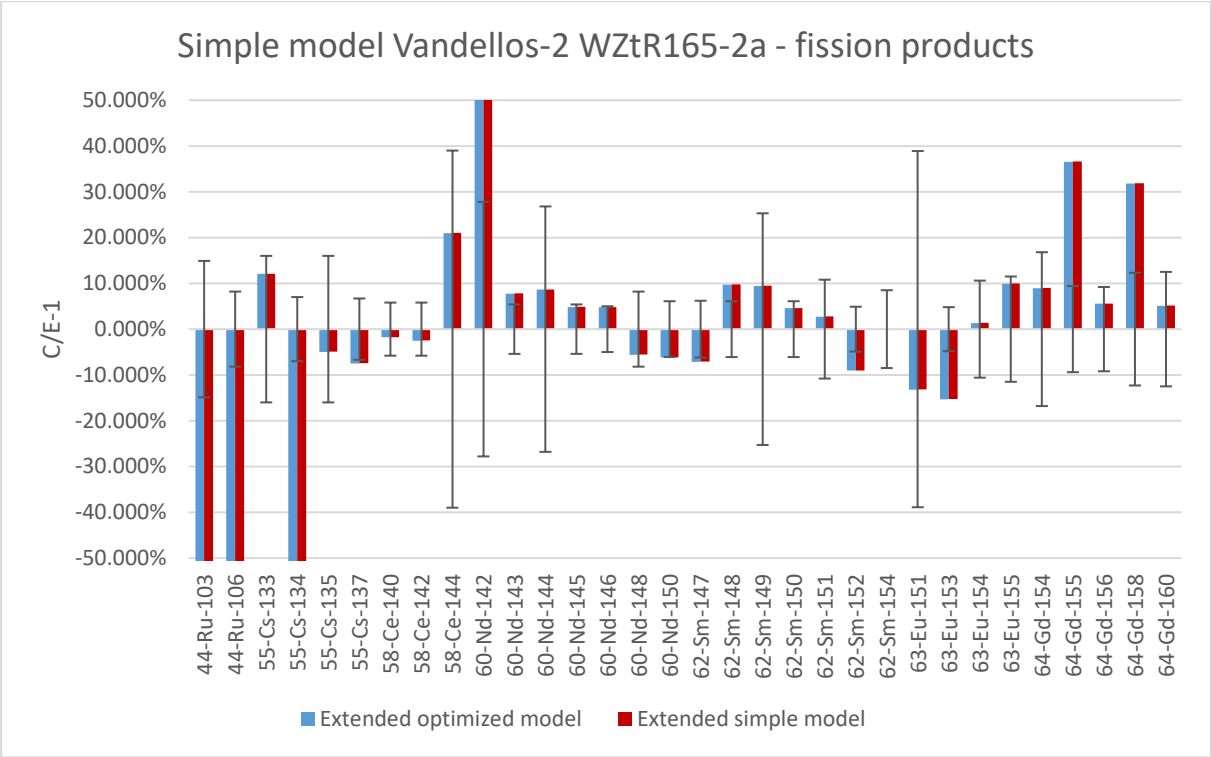

Figure 31: C/E-1 results of the optimized extended model Vandellos-2 WZtR165-2a - fission products

Optimizing the extended model barley influences the C/E-1 results of all the experimentally determined nuclides of this sample. Modeling the adjacent assemblies during cycle 7 until cycle 10 is thus redundant in this case. Still, since information concerning the adjacent assemblies is lacking, further attention must be given to correctly model this case. Additionally, the assembly is moving around the core between the irradiation cycles which could mean that reflective boundary conditions may not always be the best choice. Further analysis is needed.

4.3 Case 3: Gösgen-1 GU3

4.3.1 Simple model Gösgen-1 GU3

The MCNP geometry of assembly 1601 and 1701 are presented respectively in Figure 32 and Figure 33, showing the different modeled materials in different colors. The four different sets of C/E-1 results and the C/E-1 results obtained with the SCALE system of the actinides are presented in Figure 34 and the fission products in Figure 35, supplemented with the experimental uncertainty. A sample burn-up of 50.7 GWd/tHMi was reached in both models with the irradiation history provided in Table 11. The sample reached a burn-up of 52.07 GWd/tHMi in both cases where the model was normalized to the experimentally determined ^{148}Nd concentration. In the model with the SCALE system, a sample burn-up of 52.5 GWd/tHMi was reached. The experimental burn-up, determined based on the experimentally determined ^{148}Nd concentration and with the use of the ENDF/B-V nuclear data library, was 52.5 GWd/tHMi.

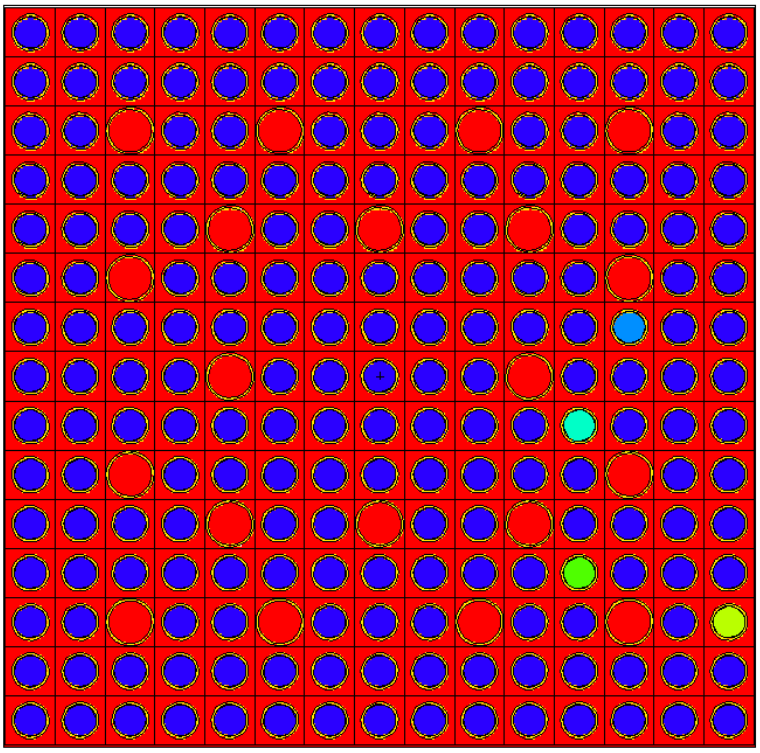

Figure 32: MCNP geometry Gösgen-1 assembly 1601

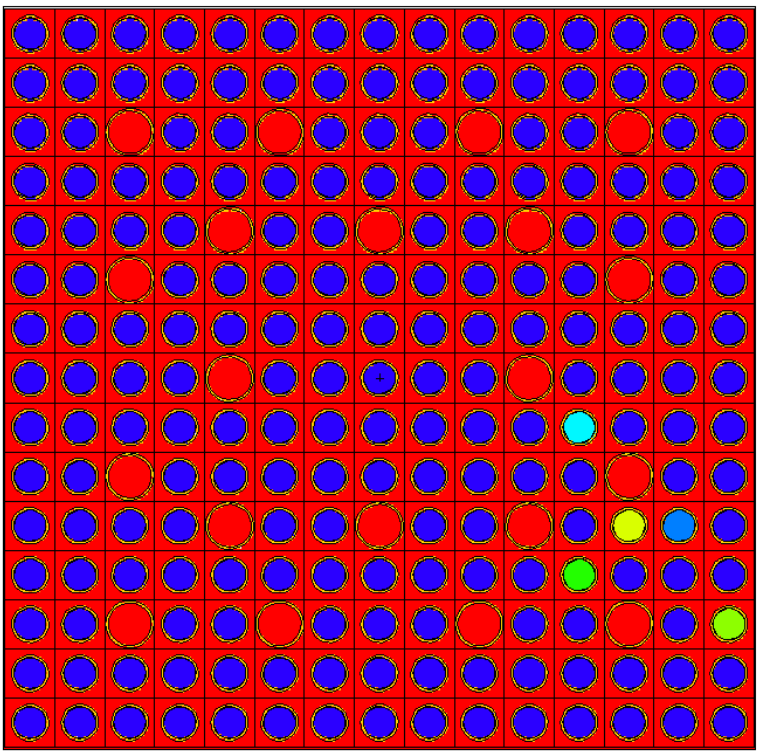

Figure 33: MCNP geometry Gösgen-1 assembly 1701

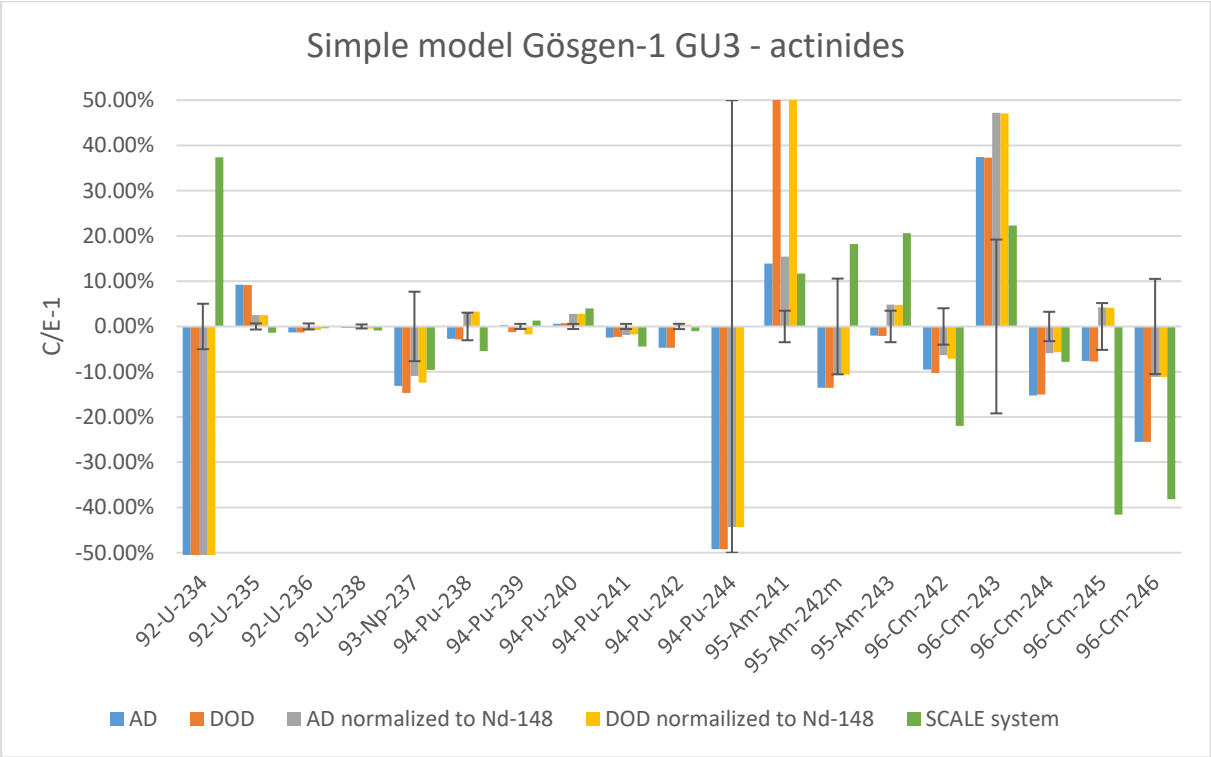

Figure 34: C/E-1 results of the simple model Gösgen-1 GU3 - actinides GU3

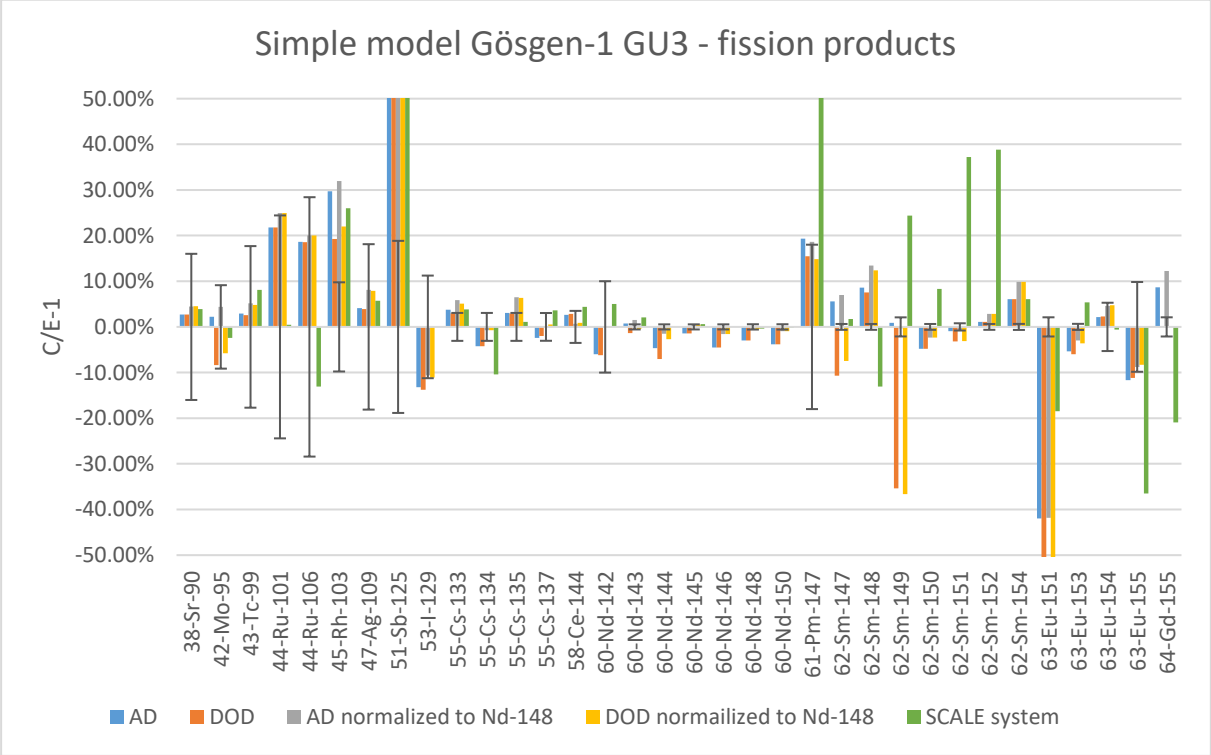

Figure 35: C/E-1 results of the simple model Gösgen-1 GU3 - fission products

The first thing to notice is again the bad agreement between the C/E-1 results with the usage of the experimental results obtained on the AD and the ones recalculated to the DOD (§4.1.1). The nuclides ^{241}Am and ^{151}Eu are both about 50% more overestimated when using the experimental results recalculated to the DOD instead of the experimental results obtained on the AD as a reference. The recalculated experimental concentration to the DOD was again negative for ^{155}Gd (§4.1.1). Additionally, ^{149}Sm is underestimated with 36% when using the experimental results recalculated to the DOD, while the C/E-1 result lies within the 95% experimental uncertainty (2.09%) when using the results obtained on the AD as a reference. As in the first case (§4.1.1), preference is given to use the experimental results obtained on the AD for the calculation of the C/E-1 values.

When the model was normalized to the experimentally determined ^{148}Nd concentration, it is noticeable that both burn-up indicators (^{137}Cs and ^{148}Nd) show better agreement with the experimental results by obtaining a C/E-1 result within the experimental uncertainty. The model without the normalization to the experimentally determined ^{148}Nd concentration, the concentration of ^{137}Cs already lies within the 95% uncertainty interval of the experimentally determined concentration, which already means (based only on this concentration) that the sample should be irradiated sufficiently. The C/E-1 result of ^{235}U shifted inside the 95% uncertainty boundaries of the experimental results after the model was normalized to the experimentally determined ^{148}Nd concentration. Therefore, preference is given to the C/E-1 results of "AD normalized to Nd-148", which is again labeled as the best simple model (same as in case 1, §4.1.1).

The fission products with strong deviating C/E-1 results in case 1 (^{95}Mo, ^{99}Tc, ^{101}Ru, ^{106}Ru, ^{103}Rh, ^{109}Ag, and ^{125}Sb), have C/E-1 results within the 95% experimental uncertainty boundaries, except for ^{125}Sb, which has a C/E-1 of almost 120%. The model with the SCALE system obtained a C/E-1 result of 62.5% [26] and 72% [51].

The best simple model shows already a good agreement with the experimental results. Still, the concentration of some nuclides deviates strongly with the experimental results (beyond the 95% uncertainty range). Since the sample rod was placed at the periphery of the assembly, it is possible that the neutron flux is not represented correctly due to the applied reflective boundary conditions and averaging of the nuclide composition over all the fuel rods in the simulation model. It is recommended to explore optimization by modeling the outer rods of the assembly as different materials. The best simple model is used for the comparison and the discussion whether or not the improvement in results is worth the extra work that went into the model.

4.3.2 Optimization Gösgen-1 GU3

After the optimization (outer rings modeled as separate materials) of the two different models (both normalization and no normalization to the experimentally determined ^{148}Nd concentration), the sample burn-up stayed the same, since the irradiation history was also kept constant. The MCNP geometry of both assemblies (1601 and 1701) are shown in Figure 36 and Figure 37, showing the different modeled materials as different colors. The C/E-1 results obtained with the optimized model and the best simple model from §4.3.1 of the actinides are presented in Figure 38 and the fission products in Figure 39, supplemented with the experimental uncertainty.

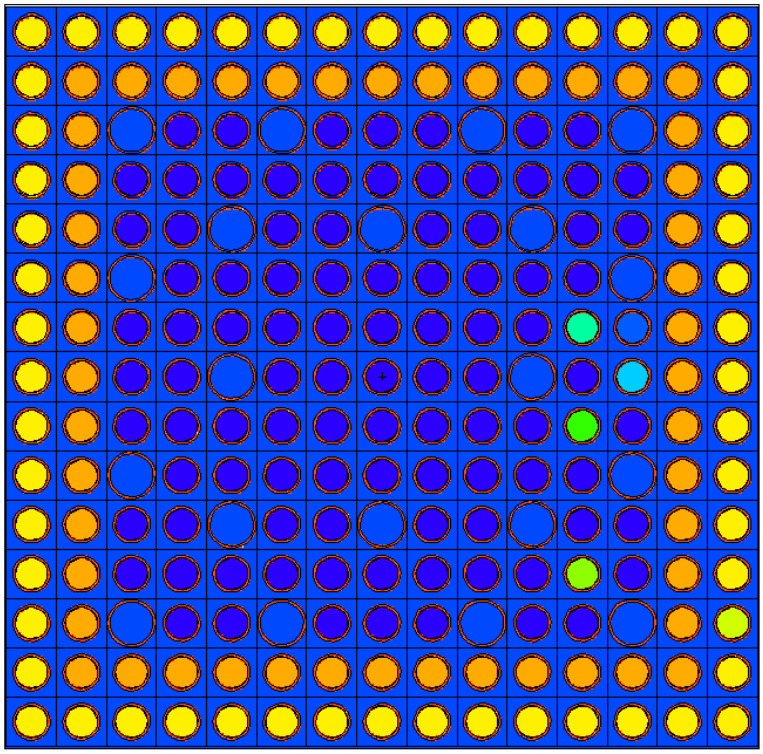

Figure 36: MCNP geometry Gösgen-1 assembly 1601 - optimized

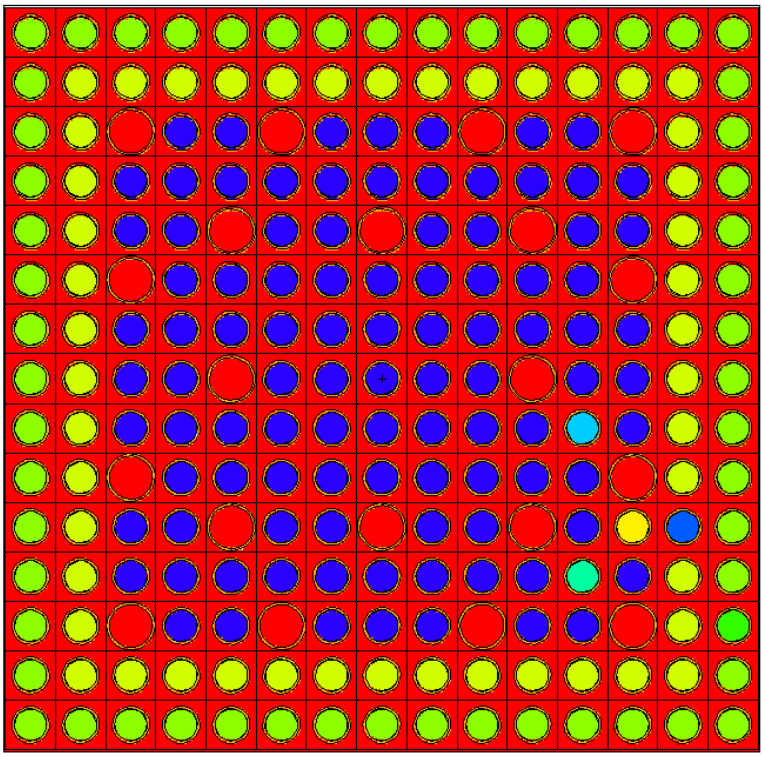

Figure 37: MCNP geometry Gösgen-1 assembly 1701 - optimized

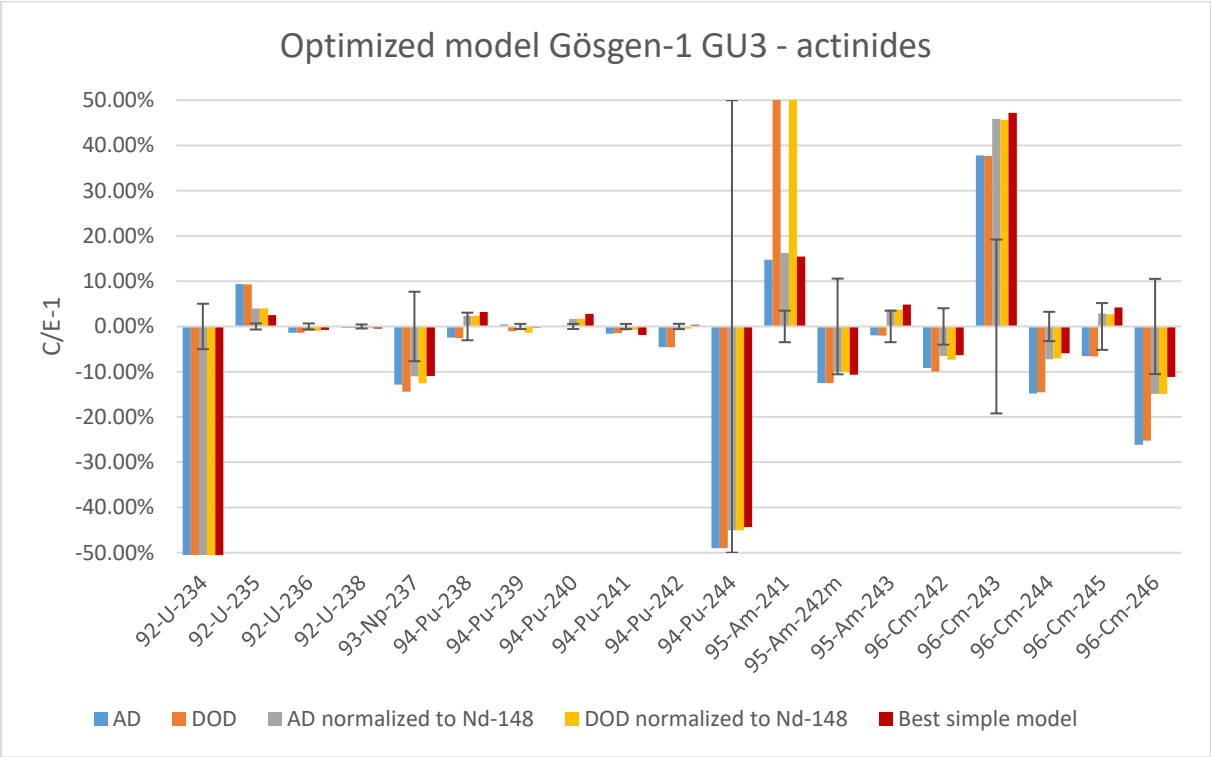

Figure 38: C/E-1 results of the optimized model Gösgen-1 GU3 - actinides

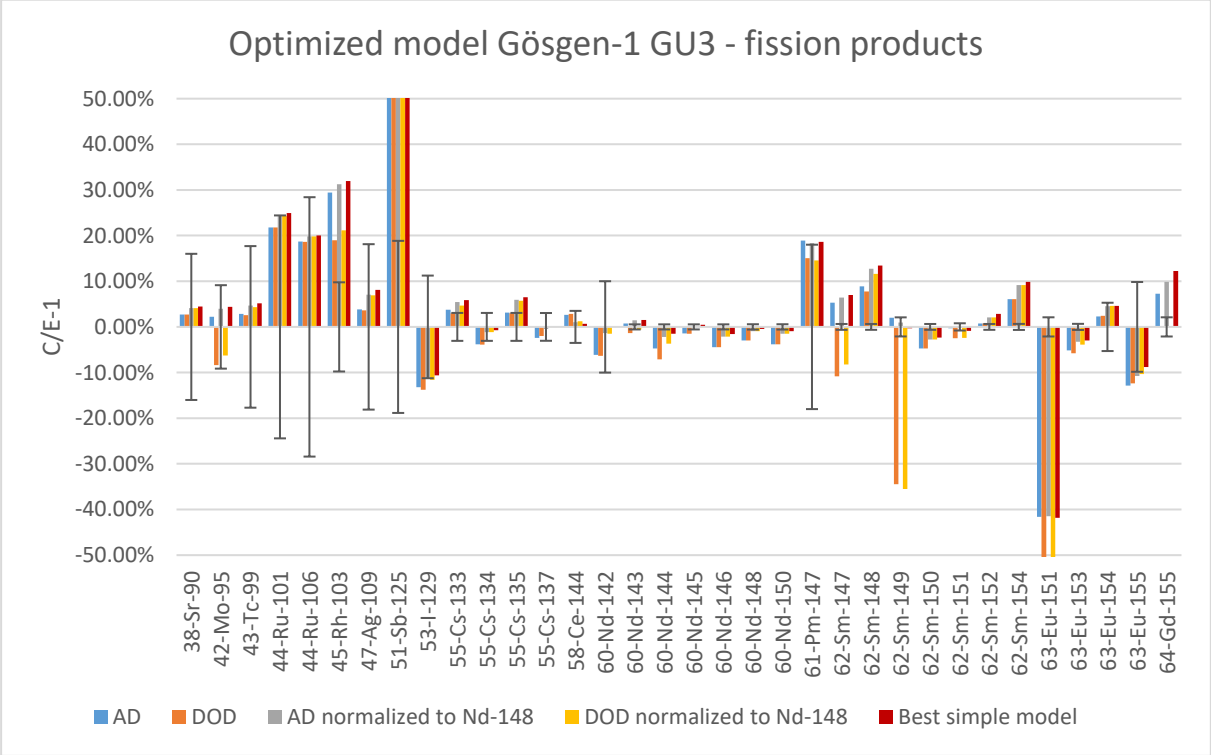

Figure 39: C/E-1 results of the optimized model Gösgen-1 GU3 - fission products

The overall best model after optimization is also the model normalized to the experimentally determined concentration of ^{148}Nd and with the experimental results obtained on the AD used as reference. In general, the C/E-1 results after optimization, when using the experimental results obtained on the AD as reference, stay within the same order of magnitude of the C/E-1 results of the best simple model. When comparing these two best models (before and after optimization), the models are evenly matched. For some important nuclides (e.g., ^{235}U, ^{239}Pu, ^{242}Pu, and ^{148}Nd), the best simple model provides slightly better C/E-1 results. On the other hand, for nuclides such as, ^{238}Pu, ^{240}Pu, and ^{243}Am, the results are slightly better for the best optimized model. The most important aspect in analyzing and assessing the C/E-1 results is whether these lie within the 95% experimental uncertainty and not to match zero. After optimization, the C/E-1 results stay within the same order of magnitude as the best simple model, which makes the optimization redundant. The extra work put in the optimization does not contribute to better results. The most recommended model to use in simulations for GU3 in the Gösgen-1 reactor is the best simple model from §4.3.1, a model normalized to the experimentally determined ^{148}Nd concentration with the experimental concentrations provided obtained on the AD as reference.

4.3.3 Influence of different nuclear data libraries

The influence of different libraries is evaluated using the best simple model in §4.3.1. The C/E-1 results of these simulated models and the best simple model from §4.3.1 of the actinides is presented in Figure 40 and the fission products in Figure 41, supplemented with the experimental uncertainty. The model simulated with the ENDF/B-VIII.0 nuclear data library and normalized to the experimentally determined ^{148}Nd concentration resulted in a burn-up of 52.38 GWd/tHMi. The burn-up reached in the other models is 50.7 GWd/tHMi since these simulations are all based on exactly the same model (irradiation history stayed the same) and in ALEPH2, the burn-up is calculated with the irradiation history.

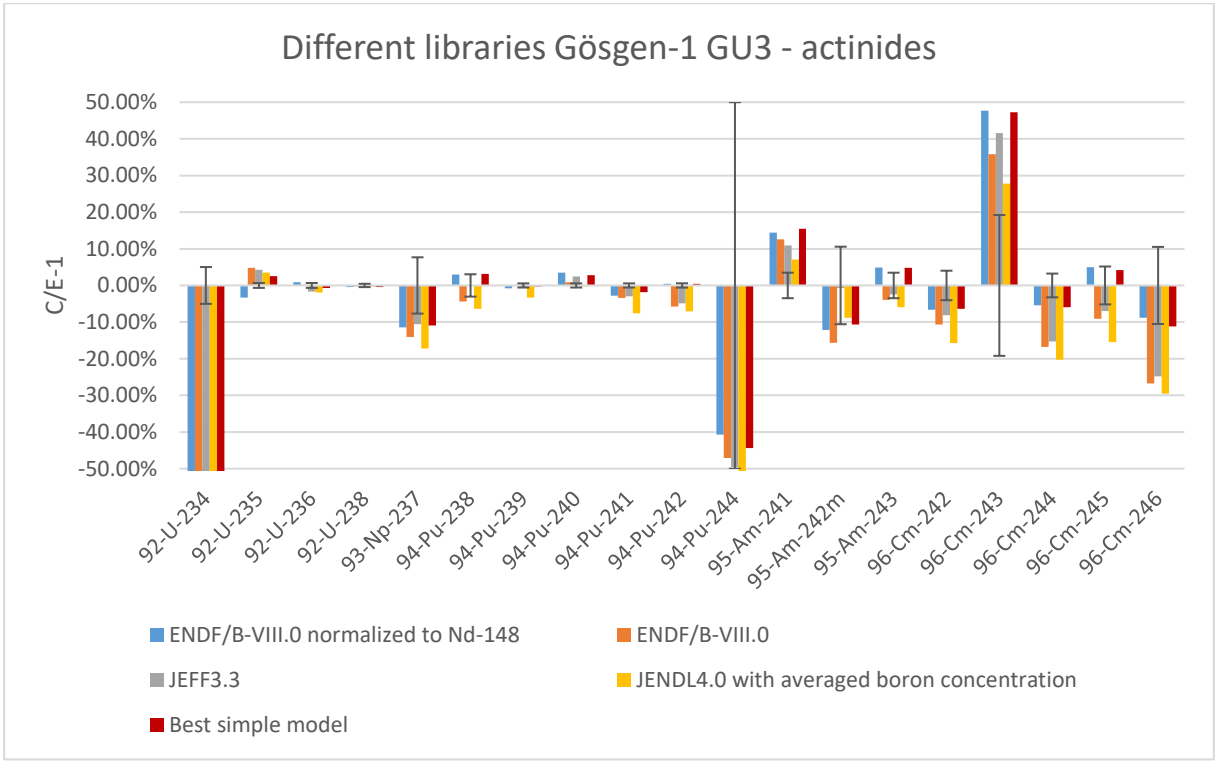

Figure 40: C/E-1 results when using different nuclear data libraries Gösgen-1 GU3 - actinides

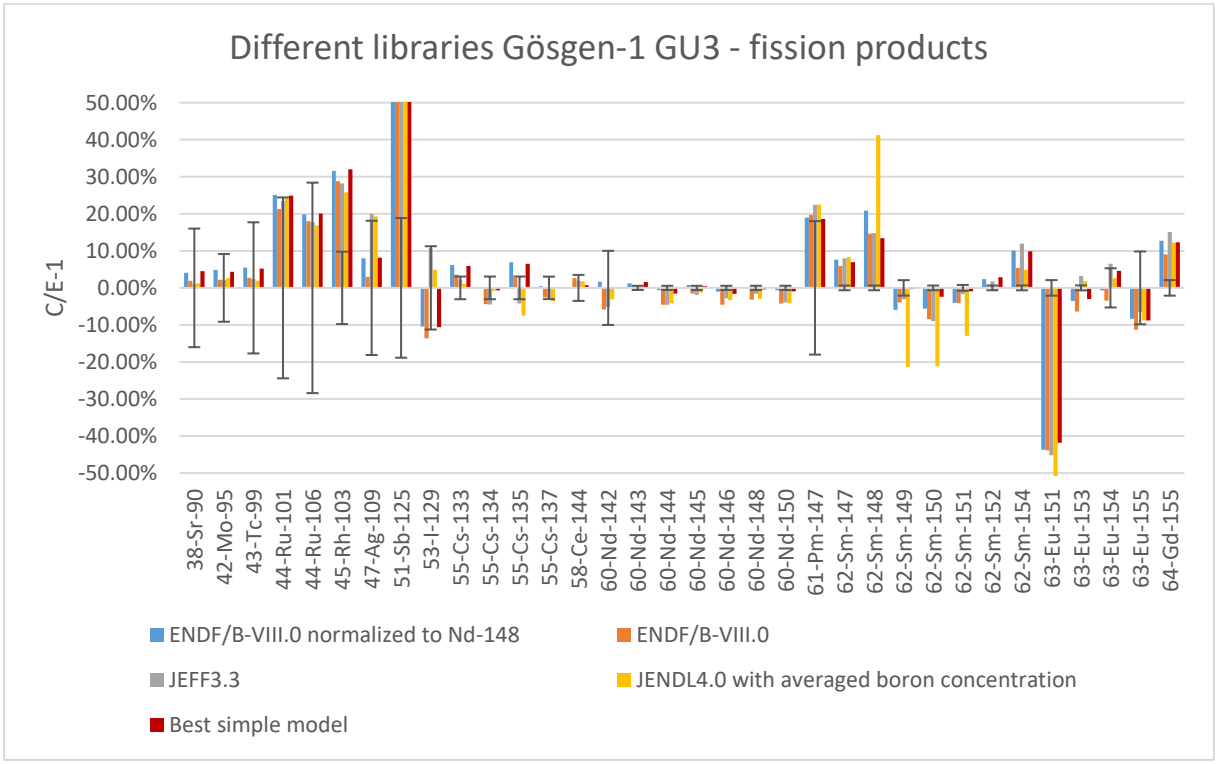

Figure 41: C/E-1 results when using different nuclear data libraries Gösgen-1 GU3 - fission products

Overall, a good agreement is found between the C/E-1 results when using different nuclear data libraries. A first exception is the C/E-1 result of ^{244}Pu when using JENDL4.0 as the nuclear data library. This nuclide is underestimated with 99%, compared to an underestimation between 40% and 49.55% (still within the experimental uncertainty boundary of 50%) for the other nuclear data libraries. This nuclide is produced through neutron capture by lighter plutonium isotopes, has a half-life of 80 million years [18], and a low capture cross section (about 100 mb [14]). This implies that the underestimation originates from the production side. However, no differences of such kind can be found in the C/E-1 results of the preceding nuclides in this production chain to explain this phenomenon.

It is also noticeable that the C/E-1 results of ^{242m}Am for the different nuclear data libraries lie around the experimental uncertainty (10.58%), except for the simulation with the JEFF3.3 nuclear data library. Here, the C/E-1 results is close to zero. This difference is not reflected in the nuclide concentrations further up the absorption/decay chain.

The C/E-1 results reflecting a different model of the boron concentration in the moderator are shown in Figure 42 for the actinide and Figure 43 for the fission products. Overall, the these results are slightly better for the simulation with the detailed boron concentration. Some improvements are found for the samarium isotopes, but still the C/E-1 results lie behind the experimental uncertainty boundary. The C/E-1 results of ^{241}Am show different trends, but the model with the detailed boron concentration provided a C/E-1 result in the same order of magnitude as the other libraries discussed in the beginning of this chapter. Same trends are found for ^{244}Cm.

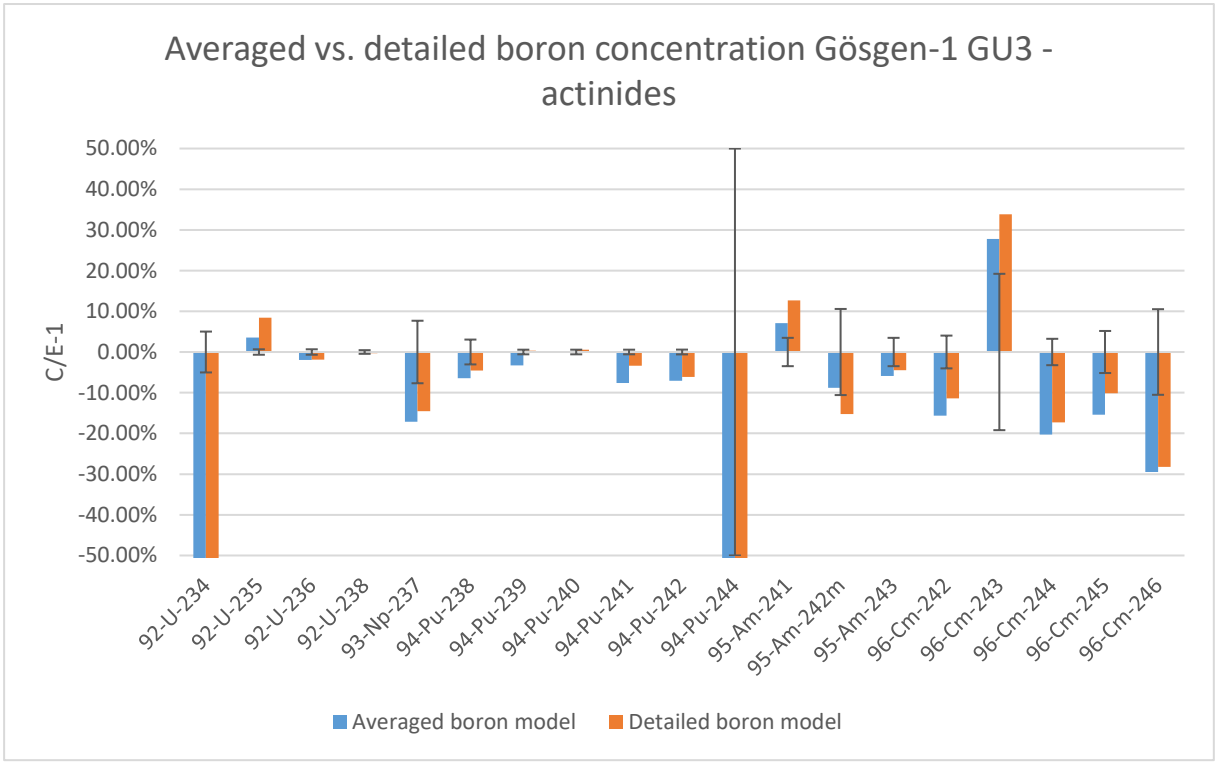

Figure 42: C/E-1 results when using averaged vs. detailed boron concentration Gösgen-1 GU3 - actinides

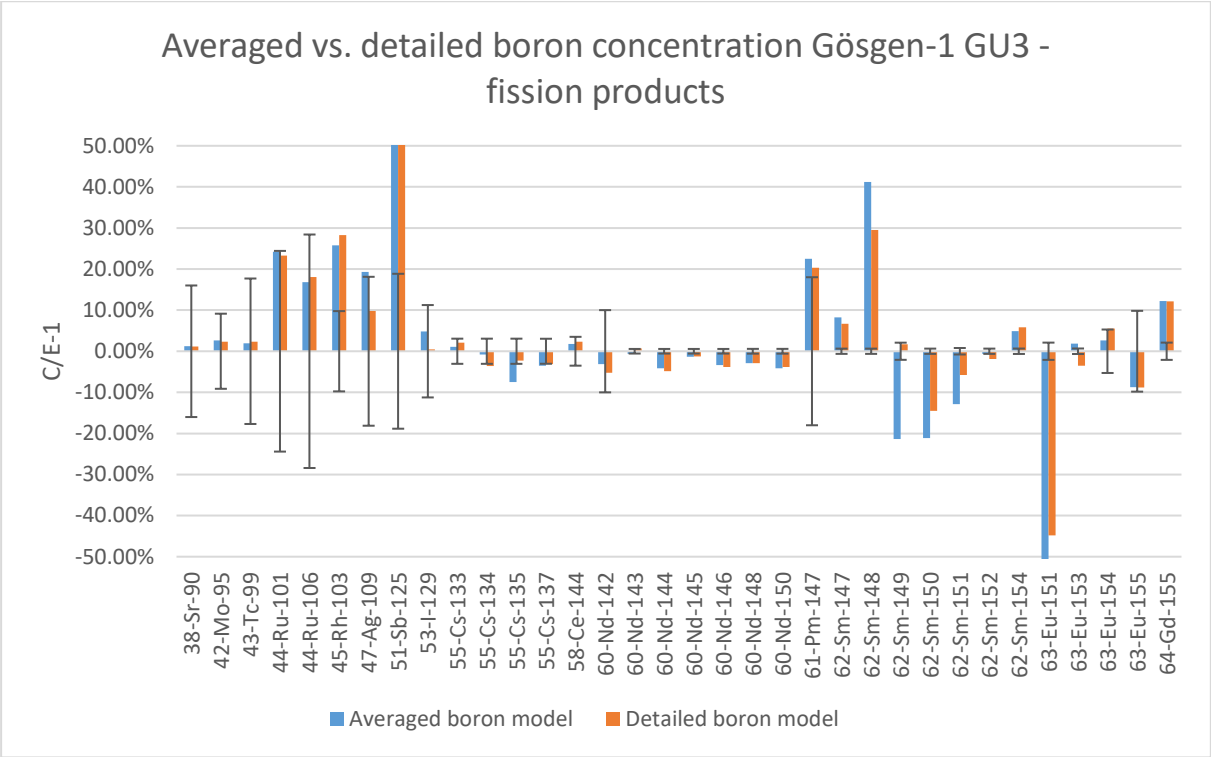

Figure 43: C/E-1 results when using averaged vs. detailed boron concentration Gösgen-1 GU3 - fission products

The severe underestimation of ^{244}Pu is not due to a different cross section but due to the way boron is modeled into the moderator. The C/E-1 result obtained with the model with the average boron concentration is -100%, whereas the C/E-1 result obtained with the model with the detailed boron concentration -64% is. This implies that the way boron is modeled in the moderator affects the neutron flux distribution which has an impact on the final nuclide composition (see §2.2).

4.4 Case 4: Beznau-1 BM5

The MCNP geometry of the assembly for both models (different cooling times of the MOX fuel) is presented in Figure 44, showing the different modeled materials as different colors. The experimental determined nuclide composition was provided with their experimental uncertainty by SCK CEN in the ARIANE report [40]. The C/E-1 results of these four different models and the C/E-1 results obtained with the SCALE system of the actinides are presented in Figure 45 and the fission products in Figure 46, supplemented with the experimental uncertainty. The experimental uncertainties of most of the neodymium and the samarium isotopes are so small (< 1%) that they are barely visible in these graphs. The experimentally determined sample burn-up is 58.9 GWd/tHMi, which is determined from the experimentally determined ^{148}Nd concentration in the sample. The burn-up simulated with ALEPH2 was 60.3 GWd/tHMi (i.e., 2% higher). No sample burn-up was provided after simulation with the SCALE system.

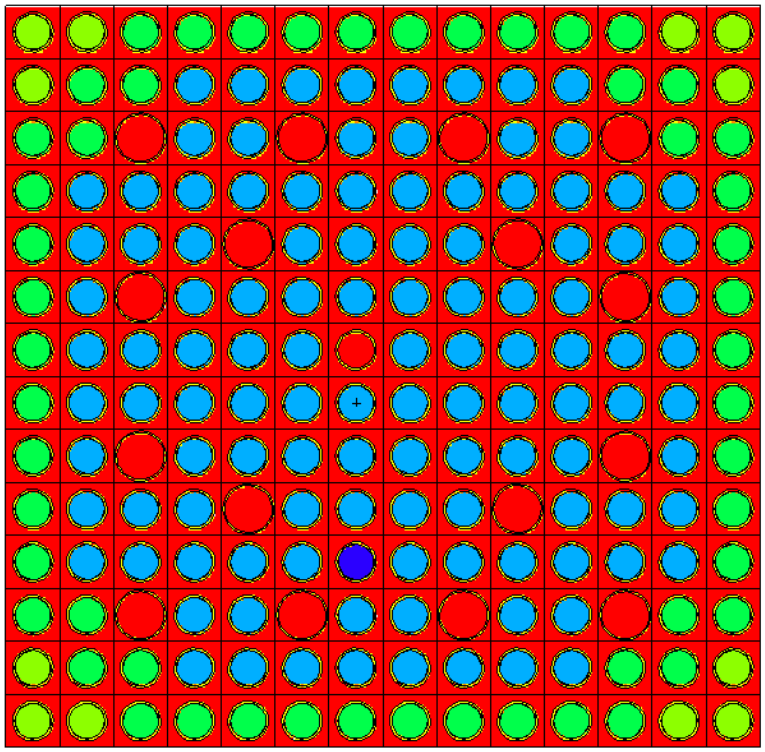

Figure 44: MCNP geometry Beznau-1 assembly M308

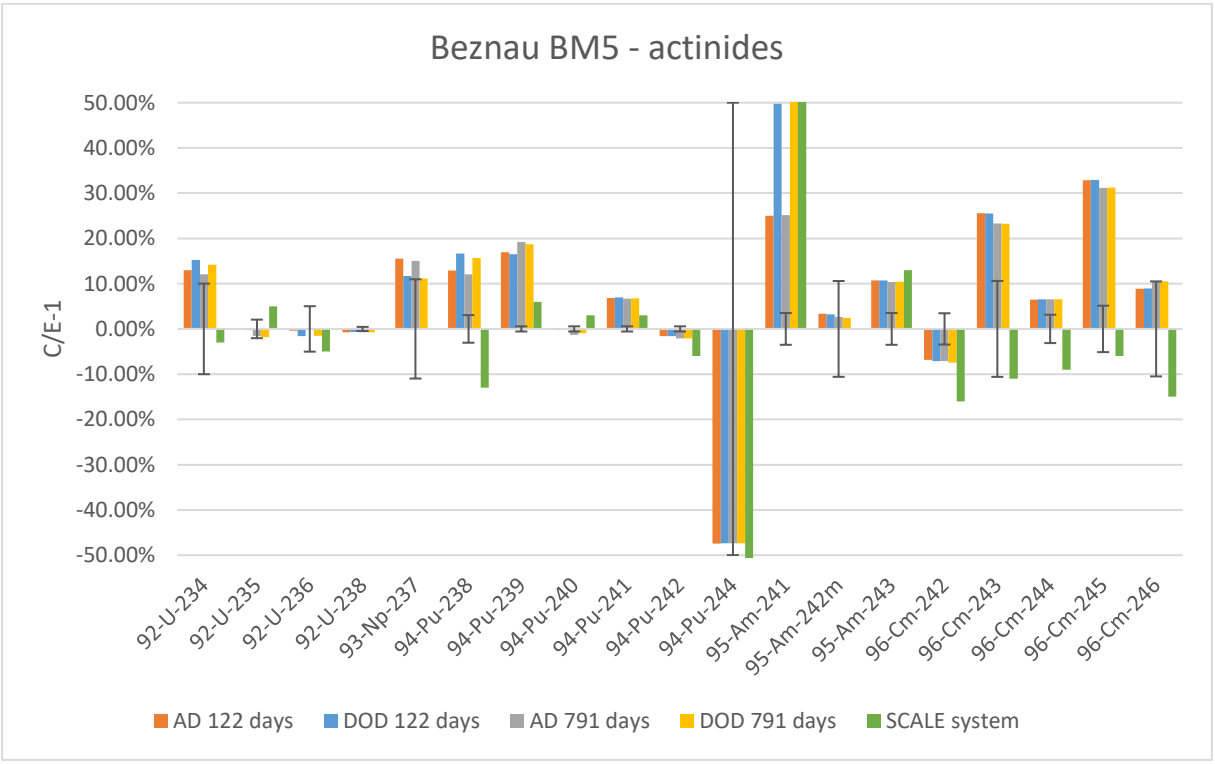

Figure 45: C/E-1 results of Beznau-1 BM5 - actinides

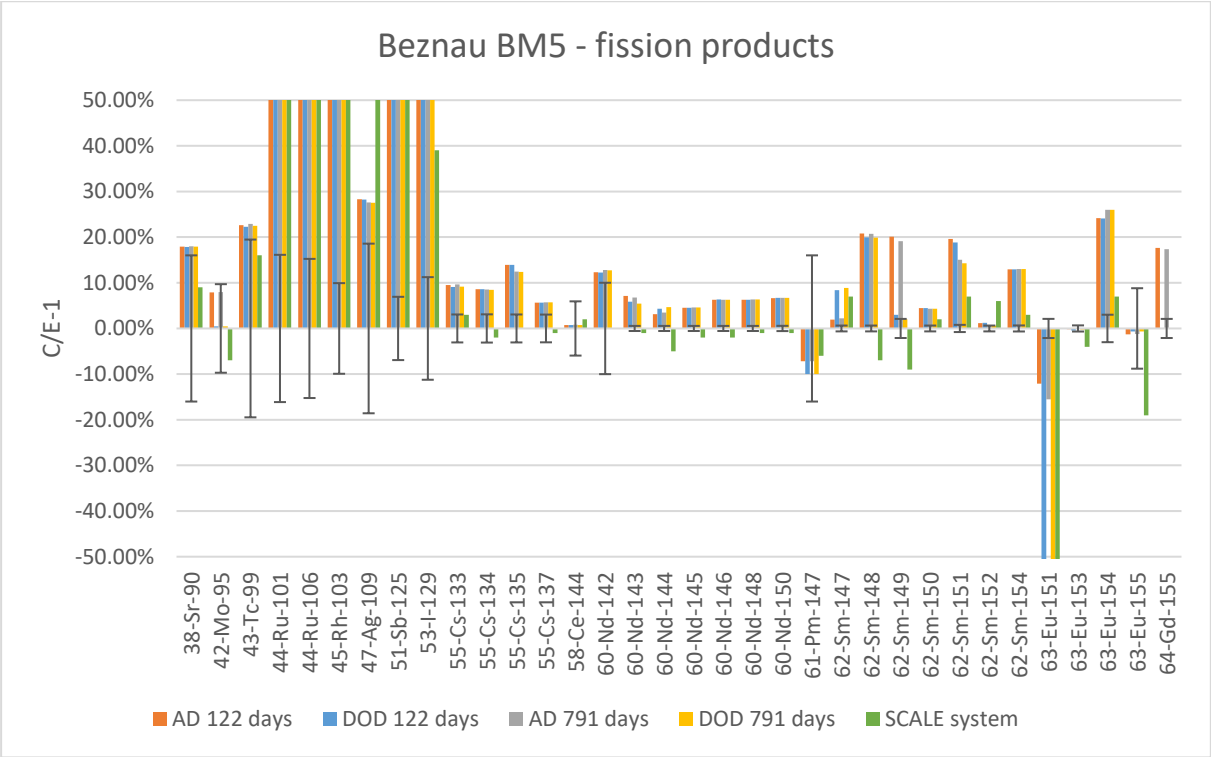

Figure 46: C/E-1 results of Beznau-1 BM5- fission products

The two different outputs (122 days or 791 days cooling time of the other MOX fuel rods besides the sample rod) show same trends when the results obtained on the AD are compared with the recalculated results to the DOD of the sample. The C/E-1 result of ^{149}Sm on the DOD lies within the experimental uncertainty (2.09%) while the result obtained on the AD 20% is. This is a stable nuclide, produced in two ways, both indirectly through fission. The first way is through the production of ^{149}Nd and two times β^--decay. The second way is through the production of ^{147}Nd, also followed by two times β^--decay and two neutron captures. The latter takes much longer to have a visible effect in the nuclide composition. This phenomenon is considered since the last irradiation cycle of the fuel sample lasts 334 days. The nuclide ^{149}Sm is seen as reactor poison because of its high thermal neutron capture cross section (56000 b) [14], [18]. Since obtained on the AD more ^{149}Sm nuclides are expected according to ALEPH2 then experimentally determined, perhaps too many fissions have occurred or too little neutron capture of ^{149}Sm have taken place. When comparing this with the C/E-1 result of the ^{148}Nd concentration (6.3%), it is possible that it is a combination of both. The nuclides ^{149}Nd and ^{149}Pm were not considered in the experimental assay because they are both very short-lived nuclides (respectively T1/2 = 1.728 h and T1/2 = 53.08 h [18]) and the measurements took place about 3 years after the fuel discharge. During the operation of the reactor the samarium concentration reaches an equilibrium independently of the operation power, since its production and disappearance rates are both equally dependent on the neutron flux [8]. It is therefore more likely that the prediction through simulation of its concentration at the DOD lies within experimental uncertainty.

The nuclide ^{151}Eu is underpredicted at both times: C/E-1 values of -13% obtained on the AD and -70% on the DOD. The uncertainty is 2.1% for the experimental results obtained on the AD. In the simulations with the SCALE system, this nuclide was underestimated by 74%. The C/E-1 of ^{95}Mo is higher when using the results obtained on the AD (8%) than recalculated to the DOD (0.5%), however all these results lie within the 95% interval of the experimental uncertainty (9.7%). In addition, the ^{155}Gd nuclide

concentration recalculated to the DOD in the official report was negative, which is technically impossible. This also shows a larger bias present on recalculated experimental results. Therefore, the C/E-1 result obtained with the experimental result recalculated to the DOD as reference was not considered for this nuclide. Overall, preference is given to use the non-recalculated experimental results as a reference.

The simulated ^{235}U concertation lies within the 95% experimental uncertainty (2.05%), whereas the C/E-1 results reported after simulation with the SCALE system 5% was [51]. Similar tendencies are found for ^{240}Pu, ^{244}Pu, ^{242m}Am, and ^{246}Cm. Most of the curium isotopes are overestimated, which could mean that too little fissions of actinides (besides ^{235}U, since its modeled concentration had a good agreement with the experimental concentration) have occurred and more and heavier actinides have been produced through neutron capture and β^--decay. In terms of fission products, simulations with the SCALE system provide overall slightly better results (but still in the same order of magnitude compared to the C/E-1 results obtained with simulations), except for ^{109}Ag, ^{151}Eu, and ^{155}Eu. No results are provided after simulation with the SCALE system for the nuclides ^{142}Nd, ^{155}Gd, ^{237}Np, and ^{242m}Am. Both ALEPH2 simulation models (two different cooling periods of the fuel before irradiation) reflect an overall good approximation of the physics within the assembly, keeping in mind that the nuclide composition of the other 178 fuel rods is practically unknown. However, it is not possible to provide a prediction of the cooling time before irradiation of the MOX fuel with these models.

4.5 Case 5: Fukushima-Daini-2 sample 1

The MCNP geometry of assembly 2F2DN23 is presented in Figure 47. Each modeled material is shown in a different color. The experimental nuclide composition is reported in the official report [48], normalized to the initial mass of uranium found in the corresponding sample. All the provided nuclide concentrations are recalculated to the DOD, except for the samarium isotopes, which are only provided on the AD. The experimental uncertainty is given for the results at reference date (on the DOD for the samarium isotopes and on the AD for the rest of the nuclides). An experimental sample burn-up of 4.15 GWd/tHMi was reported. The C/E-1 results of the actinides obtained with both models (different cooling times) and the SCALE system are presented in Figure 48 and the fission products in Figure 49, supplemented with the experimental uncertainty. For most nuclides, the experimental uncertainty is very small (0.10%, 0.30%, or 0.50%) and thus not clearly visible in the graphs presenting the C/E-1 results. The simulation with the model containing the irradiation history from Table 17 resulting in a sample burn-up of 4.15 GWd/tHMi, whereas the model normalized to the experimentally determined ^{148}Nd concentration presented a sample burn-up of 3.96 GWd/tHMi, which is 5% lower. After the simulation with the model of the SCALE system, a sample burn-up of 4.2 GWd/tHMi was reported [50], which is 1% higher than the experimental burn-up.

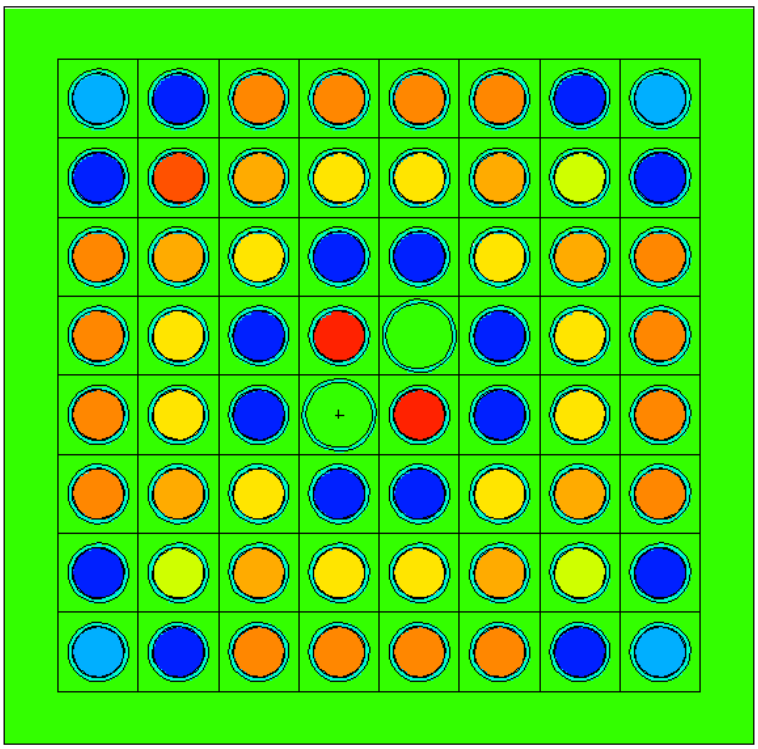

Figure 47: MCNP geometry Fukushima-Daini-2 assembly 2F2DN23

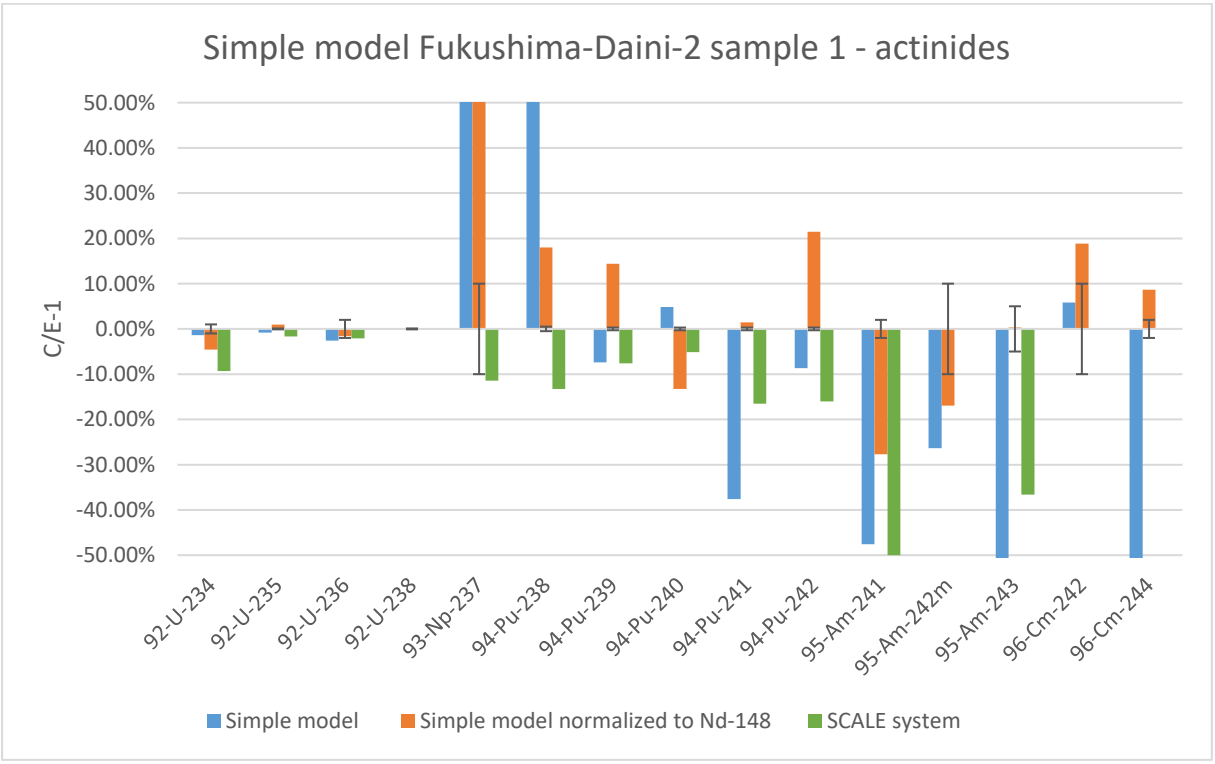

Figure 48: C/E-1 results of the simple model Fukushima-Daini-2 sample 1 - actinides

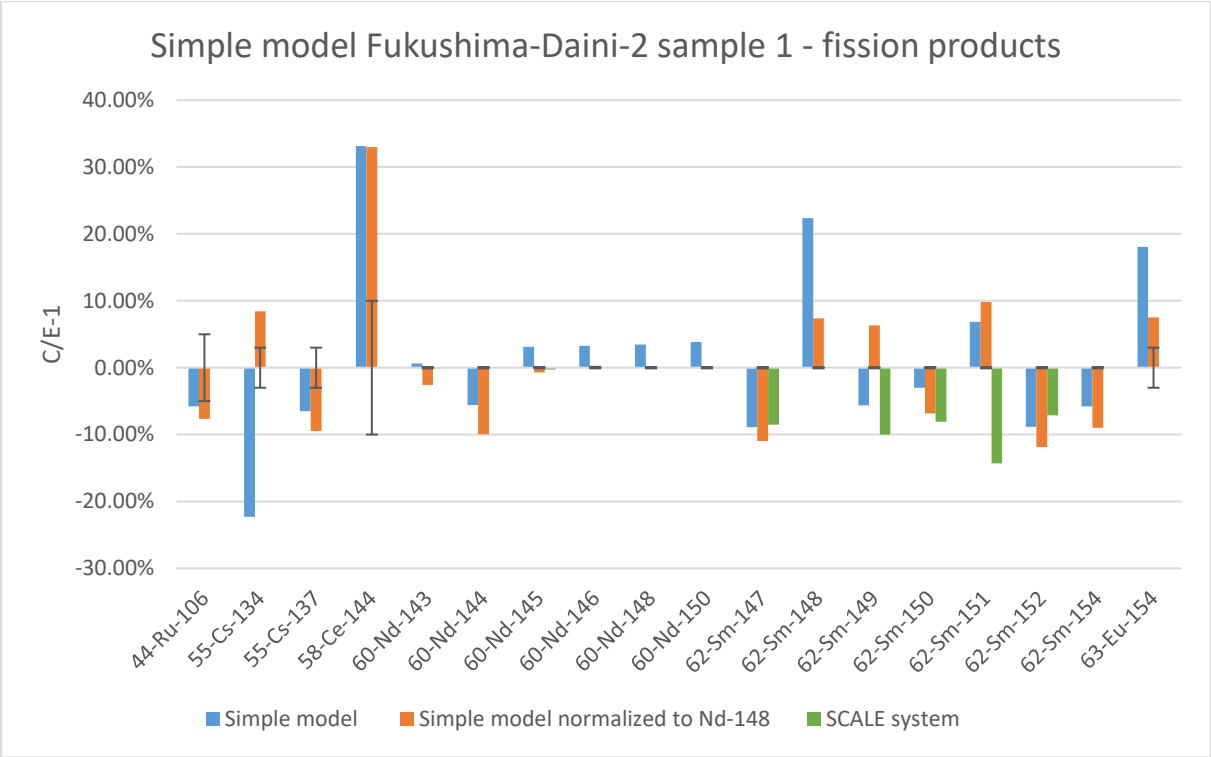

Figure 49: C/E-1 results of the simple model Fukushima-Daini-2 sample 1- fission products

Both simulations provide at first sight results in the same order of magnitude. Despite the C/E-1 result of ^{235}U is less than 1%, it still lies outside the experimental uncertainty (0.10%), opposed to a 1.7% underestimation after the simulation with the SCALE system. The model normalized to the experimentally determined ^{148}Nd concentration presents a better C/E-1 result of ^{148}Nd than the simple model, -0.03% compared to 3.47% (with 0.10% experimental uncertainty). This suggests that the sample was over irradiated in the simple model, opposed to the higher burn-up obtained with simulation with the SCALE system. The C/E-1 results of ^{235}U, ^{238}U, and ^{137}Cs are better when using the simple model, i.e., -0.81%, 0.01%, and -6.51%, respectively. Six other nuclides (i.e., ^{148}Sm, ^{154}Eu, ^{238}Pu, ^{242m}Am, ^{243}Am, and ^{244}Cm) show much better C/E-1 results for the model normalized to the experimentally determined ^{148}Nd concentration opposed to when the model was not normalized to the experimentally determined ^{148}Nd concentration, even though these results still lie outside the 95% experimental uncertainty boundary. None of both models can reproduce the experimental concentration within the experimental uncertainty. Still, simulations with the SCALE system did not provide C/E-1 results for 14 out of 33 assessed nuclides, including both of the discussed burn-up indicators, which also raises certain questions.

The reported C/E-1 results after simulation with the SCALE system did not include results for following nuclides: ^{106}Ru, ^{134}Cs, ^{137}Cs, ^{144}Ce, ^{144}Nd, ^{146}Nd, ^{148}Nd, ^{150}Nd, ^{148}Sm, ^{154}Sm, ^{145}Eu, ^{242m}Am, ^{242}Cm, and ^{244}Cm. Overall, the C/E-1 results are similar or better than the C/E-1 results obtained with the SCALE system, except for ^{237}Np, the C/E-1 result of both simulated models is more than 60%, whereas the model with the SCALE system obtained a C/E-1 value of -11%, which is just outside the 95% experimental uncertainty boundary. Because there are no other and/or better results of simulations with the SCALE system available, both models are considered a good agreement with the experimental results, except for ^{237}Np in particular, a nuclide important for the production of ^{238}Np through neutron capture, which in its turn decays through β^--decay into ^{238}Pu (a nuclide important for determining the decay

heat and neutron emission [23]). The overestimation of ^{238}Pu with the model normalized to the experimentally determined ^{148}Nd concentration is in the same range as the underestimation of the simulation with the SCALE system, which is already good. Preference is given to the model normalized to the experimentally determined ^{148}Nd concentration, but the simple model already provides acceptable nuclide compositions, except for the nuclides ^{148}Sm, ^{154}Eu, ^{238}Pu, ^{242m}Am, ^{243}Am, and ^{244}Cm. More research and modelling of this case are required. Also, the sample was placed in the periphery of the assembly and at the bottom, which means that it is possible that the neutron flux distribution is not represented correctly. Further research should involve an assessment of the extent to which the reflective boundary conditions affect the neutron flux distribution at the periphery of the assembly. Through the experience gained with the model of the sample WZtR165-2a in the Vandellos-2 reactor (§4.2), additional information must be obtained for this case to correctly model the adjacent assemblies during the irradiation of the sample.

5 Conclusion

The presented thesis describes further validation of the ALEPH2 burn-up code against experimental measures, as a part of its maintenance and verification process. ALEPH2 is a Monte-Carlo depletion code developed by SCK CEN since 2004. These burn-up codes (or depletion codes) are used to predict nuclide compositions of SNF after specific irradiation processes. Knowing the nuclide composition enables to accurately quantify integral responses such as decay heat, neutron and gamma emission, and criticality for its safe handling, transport, and storage. This validation is executed as part of its maintenance and verification process. Several LWR SNF cases were simulated by using the experimental assay data available in the SFCOMPO database. The experimentally measured nuclide compositions were compared against ALEPH2 predictions. Initially, a simple model was developed for each case, which, after analysis, was possibly refined.

The first case consisted of sample GU1, irradiated in the reactor Gösgen-1. The estimated sample burn-up (calculated with the experimentally determined ^{148}Nd concentration) is 59.66 GWd/tHMi. Two different simple models were simulated: one with the irradiation history as provided in the official reports and one where the model was normalized to the experimentally determined ^{148}Nd concentration. A sample burn-up of 59.66 and 60.47 GWd/tHMi respectively were reached. The model with the normalization to the experimentally determined ^{148}Nd concentration came up with the better C/E-1 results. Additionally, preference was given to compare the simulated results to the results determined on the AD. Some discrepancies were found between the simulated C/E-1 results and the C/E-1 results provided in the report made with the SCALE system. Additional, two other results were reported, obtained with the SCALE system and the CASMO5 code, which reported C/E-1 results agreeing to the C/E-1 results obtained in this simulation. Further optimization of the simple model consisted of dividing the sample in two halves and three annular zones, which was proven redundant since no significant better results were obtained.

The second modeled case was sample WZtR165-2a, irradiated in the reactor Vandellos-2. The estimated sample burn-up (calculated with the experimentally determined ^{148}Nd concentration) is 75 GWd/tHMi. The simple model resulted in a burn-up of 76.32 GWd/tHMi. An extended model was made due to the C/E-1 results of ^{235}U and the burn-up indicators lay too far from the experimental uncertainty. With this extended model, a sample burn-up of 79.2 GWd/tHMi was obtained. Some improvements of the model were needed because the curium isotopes showed large discrepancies. The adjacent assemblies were included in the model but this had minimal effect on the C/E-1 results.

The third modeled case was sample GU3, irradiated in the reactor Gösgen-1. The estimated sample burn-up (calculated with the experimentally determined ^{148}Nd concentration) is 52.5 GWd/tHMi. Two different simple models were simulated: one with the irradiation history as provided in the official reports and one where the model was normalized to the experimentally determined ^{148}Nd concentration. A sample burn-up of 50.7 and 52.07 GWd/tHMi respectively were reached. The model with the normalization to the experimentally determined ^{148}Nd concentration came up with the better C/E-1 results. Additionally, preference was given to compare the simulated results to the results obtained to the AD. The results obtained with this model already provided a good agreement with the experimental results and overall better results compared to the results obtained with the SCALE system. Further optimization, modeling the outer two rings of the assembly as different materials, was proven redundant since these results were very similar to the results obtained with the best simple model. In addition, the influence of using different nuclear data libraries was tested with the best simple model.

Some minor discrepancies are found when using the different nuclear data libraries. This was expected since the calculation of the nuclide compositions relies entirely on the nuclear data.

The fourth case was sample BM5, irradiated in the reactor Beznau-1. The estimated sample burn-up (calculated with the experimentally determined ^{148}Nd concentration) is 58.9 GWd/tHMi. With the simulated model, a sample burn-up of 60.3 GWd/tHMi was reached. Due to the large experimental uncertainty on the burn-up indicators, it was not possible to normalize the model to one of these concentrations. The cooling time of the fuel in the assembly was not mentioned in the official reports, except for the sample rod itself. This crucial information since the fuel composition changes due to the decay of the plutonium isotopes. Two different decay periods of this fuel were modeled. Additionally, preference was given to compare the simulated results to the results determined on the AD. Both models reflect an overall good approximation of the physics within the assembly, keeping in mind that the nuclide composition of the other 178 fuel rods is practically unknown.

The last modeled case was sample 1, irradiated in the reactor Fukushima-Daini-2. The estimated sample burn-up (calculated with the experimentally determined ^{148}Nd concentration) is 4.15 GWd/tHMi. With the simulated model, a sample burn-up of 4.15 GWd/tHMi was reached with the simple model and 3.96 GWd/tHMi with the model normalized to the experimentally determined ^{148}Nd concentration. The report presenting the results of models with the SCALE system did not provide C/E-1 results for all the nuclides for which an experimental concentration was reported, which complicated the assessment of the C/E-1 results obtained with the models. Still, comparing the results obtained with the SCALE system, the results obtained with the models provided a better agreement with the experimental concentrations. Preference was given to the model normalized to the experimentally determined ^{148}Nd concentration. More research and modelling of adjacent assemblies is required for this case since the sample is placed in the periphery of the assembly, with the risk of not representing the neutron flux correctly.

A good agreement between the calculated nuclide concentrations and measured data was found and therefore, ALEPH2 provides a good representation of the actual nuclide composition.

6 Outlook

As an outlook, further validation of the ALEPH2 burn-up code with other SNF cases is recommended. Additionally, two cases used in this validation need more attention: BM5 in reactor Beznau-1 and sample 1 in reactor Fukushima-Daini-2.

During the modeling of sample BM5 from reactor Beznau-1, little to no information of the nuclide composition of the other fuel rods in the assembly was known, which resulted in a model with a lot of assumptions. Despite an overall preference for the newly made models, knowing the nuclide composition of the other fuel rods in the model of the SCALE system would be an added value. An additional simulation is recommended if this information could be obtained.

Concerning sample 1, retrieved from the reactor Fukushima-Daini-2, little to no prior validation has been done with the information of this sample. This makes the simulation in this thesis one of the first complete evaluations. Even thought, sufficient prior simulations have been executed with the other samples in rod SF98, it is necessary to be able to provide accurate nuclide compositions for samples taken at the periphery of the assembly, even because these simulations are a little more complex. More validation of such a kind is encouraged.

Finally, further improvement of the model of the WZtR165-2a sample is encouraged. Still some discrepancies are found between the simulations and the experimental results, especially concerning ^{241}Am and the curium isotopes. Since information is lacking concerning the adjacent assemblies, further investigation is needed to correctly model the nuclide composition of these assemblies. Additionally, since the assembly is moving around the core between the irradiation cycles, reflective boundary conditions may not be the best choice. Further analysis is needed.

References

[1] M. I. Ojovan, W. E. Lee, and S. N. Kalmykov, *An introduction to nuclear waste immobilisation*. Elsevier, 2019.

[2] "ONDRAF/NIRAS Research, Development and Demonstration (RD&D) Plan for the geological disposal of high-leven and/or long-lived radioactive waste including irradiated fuel if considered as waste," 2013.

[3] L. Fiorito, D. Piedra, O. Cabellos, and C. J. Diez, "Inventory calculation and nuclear data uncertainty propagation on light water reactor fuel using ALEPH-2 and SCALE 6.2," *Ann. Nucl. Energy*, vol. 83, pp. 137–146, Sep. 2015, doi: 10.1016/j.anucene.2015.03.046.

[4] G. You, C. Zhang, and X. Pan, "Introduction of burn-up credit in nuclear criticality safety analysis," in *Procedia Engineering*, Jan. 2012, vol. 43, pp. 297–301, doi: 10.1016/j.proeng.2012.08.051.

[5] F. Michel-Sendis *et al.*, "SFCOMPO-2.0: An OECD NEA database of spent nuclear fuel isotopic assays, reactor design specifications, and operating data," *Ann. Nucl. Energy*, vol. 110, pp. 779–788, Dec. 2017, doi: 10.1016/j.anucene.2017.07.022.

[6] P. Cook, P. Dyck, R. Einziger, H. P. Fuchs, and A. Gerasimov, "Impact of High Burnup Uranium Oxide and Mixed Uranium-Plutonium Oxide Water Reactor Fuel on Spent Fuel Management," 2011. Accessed: Oct. 01, 2020. [Online]. Available: http://www.iaea.org/Publications/index.html.

[7] K. Khattab, H. Omar, and N. Ghazi, "The effect of temperature and control rod position on the spatial neutron flux distribution in the Syrian miniature neutron source reactor," *Nucl. Eng. Des.*, vol. 236, no. 23, pp. 2419–2423, Dec. 2006, doi: 10.1016/j.nucengdes.2006.03.003.

[8] J. R. Lamarsh and A. J. Baratta, *Introduction to Nuclear Engineering*. 2001.

[9] "Deliverable 8.1: State-of-the-art report," 2019.

[10] "Spent Nuclear Fuel Assay Data for Isotopic Validation State-of-the-art Report," 2011. Accessed: Apr. 25, 2021. [Online]. Available: www.oecd-nea.org.

[11] F. Michel-Sendis, J. Martinez-González, and I. Gauld, "SFCOMPO 2.0 - A relational database of spent fuel isotopic measurements, reactor operational histories, and design data," in *EPJ Web of Conferences*, Sep. 2017, vol. 146, p. 6015, doi: 10.1051/epjconf/201714606015.

[12] H. J. Krappe and K. Pomorski, *Theory of Nuclear Fission*, vol. 838. Berlin, Heidelberg: Springer Berlin Heidelberg, 2012.

[13] M. Herman and A. Trkov, "ENDF-6 Formats Manual: Data Formats and Procedures for the Evaluated Nuclear Data Files ENDF/B-VI and ENDF/B-VII," New York, Jul. 2010. Accessed: Mar. 10, 2021. [Online]. Available: www.nndc.bnl.gov.

[14] "Nuclear Energy Agency (NEA) - JANIS." https://www.oecd-nea.org/jcms/pl_39910/janis (accessed Feb. 28, 2021).

[15] D. Wootan, K. Burns, R. Gates, G. Longoni, and B. Schmitt, "A Concept For a Flexible Neutron Source," *Trans. Am. Nucl. Soc.*, vol. 112, pp. 340–344, Jun. 2015.

[16] "Spent Nuclear Fuel - Used Nuclear Fuel." https://www.nuclear-power.net/nuclear-power-plant/nuclear-fuel/spent-fuel/ (accessed Feb. 13, 2021).

[17] K. Dayman, S. Biegalski, and D. Haas, "Determination of short-lived fission product yields with gamma spectrometry," *J. Radioanal. Nucl. Chem.*, vol. 305, no. 1, pp. 213–223, Jul. 2015, doi: 10.1007/s10967-015-3993-9.

[18] "Livechart - Table of Nuclides - Nuclear structure and decay data." https://www-nds.iaea.org/relnsd/vcharthtml/VChartHTML.html (accessed Mar. 01, 2021).

[19] P. Reuss, *Neutron Physics*. EDP Sciences, 2008.

[20] "What is Fuel Depletion - Isotopic Changes - Definition." https://www.reactor-physics.com/what-is-fuel-depletion-isotopic-changes-definition/ (accessed Feb. 16, 2021).

[21] T. P. Makarova, B. A. Bibichev, and V. D. Domkin, "Destructive analysis of the nuclide composition of spent fuel of WWER-440, WWER-1000, and RBMK-1000 reactors," *Radiochemistry*, vol. 50, no. 4, pp. 414–426, Aug. 2008, doi: 10.1134/S1066362208040152.

[22] L. McManniman and S. Krikorian, "New CRP: Spent Fuel Characterization (T13018) ," *iaea.org*, May 29, 2020. https://www.iaea.org/newscenter/news/new-crp-spent-fuel-characterization-t13018 (accessed May 17, 2021).

[23] G. Žerovnik *et al.*, "Observables of interest for the characterisation of Spent Nuclear Fuel," 2018. doi: 10.2760/418524.

[24] I. Guenther-Leopold, B. Wernli, and Z. Kopajtic, "Characterization of spent nuclear fuels by an online combination of chromatographic and mass spectrometric techniques," 2003, doi: 10.11484/JAERI-CONF-2003-019-PART2.

[25] A. S. Chesterman, B. International, A. Simpson, and M. Clapham, "Burnup Credit Measurements for Cask Loading Compliance-A Review of Techniques and Calibration Philosophies-11194," 2011, p. 10, Accessed: Mar. 02, 2021. [Online]. Available: http://www.nrc.gov/waste/.

[26] G. Ilas, I. C. Gauld, and B. D. Murphy, "Analysis of Experimental Data for High Burnup PWR Spent Fuel Isotopic Validation-ARIANE and REBUS Programs (UO2 Fuel)," 2010.

[27] A. Stankovskiy and G. Van den Eynde, "Advanced method for calculations of core burn-up, activation of structural materials, and spallation products accumulation in accelerator-driven systems," *Sci. Technol. Nucl. Install.*, vol. 2012, 2012, doi: 10.1155/2012/545103.

[28] "Los Alamos National Laboratory: MCNP Home Page." https://mcnp.lanl.gov/ (accessed Oct. 19, 2020).

[29] N. A. Hanan, A. P. Olson, R. B. Pond, J. E. Matos, and S. Paulo, "A MONTE CARLO BURNUP CODE LINKING MCNP AND REBUS*," Argonne, Illinois, 1998.

[30] B. Ebiwonjumi, H. Lee, W. Kim, and D. Lee, "Validation of nuclide depletion capabilities in Monte Carlo code MCS," *Nucl. Eng. Technol.*, vol. 52, no. 9, pp. 1907–1916, Sep. 2020, doi: 10.1016/j.net.2020.02.017.

[31] A. Stankovskiy, G. Van den Eynde, and L. Fiorito, "ALEPH: A Monte Carlo Depletion Code - Version 2.8," Brussel, 2021.

[32] CEA, "Depletion and activation calculations," Nov. 29, 2018. https://www.cea.fr/energies/tripoli-4/Pages/Code features/Depletion-and-activation-calculations.aspx (accessed Dec. 05, 2020).

[33] A. G. Croff, "A User's Manual for the ORIGEN2 Computer Code ," 1980.

[34] A. Stankovskiy, G. Van den Eynde, and T. Vidmar, "Development and validation of ALEPH Monte Carlo burn-up code," *Nucl. Meas. Eval. Appl.*, pp. 161–170, 2011.

[35] L. Fiorito, A. Stankovskiy, G. Van den Eynde, and P. E. Labeau, "Development of time-dependent reaction rates to optimise predictor-corrector algorithm in ALEPH burn-up code," *Ann. Nucl. Energy*, vol. 62, pp. 307–315, Dec. 2013, doi: 10.1016/j.anucene.2013.05.046.

[36] K. Suyama, A. Nouri, H. Mochizuki, and Y. Nomura, "SFCOMPO: A database for isotopic composition of nuclear spent fuel; current status and future development." 2003, Accessed: Oct. 12, 2020. [Online]. Available: http://inis.iaea.org/Search/search.aspx?orig_q=RN:34047379.

[37] Y. Naito, M. Kurosawa, and T. Kaneko, "Databook of the isotopic composition of spent fuel in light water reactors." 1993, Accessed: Oct. 12, 2020. [Online]. Available:

http://inis.iaea.org/Search/search.aspx?orig_q=RN:25005325.

[38] “Nuclear Energy Agency (NEA) - SFCOMPO 2.0 (Spent Fuel Isotopic Composition).” https://www.oecd-nea.org/jcms/pl_21515/sfcompo-2-0-spent-fuel-isotopic-composition (accessed Feb. 28, 2021).

[39] “SCALE: A modular code system for performing Standardized Computer Analyses for Licensing Evaluation,” U.S. Nuclear Regulatory Commission. Spent Fuel Project Office., Oak Ridge, TN, Mar. 1997. doi: 10.2172/481563.

[40] R. T. Primm, “ARIANE International Programme Final Report,” Apr. 2002. Accessed: Nov. 23, 2020. [Online]. Available: http://www.osti.gov/contact.html.

[41] M. B. Chadwick *et al.*, “ENDF/B-VII.1 nuclear data for science and technology: Cross sections, covariances, fission product yields and decay data,” *Nucl. Data Sheets*, vol. 112, no. 12, pp. 2887–2996, Dec. 2011, doi: 10.1016/j.nds.2011.11.002.

[42] D. A. Brown *et al.*, “ENDF/B-VIII.0: The 8th Major Release of the Nuclear Reaction Data Library with CIELO-project Cross Sections, New Standards and Thermal Scattering Data,” *Nucl. Data Sheets*, vol. 148, pp. 1–142, Feb. 2018, doi: 10.1016/j.nds.2018.02.001.

[43] A. Santamarina, D. Bernard, P. Blaise, and M. Coste, “Nuclear Energy Agency (NEA) - The JEFF-3.1.1 Nuclear Data Library,” 2009. Accessed: Dec. 07, 2020. [Online]. Available: https://www.oecd-nea.org/jcms/pl_14470.

[44] “Synthesis of the subgroup 7 activities: Specification of a benchmark on Sensitivity / Uncertainty Analysis of used PWR UOx fuel,” 2020.

[45] K. Shibata *et al.*, “JENDL-4.0: A new library for nuclear science and engineering,” *J. Nucl. Sci. Technol.*, vol. 48, no. 1, pp. 1–30, 2011, doi: 10.1080/18811248.2011.9711675.

[46] P. Ortego, “Expert Group on Assay Data for Spent Nuclear Fuel: Evaluation of ARIANE Experiments - Beznau BM1 sample measurements,” 2011.

[47] U. Mertyurek, M. W. Francis, and I. C. Gauld, “SCALE 5 Analysis of BWR Spent Nuclear Fuel Isotopic Compositions for Safety Studies,” 2010. Accessed: May 19, 2021. [Online]. Available: http://www.osti.gov/contact.html.

[48] Y. Nakahara *et al.*, “Nuclide composition benchmark data set for verifying burnup codes on spent light water reactor fuels,” *Nucl. Technol.*, vol. 137, no. 2, pp. 111–126, 2002, doi: 10.13182/NT02-2.

[49] G. Ilas and I. Gauld, “Analysis of Experimental Data for High Burnup PWR Spent Fuel Isotopic Validation - Vandellos II Reactor,” Oak Ridge, TN (United States), Jan. 2011. doi: 10.2172/1003739.

[50] I. Gauld and U. Mertyurek, “Margins For Uncertainty In The Predicted Spent Fuel Isotopic Inventories For BWR Burnup Credit ,” Oak Ridge, 2018. Accessed: May 26, 2021. [Online]. Available: https://www.nrc.gov/reading-rm/doc-collections/nuregs/contract/cr7251/index.html.

[51] S. Azzaoui, M. Micaulaut, K. Govers, and M. Verwerft, “SCALE-6 fuel depletion analyses: Application to the ARIANE program,” Sorbonne Universités.

[52] D. Rochman, A. Vasiliev, H. Ferroukhi, and M. Hursin, “Analysis for the ARIANE GU1 sample: Nuclide inventory and decay heat,” *Ann. Nucl. Energy*, vol. 160, p. 108359, Sep. 2021, doi: 10.1016/j.anucene.2021.108359.

[53] H.-U. Zwicky and J. Low, “Fuel Pellet Isotopic Analyses of Vandellós 2 Rods WZtR165 and WZR0058: Complementary Report,” 2008.

Appendix A: Inconsistencies between SFCOMPO database and official reports

In context of the realization of the thesis “Validation of ALEPH2 burn-up code using benchmarks from SFCOMPO”, this report has been made to point out found inconsistencies between the SFCOMPO database and the official reports providing the information. There was some information missing concerning several reactors, for example, no irradiation history was provided for the irradiation of the samples (something that makes a correct modeling very hard) and no information at all provided concerning the spatial arrangement of the fuel rods in assembly LYD396 in the reactor Quad Cities-1 reactor. The reason this information is missing, is because it was not available for the public.

On the other hand, during this assignment, errors were found in the presented information of the Fukushima-Daini-2 reactor. There are some inconsistencies in the presentation of the fuel type of different rods in the different assemblies. In assembly 2F2D1, rod B3 has the nuclide composition of the fuel defined as “Gadolinium-2”. When looking specifically at the information of this rod, the rod type is defined to be “Fuel-6”, which is incorrect. Additionally, sample TU103 and TU104 are taken respectively 3342.5 mm and 2742.5 mm from the bottom of the fuel stack. Since the rod itself is only defined to be 2473.3 mm long, those sample don’t seem to be taken from the rod itself, while the active fuel length is 371 mm. In that same assembly, rod F6 is composed out of “Fuel-6”, while in SFCOMPO “Fuel-7” is displayed. In assembly 2F2D2, this same error was made only for rod 6. In assembly 2F2D3, rod A4 and H5 are said to be “Fuel-6”, while this should be “Fuel-8”. Finally, in assembly 2F2D4 this is also the case for rod A4, H4, and H5.

Appendix B: Input ALEPH2 - Gösgen-1 GU1 simple model normalized to experimental ^{148}Nd concentration

```
DATN /srv/sci/pack/mcnp/aleph/data/libn/endfb71_v25
MCNP /srv/sci/pack/mcnp/aleph/code/mcnp62_aleph.sh 72 $ 72 CPU
OUT tpd inv act abs

BURN 1 10 9 8 7 4
VOL 1310.155 6.518 6.518 6.518 6.518 2730.086          $ total volume
DENS -10.4 -10.4 -10.4 -10.4 -10.4 -0.712              $ density
TAL 4
TRACE ind 601480 -7.23804347826E-4 0.0059 10
c ################################
c IRRADIATION HISTORY
c ################################
c cycle 12
IRP S 10 3.771506E-03 d 6
PPM 4 50000 1511
IRP S 10 4.169076E-03 d 144
PPM 4 50000 1179
IRP S 10 3.880447E-03 d 144.2
PPM 4 50000 565
IRP S 10 3.551016E-03 d 22.8
PPM 4 50000 8
DEC d 32
c cycle 13
IRP S 10 2.822983E-03 d 6
PPM 4 50000 1477
IRP S 10 2.998479E-03 d 144
PPM 4 50000 1145
IRP S 10 3.328065E-03 d 142.3
PPM 4 50000 542
IRP S 10 3.111901E-03 d 29
PPM 4 50000 7
DEC d 16
c cycle 14
IRP S 10 2.201927E-03 d 6
PPM 4 50000 1517
IRP S 10 2.865328E-03 d 144
PPM 4 50000 1178
IRP S 10 2.842569E-03 d 140.14
PPM 4 50000 549
IRP S 10 3.542159E-03 d 41.2
PPM 4 50000 5
DEC d 26
c cycle 15
IRP S 10 2.371306E-03 d 6
PPM 4 50000 1594
IRP S 10 2.533628E-03 d 144
PPM 4 50000 1243
IRP S 10 2.380004E-03 d 151.9
PPM 4 50000 605
IRP S 10 2.223782E-03 d 24.8
PPM 4 50000 5
DEC d 1000
DEC d 40
DEC d 11
DEC d 2
DEC d 1
DEC d 6
DEC d 31
DEC d 5
DEC d 20
```

```
DEC d 1021

MESSAGE: xsdir=/srv/sci/pack/mcnp/xs_aleph_big/mcnpx/xsdirb71_lambda

Gosgen-1, GU1 sample
c ##############################
c CELLS
c ##############################
c fuel 12-13
100 1  -10.4          -10 IMP:N=1 u=1  TMP=7.756E-08 $ fuel pellet
101 3  -0.0020907 10 -11 IMP:N=1 u=1  TMP=5.170E-08 $ He
102 2  -6.5093    11 -12 IMP:N=1 u=1  TMP=5.170E-08 $ cladding of rod
103 4  -0.712     12     IMP:N=1 u=1  TMP=5.170E-08 $ moderator
c rod 14H13
200 10 -10.4          -10 IMP:N=1 u=2  TMP=7.756E-08 $ fuel pellet
201 3  -0.0020907 10 -11 IMP:N=1 u=2  TMP=5.170E-08 $ He
202 2  -6.5093    11 -12 IMP:N=1 u=2  TMP=5.170E-08 $ cladding of rod
203 4  -0.712     12     IMP:N=1 u=2  TMP=5.170E-08 $ moderator
c rod M12
900 9  -10.4          -10 IMP:N=1 u=9  TMP=7.756E-08 $ fuel pellet
901 3  -0.0020907 10 -11 IMP:N=1 u=9  TMP=5.170E-08 $ He
902 2  -6.5093    11 -12 IMP:N=1 u=9  TMP=5.170E-08 $ cladding of rod
903 4  -0.712     12     IMP:N=1 u=9  TMP=5.170E-08 $ moderator
c rod M14
800 8  -10.4          -10 IMP:N=1 u=8  TMP=7.756E-08 $ fuel pellet
801 3  -0.0020907 10 -11 IMP:N=1 u=8  TMP=5.170E-08 $ He
802 2  -6.5093    11 -12 IMP:N=1 u=8  TMP=5.170E-08 $ cladding of rod
803 4  -0.712     12     IMP:N=1 u=8  TMP=5.170E-08 $ moderator
c rod N13
700 7  -10.4          -10 IMP:N=1 u=7  TMP=7.756E-08 $ fuel pellet
701 3  -0.0020907 10 -11 IMP:N=1 u=7  TMP=5.170E-08 $ He
702 2  -6.5093    11 -12 IMP:N=1 u=7  TMP=5.170E-08 $ cladding of rod
703 4  -0.712     12     IMP:N=1 u=7  TMP=5.170E-08 $ moderator
c guide tube
400 4 -0.712       -30   IMP:N=1 u=4  TMP=5.170E-08 $ moderator in guide
tube
401 2 -6.5093     30 -31 IMP:N=1 u=4  TMP=5.170E-08 $ zircaloy guide tube
402 4 -0.712      31     IMP:N=1 u=4  TMP=5.170E-08 $ moderator outside
tube
c assembly
2 0           20 -21 22 -23        lat=1  IMP:N=1    u=10
          fill=-7:7 -7:7 0:0
     1 1 1 1 1 1 1 1 1 1 1 1 1 1 1
     1 1 1 1 1 1 1 1 1 1 8 1 1 1 1
     1 1 4 1 1 4 1 1 1 4 2 7 4 1 1
     1 1 1 1 1 1 1 1 1 1 9 1 1 1 1
     1 1 1 1 4 1 1 4 1 1 4 1 1 1 1
     1 1 4 1 1 1 1 1 1 1 1 1 4 1 1
     1 1 1 1 1 1 1 1 1 1 1 1 1 1 1
     1 1 1 1 4 1 1 1 1 1 4 1 1 1 1
     1 1 1 1 1 1 1 1 1 1 1 1 1 1 1
     1 1 4 1 1 1 1 1 1 1 1 1 4 1 1
     1 1 1 1 4 1 1 4 1 1 4 1 1 1 1
     1 1 1 1 1 1 1 1 1 1 1 1 1 1 1
     1 1 4 1 1 4 1 1 1 4 1 1 4 1 1
     1 1 1 1 1 1 1 1 1 1 1 1 1 1 1
     1 1 1 1 1 1 1 1 1 1 1 1 1 1 1
3 0        -80                      fill=10                IMP:N=1
4 4 -0.712 -90 #3                           TMP=5.170E-08 IMP:N=1
5 0         90                                            IMP:N=0

c ##############################
c SURFACES
c ##############################
```

```
c fuel and cladding
10 cz 0.4555       $ fuel pellet outer radius
11 cz 0.465        $ clad inner radius
12 cz 0.5375       $ clad outer radius
c lattice cell
20 px -0.715
21 px 0.715
22 py -0.715
23 py 0.715
c guide tube
30 cz 0.62         $ inner radius guide tube
31 cz 0.69         $ outer radius guide tube
c assembly wrapper
80  rpp -10.725 10.725 -10.725 10.725 -5 5  $ inner box
*90 rpp -10.78  10.78  -10.78  10.78  -5.001 5.001  $ outer box

c ################################
c MATERIALS
c ################################
m1   8016.09c   1.340323E-03           $ fuel
     92234.09c  6.276205E-05
     92235.09c  6.075749E-03
     92238.09c  1.653326E-01
m10  8016.09c   1.340323E-03           $ fuel rod 14H13
     92234.09c  6.276205E-05
     92235.09c  6.075749E-03
     92238.09c  1.653326E-01
m9   8016.09c   1.340323E-03           $ fuel rod M12
     92234.09c  6.276205E-05
     92235.09c  6.075749E-03
     92238.09c  1.653326E-01
m8   8016.09c   1.340323E-03           $ fuel rod M14
     92234.09c  6.276205E-05
     92235.09c  6.075749E-03
     92238.09c  1.653326E-01
m7   8016.09c   1.340323E-03           $ fuel rod N13
     92234.09c  6.276205E-05
     92235.09c  6.075749E-03
     92238.09c  1.653326E-01
m2   40090.06c  5.06062E-01        $ Zircaloy-4 Clad
     40091.06c  1.10360E-01
     40092.06c  1.68688E-01
     40094.06c  1.70950E-01
     40096.06c  2.75408E-02
     50112.06c  9.54091E-03
     50114.06c  6.49176E-03
     50115.06c  3.34424E-03
     50116.06c  1.43016E-01
     50117.06c  7.55405E-02
     50118.06c  2.38228E-01
     50119.06c  8.44913E-02
     50120.06c  3.20457E-01
     50122.06c  4.55407E-02
     50124.06c  5.69505E-02
     26054.06c  2.00764E-04
     26056.06c  3.15158E-03
     26057.06c  7.27836E-05
     26058.06c  9.68616E-06
     24050.06c  7.63306E-05
     24052.06c  1.47196E-03
     24053.06c  1.66909E-04
     24054.06c  4.15471E-05
     72174.06c  8.18837E-08
     72176.06c  2.69192E-06
```

```
     72177.06c  9.51894E-06
     72178.06c  1.39611E-05
     72179.06c  6.97035E-06
     72180.06c  1.79530E-05
m3   2003.06c   1.3200E-06        $ He
     2004.06c   0.99999866
m4   1001.06c   0.6659            $ water
     8016.06c   0.33254
     8017.06c   1.2666667E-04
mt4 lwtr.16t
c
c tallies
kcode 100000  1  30  280
ksrc -10.01 -10.01 0
     -8.58  -10.01 0
     -7.15  -10.01 0
     -5.72  -10.01 0
     -4.29  -10.01 0
     -2.86  -10.01 0
     -1.43  -10.01 0
     0      -10.01 0
     1.43   -10.01 0
     2.86   -10.01 0
     4.29   -10.01 0
     5.72   -10.01 0
     7.15   -10.01 0
     8.58   -10.01 0
     10.01  -10.01 0
     -10.01 -8.58  0
     -8.58  -8.58  0
     -7.15  -8.58  0
     -5.72  -8.58  0
     -4.29  -8.58  0
     -2.86  -8.58  0
     -1.43  -8.58  0
     0      -8.58  0
     1.43   -8.58  0
     2.86   -8.58  0
     4.29   -8.58  0
     5.72   -8.58  0
     7.15   -8.58  0
     8.58   -8.58  0
     10.01  -8.58  0
     -10.01 -7.15  0
     -8.58  -7.15  0
     -7.15  -7.15  0
     -5.72  -7.15  0
     -4.29  -7.15  0
     -2.86  -7.15  0
     -1.43  -7.15  0
     0      -7.15  0
     1.43   -7.15  0
     2.86   -7.15  0
     4.29   -7.15  0
     5.72   -7.15  0
     7.15   -7.15  0
     8.58   -7.15  0
     10.01  -7.15  0
     -10.01 -5.72  0
     -8.58  -5.72  0
     -7.15  -5.72  0
     -5.72  -5.72  0
     -4.29  -5.72  0
     -2.86  -5.72  0
```

```
-1.43  -5.72  0
0      -5.72  0
1.43   -5.72  0
2.86   -5.72  0
4.29   -5.72  0
5.72   -5.72  0
7.15   -5.72  0
8.58   -5.72  0
10.01  -5.72  0
-10.01 -4.29  0
-8.58  -4.29  0
-7.15  -4.29  0
-5.72  -4.29  0
-4.29  -4.29  0
-2.86  -4.29  0
-1.43  -4.29  0
0      -4.29  0
1.43   -4.29  0
2.86   -4.29  0
4.29   -4.29  0
5.72   -4.29  0
7.15   -4.29  0
8.58   -4.29  0
10.01  -4.29  0
-10.01 -2.86  0
-8.58  -2.86  0
-7.15  -2.86  0
-5.72  -2.86  0
-4.29  -2.86  0
-2.86  -2.86  0
-1.43  -2.86  0
0      -2.86  0
1.43   -2.86  0
2.86   -2.86  0
4.29   -2.86  0
5.72   -2.86  0
7.15   -2.86  0
8.58   -2.86  0
10.01  -2.86  0
-10.01 -1.43  0
-8.58  -1.43  0
-7.15  -1.43  0
-5.72  -1.43  0
-4.29  -1.43  0
-2.86  -1.43  0
-1.43  -1.43  0
0      -1.43  0
1.43   -1.43  0
2.86   -1.43  0
4.29   -1.43  0
5.72   -1.43  0
7.15   -1.43  0
8.58   -1.43  0
10.01  -1.43  0
-10.01  0     0
-8.58   0     0
-7.15   0     0
-5.72   0     0
-4.29   0     0
-2.86   0     0
-1.43   0     0
0       0     0
1.43    0     0
2.86    0     0
```

```
4.29    0     0
5.72    0     0
7.15    0     0
8.58    0     0
10.01   0     0
-10.01  10.01 0
-8.58   10.01 0
-7.15   10.01 0
-5.72   10.01 0
-4.29   10.01 0
-2.86   10.01 0
-1.43   10.01 0
0       10.01 0
1.43    10.01 0
2.86    10.01 0
4.29    10.01 0
5.72    10.01 0
7.15    10.01 0
8.58    10.01 0
10.01   10.01 0
-10.01  8.58  0
-8.58   8.58  0
-7.15   8.58  0
-5.72   8.58  0
-4.29   8.58  0
-2.86   8.58  0
-1.43   8.58  0
0       8.58  0
1.43    8.58  0
2.86    8.58  0
4.29    8.58  0
5.72    8.58  0
7.15    8.58  0
8.58    8.58  0
10.01   8.58  0
-10.01  7.15  0
-8.58   7.15  0
-7.15   7.15  0
-5.72   7.15  0
-4.29   7.15  0
-2.86   7.15  0
-1.43   7.15  0
0       7.15  0
1.43    7.15  0
2.86    7.15  0
4.29    7.15  0
5.72    7.15  0
7.15    7.15  0
8.58    7.15  0
10.01   7.15  0
-10.01  5.72  0
-8.58   5.72  0
-7.15   5.72  0
-5.72   5.72  0
-4.29   5.72  0
-2.86   5.72  0
-1.43   5.72  0
0       5.72  0
1.43    5.72  0
2.86    5.72  0
4.29    5.72  0
5.72    5.72  0
7.15    5.72  0
8.58    5.72  0
```

```
      10.01   5.72  0
      -10.01  4.29  0
      -8.58   4.29  0
      -7.15   4.29  0
      -5.72   4.29  0
      -4.29   4.29  0
      -2.86   4.29  0
      -1.43   4.29  0
      0       4.29  0
      1.43    4.29  0
      2.86    4.29  0
      4.29    4.29  0
      5.72    4.29  0
      7.15    4.29  0
      8.58    4.29  0
      10.01   4.29  0
      -10.01  2.86  0
      -8.58   2.86  0
      -7.15   2.86  0
      -5.72   2.86  0
      -4.29   2.86  0
      -2.86   2.86  0
      -1.43   2.86  0
      0       2.86  0
      1.43    2.86  0
      2.86    2.86  0
      4.29    2.86  0
      5.72    2.86  0
      7.15    2.86  0
      8.58    2.86  0
      10.01   2.86  0
      -10.01  1.43  0
      -8.58   1.43  0
      -7.15   1.43  0
      -5.72   1.43  0
      -4.29   1.43  0
      -2.86   1.43  0
      -1.43   1.43  0
      0       1.43  0
      1.43    1.43  0
      2.86    1.43  0
      4.29    1.43  0
      5.72    1.43  0
      7.15    1.43  0
      8.58    1.43  0
      10.01   1.43  0
f4:n 100 200 900 800 700 (103 203 903 803 703 400 402)
sd4 1 1 1 1 1 1
```